

American Conference on Neutron Scattering

June 23–27, 2002

The Radisson Summit Hill–Knoxville
401 Summit Hill Drive
Knoxville, Tennessee 37902

www.sns.gov/acns

Conference Contacts

Rob Briber, General Chair
Julie Borchers and Paul Butler, Program Co-Chairs
Jim Rhyne, NSSA President
Dave Belanger, NSSA-SHUG Liaison
Rob McQueeney, SHUG Representative
Anne Mayes, Treasurer
Al Ekkebus, Local Committee
Ann Jordan, Local Committee

Sponsors

In response to numerous requests from its membership, the Neutron Scattering Society of America (NSSA), in conjunction with the SNS-HFIR User Group (SHUG), has organized this first American Conference on Neutron Scattering. The conference is sponsored by the national neutron centers and is planned to be held at one of the centers every other year, in years that do not coincide with either the international or European conferences on neutron scattering.

Inaugural American Conference on Neutron Scattering

We want to welcome all in attendance at the first American Conference on Neutron Scattering (ACNS) on behalf of the Neutron Scattering Society of America (NSSA) and the Spallation Neutron Source (SNS) and High Flux Isotope Reactor (HFIR) User Group (SHUG). This inaugural conference is the realization of a long-term dream of many members and officers of NSSA. In the spirit of the NSSA cross-disciplinary organization, it is an opportunity to bring together scientists for talks and discussion from a spectrum of disciplines who have common interests in the use of neutron scattering for research. The papers to be presented at this ACNS include substantial representation from polymer sciences, biology, condensed matter physics and magnetism, materials science and engineering, and neutron instrument development.

It is the intent to hold this conference every two years, except in years coinciding with the International Conference on Neutron Scattering (ICNS). This first conference is being held at Knoxville, Tennessee. In subsequent years, it is planned to have a rotating venue among locations close to the major national neutron centers.

The conference has received significant funding from the National Science Foundation and the U.S. Department of Energy. In addition, financial and in-kind support was provided by the national neutron centers—the Oak Ridge Spallation Neutron Source and High Flux Isotope Reactor, the National Institute of Standards and Technology Center for Neutron Research, the Los Alamos Manuel Lujan Neutron Scattering Center, and the Argonne Intense Pulsed Neutron Source. We are most appreciative of this support that has made the conference possible and for the vote of confidence it gives for the future of neutron scattering in the United States.

The success of this conference depends heavily on many people working behind the scenes. In particular, we want to mention Julie Borchers and Paul Butler, program co-chairs; Anne Mayes, NSSA treasurer; Al Ekkebus, Ann Jordan, and Charlie Horak, local committee chairs; along with many others who served on various committees.

We hope you enjoy this conference, and we welcome your feedback and suggestions on ways to improve future conferences. A comment form is included at the back of this program, and comments can be sent to nssa@neutronscattering.org, given to any of the officers of NSSA identified by special badges, or turned in at the NSSA booth here at the conference. For announcements of other conferences and workshops and general news relating to neutron scattering, we hope you will consult the NSSA web site at www.neutronscattering.org.

Jim Rhyne
President, Neutron Scattering Society of America

Robert Briber
Vice President, Neutron Scattering Society of America
ACNS, General Chair

on behalf of the officers of NSSA and SHUG

Contents

Conference Organization	4
Conference Information	6
Presentation Guidelines	9
Displays and Exhibits	10
Hotel Floor Plan	11
Conference Schedule	12
Monday, June 24, 2002, Abstracts	19
Tuesday, June 25, 2002, Abstracts	55
Wednesday, June 26, 2002, Abstracts	93
Author Index	121
Vendor Advertisements	130
Conference Comment Form	133

Conference Organization

Sponsors

The ACNS has received generous support from the following sponsors:

Argonne National Laboratory Intense Pulsed Neutron Source
Los Alamos National Laboratory Manuel Lujan Neutron Scattering Center
National Institute of Standards and Technology Center for Neutron Research
National Science Foundation
Oak Ridge National Laboratory High Flux Isotope Reactor
Oak Ridge National Laboratory Spallation Neutron Source
U.S. Department of Energy

Steering Committee:

General Chair	Robert Briber (University of Maryland)
Program Co-Chairs	Julie Borchers (National Institute of Standards and Technology) Paul Butler (Oak Ridge National Laboratory)
NSSA President	James Rhyne (University of Missouri)
NSSA-SHUG Liaison	David Belanger (University of California, Santa Cruz)
SHUG President	John Tranquada (Brookhaven National Laboratory)
SHUG Representative	Robert McQueeney (Los Alamos Manuel Lujan Neutron Science Center)
NSSA Treasurer	Anne Mayes (Massachusetts Institute of Technology)

Local Committee:

Al Ekkebus, Ann Jordan, and Charlie Horak (Oak Ridge National Laboratory Spallation Neutron Source)

Program Committee

A. Neutron Sources Developments

B. Neutron Instrumentation

1. Modeling and Simulations

2. New Instrumentation

3. New Techniques

Jack Carpenter (Intense Pulsed Neutron Source)

Dan Neumann (National Institute of Standards and Technology)

Lee Robertson (Oak Ridge National Laboratory)

C. Soft Condensed Matter

Ramanan Krishnamoorti (University of Houston)

Nitash Balsara (University of California, Berkeley)

Mark Foster (University of Akron)

Mark Dadmun (University of Tennessee)

D. Magnetism

Bruce Gaulin (McMaster University)

Jaime Fernandez-Baca (Oak Ridge National Laboratory)

Mike Fitzsimmons (Los Alamos Manuel Lujan Neutron Science Center)

Suzanne te Velthuis (Intense Pulsed Neutron Source)

E. Material Science

Steve Nagler (Oak Ridge National Laboratory)

Angus Wilkinson (Georgia Institute of Technology)

Rob McQueeney (Los Alamos Manuel Lujan Neutron Science Center)

F. Biology

Doug Tobias (University of California, Irvine)

Susan Krueger (National Institute of Standards and Technology)

Dieter Schneider (Brookhaven National Laboratory)

G. Chemistry and Chemical Physics

Josef Zwanziger (Indiana University)

Patrick Woodward (Ohio State University)

Juergen Eckert (Los Alamos Manuel Lujan Neutron Science Center)

H. Industrial Applications

John Root (Chalk River Laboratories)

Thomas Mason (ExxonMobil)

I. Fundamental Physics

Mike Snow (Indiana University)

David Jacobson (National Institute of Standards and Technology)

Conference Information

Conference Structure

The ACNS features a combination of keynote, invited, and contributed talks, along with poster sessions. A session on Tuesday, June 25, will highlight the capabilities of the instrumentation available for users at the major neutron centers in North America and will provide a forum for users to ask questions and raise issues that relate to using these facilities. This session will be followed by business meetings for user groups that have requested time. Also featured are breakout sessions for in-depth discussions and working groups on focussed topics.

The conference web site is www.sns.gov/acns/.

NSSA Membership Information

The Neutron Scattering Society of America (NSSA) was formed in 1992 and is an organization of persons who have an interest in neutron-scattering research in a wide spectrum of disciplines. Membership in the society is open to individuals in academia, industry, and government. Graduate students and recent Ph.D.s are especially encouraged to join. There is no cost to be a member, and all members receive a complementary copy of *Neutron News*. Additional information and membership forms are available at the NSSA display in front of the Tennessee Ballroom or at the NSSA web site: www.neutronsattering.org.

Transportation

A Delta Airlines discount (5%) has been arranged for ACNS meeting attendees. For reservations, please call Delta at 1-800-241-6760 and refer to File No. DMN185553A.

Taxis (about \$20 to the Radisson Summit Hill Hotel) and major automobile rental agencies such as Alamo, Avis, Budget, Hertz, National, and Thrifty are located in the baggage claim area of McGhee Tyson Airport in Knoxville.

Additionally, a shuttle service with a lower rate than the taxi services may be available. Please check the web site for details.

Conference Hotel

The Radisson Summit Hill is conveniently located to transportation, shopping, and local attractions. A historic shopping district, the Old City, is just two blocks away, and other area attractions are all within a 10-minute drive. Parking at the Radisson is complementary for all guests and attendees. To receive the conference rate of \$79.00 per night, reservations may be made directly with the hotel at 865-522-2600. State and local taxes are 16.25%. Hotel rooms can also be reserved on-line via the conference web site (www.sns.gov/acns). Suggestions for alternate hotel arrangements (or for Saturday night accommodations) are listed on the conference web site under "Regional Attractions." In particular, rooms might be available on Saturday night at the Hampton Inn Knoxville Airport (1-865-983-1101), Scottish Inn Airport (1-800-251-1962), Fairfield Inn Knoxville Airport (1-865-984-9350), or Alcoa Days Inn Knoxville Airport (1-865-970-3060).

Registration

Registration is available on-line at the conference web site. Payment can be made by check in U.S. dollars or by credit card. Checks should be made payable to ACNS. Advance registration closed on May 15, 2002. On-site registration is also available. All conference attendees must register and wear their badges during the meeting. The conference registration desk is located on the Mezzanine level of the Radisson. The registration desk will be open on Sunday, June 23, from 3:00–7:00 p.m. On Monday through Wednesday, June 24–26, the desk will be open from 8:00 a.m.–5:00 p.m.

Registration fees are:

Advance student registration	\$100
On-site student registration	\$150
Advance registration	\$250
On-site registration	\$300

All registrants will receive a badge, a copy of the program book, a bag with the ACNS logo, continental breakfast on Monday through Thursday, and buffet lunch on Monday through Wednesday. Copies of the latest issue of *Neutron News* will be available at the NSSA booth for all registrants.

Travel Reimbursements

Limited travel support is available to partially support the travel expenses of some conference participants, particularly students, postdocs, and junior faculty in the United States. Application forms are available on-line at the conference web site. Support decisions for those registering by May 1 will be conveyed to applicants by May 15. Later applications will be considered until June 1. Reimbursement checks will be available soon after the meeting. The registration fee must be paid in advance. To receive reimbursements, receipts must be presented for expenses incurred. Additional information about reimbursements is available at the NSSA booth outside of the Tennessee Ballroom.

Nanophase Materials Sciences Workshop

In conjunction with the ACNS meeting, the second Oak Ridge National Laboratory Nanophase Materials Sciences Workshop will be held June 23–25 at the Holiday Inn Select and Knoxville Convention Center in Knoxville. On Sunday, June 23, the workshop features a symposium that will include plenary tutorial talks on distinctly “nano” neutron-scattering methods, followed by parallel sessions illustrating their use in contemporary nanoscience research, all presented by national and international experts. Additional information is available at the workshop web site: www.ssd.ornl.gov/CNMS/workshops/.

Receptions and Conference Banquets

A reception will be held on Sunday, June 23, from 5:30–7:00 p.m. in Summit Grand Ballroom II. All conference registrants are invited to attend.

The Los Alamos Manuel Lujan Neutron Scattering Center will sponsor another reception on Monday, June 24, from 8:00–9:30 p.m. in Summit Grand Ballroom I in conjunction with the Monday evening poster session in Summit Grand Ballroom II.

The Conference Banquet will be held on Tuesday, June 25, at 7:30 p.m. at the Foundry Restaurant. A reception will begin at 7:00 p.m. The Foundry is a beautifully restored iron foundry that was built in 1865. Today it houses one of the finest gathering places for special events and has been placed on the historic registry. The price of the banquet is \$40 and includes hors d'oeuvres, sit-down dinner, and beverage tickets. The Foundry is located within easy walking distance of the Radisson. Shuttle service will be available to and from the Foundry for a limited number of conference attendees. Attendees should meet the shuttle outside of the Radisson front entrance at 6:45 p.m. Priority seating should be given to those in need.

Breakfast, Lunch, and Coffee Breaks

Continental breakfast will be served on Monday–Thursday, June 24–27, in Summit Grand Ballroom I from 7:30–8:30 a.m. Buffet lunch will be served on Monday–Wednesday, June 24–26, in Summit Grand Ballroom I at the time listed in the conference schedule. Coffee and tea will be available in Summit Grand Ballroom I and in the foyer of Summit Grand Ballroom during coffee breaks.

Internet Café

Five computers with Internet access will be available on the Mezzanine level. Wireless (802.11b) Internet access is also planned for the conference site.

Presentation Guidelines

Oral Presentations:

Keynote talks are 25 minutes plus 5 minutes for questions. Invited and contributed talks are 13 minutes plus 2 minutes for questions. Overhead projectors and LCD projectors will be available in each room. Speakers are encouraged to use LCD projectors. All computer-based presentations should be in Microsoft PowerPoint 2000 format. Computers will be available with the following software installed:

Windows 2000
Microsoft Office 2000
Adobe Acrobat 5.0 reader
Windows Media Player 7.01

If presenters have additional requirements, they should contact Dan Ciarlette (ciarletted@sns.gov) before the conference. The computer network in the Internet Café will have software similar to those in the conference areas and will be available for presenters to use for compatibility checks.

Poster Presentations:

Poster sessions will be in Summit Grand Ballroom II, and poster spaces will be identified by number. Posters should be available for viewing two hours before the start of the poster session. Presenters should stand by their posters throughout the session.

**Posters will be attached ONLY by velcro tabs available at the conference registration desk.
Pins CANNOT be used.**

Dimensions of the usable poster display area is about 46 by 72 inches.

Setup times for posters:

Monday evening session—set up during lunch on Monday
Tuesday morning session—set up during breakfast on Tuesday
Wednesday morning session—set up during breakfast on Wednesday

All posters should be removed by the end of the day of the applicable session.

Displays and Exhibits

Neutron-Scattering Facilities Displays

Displays from each of the neutron-scattering facilities in North America will be set up on the Mezzanine outside the Tennessee Ballroom. These facilities include the Oak Ridge National Laboratory Spallation Neutron Source and High Flux Isotope Reactor, the National Institute of Standards and Technology Center for Neutron Research, the Los Alamos Manuel Lujan Neutron Scattering Center, the Argonne National Laboratory Intense Pulsed Neutron Source, and Neutron Program for Materials Research at Chalk River Laboratories.

Exhibits

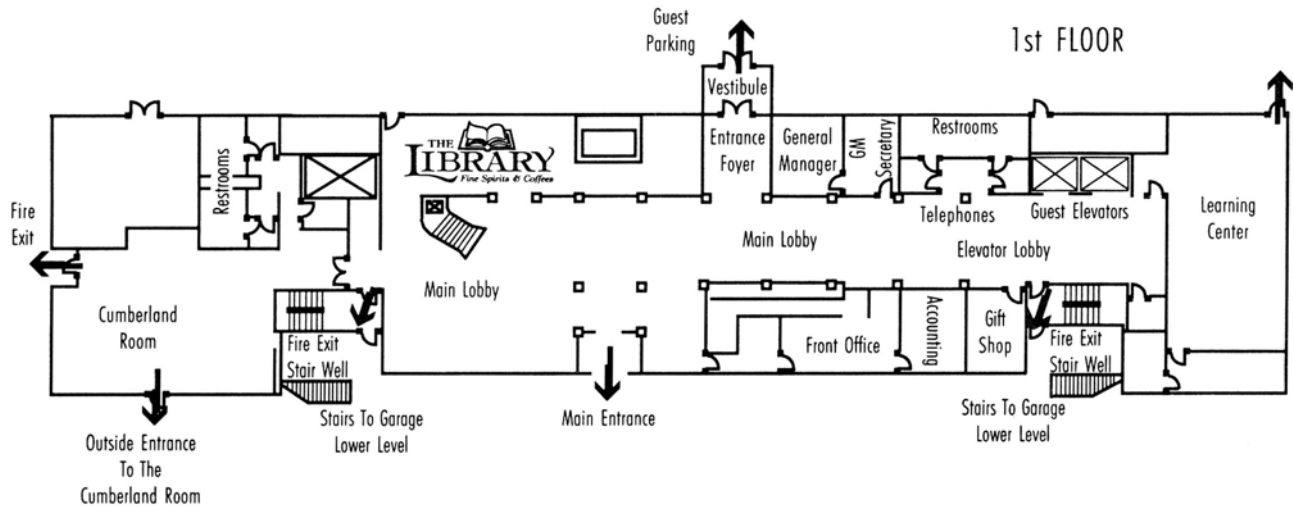
The ACNS will feature ten exhibitors in Summit Grand Ballroom II, adjacent to the poster presentations. Hours for the exhibits will be posted at the meeting.

Exhibitors are:

Advanced Design Consulting
Astrium GmbH (Dornier)
Kurt Lesker Co.
Molecular Metrology, Inc.
Ordela, Inc.
Oxford Instruments
Struck Innovative Systeme
Thermo Reax
Varian Vacuum Technologies
CAEN & WIENER

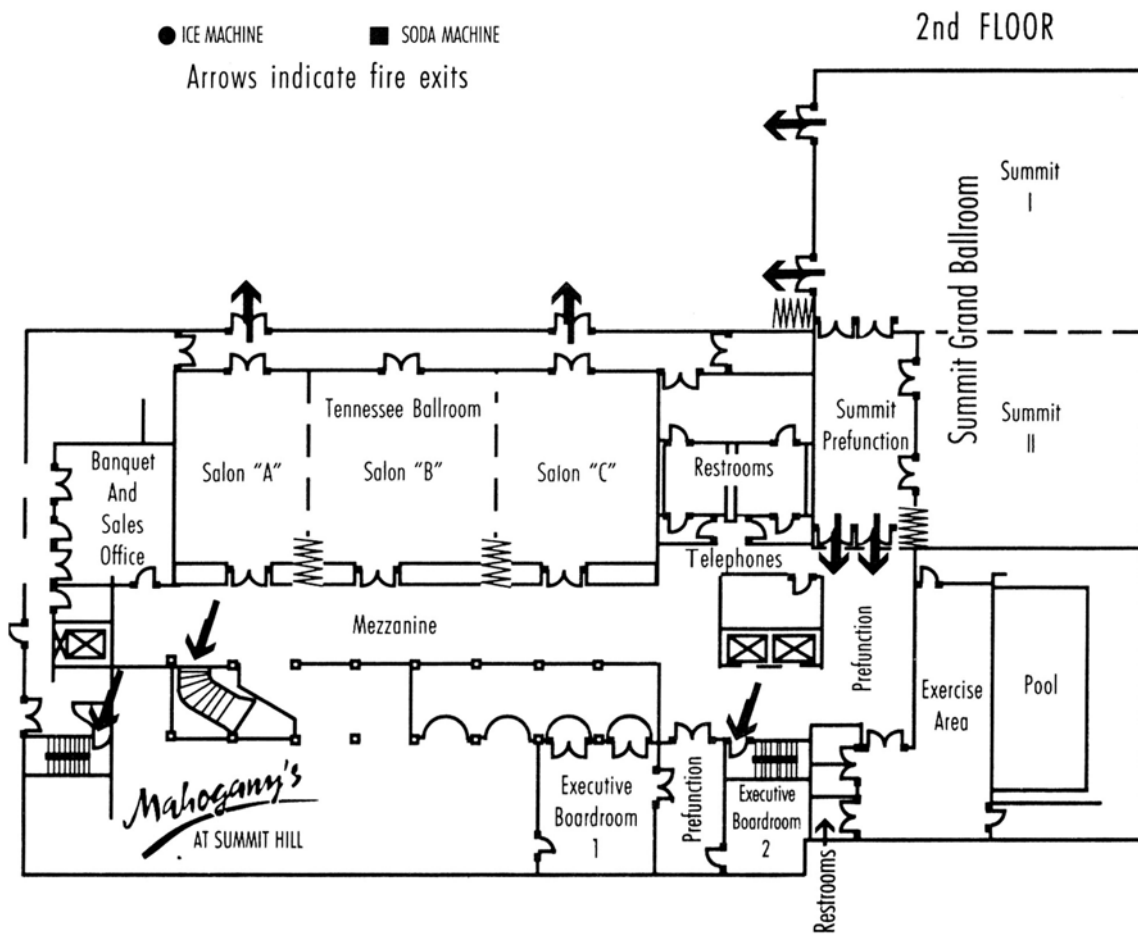
Hotel Floor Plan

Property Layout



● ICE MACHINE ■ SODA MACHINE

Arrows indicate fire exits



Conference Schedule

Sunday Evening 6/23/02

Time	Session	Location
3:00 PM - 7:00 PM	Registration	Mezzanine
5:30 PM - 7:00 PM	Reception	Summit Grand Ballroom I

Monday Morning 6/24/02

Time	Session	Location
7:30 AM	Continental Breakfast	Summit Grand Ballroom I
	Session A: Introduction Chair: Rob Briber (Univ. Maryland) and Dave Belanger (UCSC)	Tennessee Ballroom A, B, C
8:20 AM	NSSA/SHUG Welcome Jim Rhyne (NSSA) and John Tranquada (SHUG)	
8:30 AM	DOE BES Welcome Pat Dehmer (DOE)	
8:40 AM	DOC NIST Welcome Mike Rowe (NIST)	
8:50 AM	NSF Welcome Tom Weber (NSF)	
9:00 AM	Review of U.S. Neutron Sources Paul Sokol (Penn. State)	
9:30 AM	Review of World Neutron Sources Gerry Lander (EITU)	
10:00 AM	Coffee Break	Summit Grand Ballroom I
	Session B: Plenary Chair: Jim Rhyne (Univ. Missouri/NSSA)	Tennessee Ballroom A, B, C
10:30 AM	SNS Overview Thom Mason (SNS)	
11:30 AM	Plenary Talk Robert Cava (Princeton University)	

Monday Afternoon 6/24/02

Time	Session	Location
12:30 PM	Lunch	Summit Grand Ballroom I
1:30 PM	Session C: Oral Presentations CA: Colloids, Micelles and Biomolecules Chair: Lee Magid (Univ. Tennessee)	Tennessee Ballroom A
	CB: Magnetism I Chair: Bruce Gaulin (McMaster Univ.)	Tennessee Ballroom B
	CC: Materials Chemistry Chair: Josef Zwanziger (Indiana Univ.)	Tennessee Ballroom C

3:15 PM	Coffee Break	Summit Grand Ballroom I
3:45 PM	Session D: Oral Presentations	
	DA: Polymer Structure and Thermodynamics I Chair: Mark Dadmun (Univ. Tennessee)	Tennessee Ballroom A
	DB: Magnetism II Chair: John Tranquada (Brookhaven National Laboratory)	Tennessee Ballroom B
	DC: Materials I Chair: Xun-Li Wang (Spallation Neutron Source)	Tennessee Ballroom C
	DD: Neutron Optics Chair: Ian Anderson (Spallation Neutron Source)	Cumberland Room
5:30 PM	Finished	

Monday Evening 6/24/02

Time	Session	Location
8:00 PM – 9:30 PM	Session E: Poster Presentations EP: Instrumentation EQ: Chemistry ER: Materials ES: Soft Condensed Matter	Summit Grand Ballroom II
8:00 PM – 9:30 PM	LANSCE Reception	Summit Grand Ballroom I

Tuesday Morning 6/25/02

Time	Session	Location
7:30 AM	Continental Breakfast	Summit Grand Ballroom I
8:30 AM	Session F: Oral Presentations	
	FA: Soft Matter Dynamics Chair: Darrin Pochan (Univ. Delaware)	Tennessee Ballroom A
	FB: Neutron Techniques Chair: Patrick Gallagher (NIST)	Tennessee Ballroom B
	FC: Materials II Chair: Arthur Schultz (Argonne National Laboratory)	Tennessee Ballroom C
	FD: Nuclear/Particle/Astrophysics with Neutrons I Chair: Michael Snow (Indiana Univ.)	Cumberland Room
10:15 AM	Coffee Break	Summit Grand Ballroom I
10:30 AM - 12:00 PM	Session G: Poster Presentations GP: Instrumentation GQ: Magnetism GR: Materials	Summit Grand Ballroom II

Tuesday Afternoon 6/25/02

Time	Session	Location
12:00 PM	Lunch	Summit Grand Ballroom I
1:15 PM	Session H: Oral Presentations HA: Biological/Biomimetic Systems I Chair: Mathias Lösche (Leipzig Univ.) HB: Industrial Applications Chair: John Root (National Research Council of Canada) HC: Surfaces and Adsorption Chair: Dan Neumann (NIST) HD: Research Frontiers in Artificially Structured Materials Chair: Suzanne te Velthuis (Argonne National Laboratory)	Tennessee Ballroom A Tennessee Ballroom B Tennessee Ballroom C Cumberland Room
3:00 PM	Coffee Break	Summit Grand Ballroom I

Tuesday Afternoon 6/25/02

Time	Session	Location
3:30 PM	Session I: Moderated Discussion and User Group Chair: Thomas Russell (Univ. Massachusetts) Introduction: "Tales of an Experienced User" Thomas Russell	Tennessee Ballroom A, B, C
4:00 PM	Moderated Panel Discussion to discuss user needs and opportunities at national neutron facilities with representatives from IPNS, LANSCE, NCNR, and ORNL	
4:40 PM	JINS Presentation	
5:00 PM	CINS Business Meeting	
5:20 PM	SHUG Business Meeting	
5:40 PM	LANSCE Business Meeting	
6:00 PM	IPNS Business Meeting	
6:20 PM	Finished	

Tuesday Evening 6/25/02

Time	Session	Location
7:00 PM	Banquet Dinner at the Foundry	Foundry Restaurant

Wednesday Morning 6/26/02

Time	Session	Location
7:30 AM	Continental Breakfast	Summit Grand Ballroom I
8:30 AM	Session J: Oral Presentations JA: Biological/Biomimetic Systems II Chair: Kalina Hristova (Johns Hopkins University) JB: Magnetism III Chair: Jaime Fernandez-Baca (Oak Ridge National Laboratory)	Tennessee Ballroom A Tennessee Ballroom B

	JC: Hydrides and Hydrogen Bonds Chair: Juergen Eckert (UCSB/LANSCE)	Tennessee Ballroom C
	JD: Nuclear/Particle/Astrophysics with Neutrons II Chair: David Jacobson (NIST)	Cumberland Room
10:00 AM	Coffee Break	Summit Grand Ballroom I
10:15 AM – 12:00 PM	Session K: Poster Presentations KP: Instrumentation KQ: Chemistry KR: Soft Condensed Matter KS: Biology	Summit Grand Ballroom II

Wednesday Afternoon 6/26/02

Time	Session	Location
12:00 PM	Lunch	Summit Grand Ballroom I
1:15 PM	Session L: Oral Presentations LA: Polymer Structure and Thermodynamics II Chair: Robert Briber (Univ. Maryland) LB: Sample Environment and Neutron Detection Chair: Jack Carpenter (Argonne National Laboratory) LC: Materials III Chair: Rob McQueeney (LANSCE)	Tennessee Ballroom A Tennessee Ballroom B Tennessee Ballroom C
2:45 PM	Coffee Break	Summit Grand Ballroom I
3:15 PM	Session M: Breakout I MA: Cold Neutron Chopper Spectrometer IDT Chair: Paul Sokol (Penn. State) MB: Canadian Institute of Neutron Scattering (CINS) I MC: Engineering Materials Chair: Hahn Choo (Univ. Tennessee) MD: Who Needs Better Sample Environments? Chair: Louis Santodonato (SNS) ME: Status of the SNS Magnetism Reflectometer Chair: Suzanne te Velthuis (Argonne National Lab.) MF: New High Flux Instrumentation for Large Scale Structure Studies at HFIR Chair: Paul Butler (Oak Ridge National Lab.)	Tennessee Ballroom A Tennessee Ballroom B Tennessee Ballroom C Cumberland Room Summit Grand Ballroom I Summit Grand Ballroom I
4:45 PM	Session N: Breakout II NA: Backscattering IAT Chair: Grant Smith (Univ. Utah) NB: Canadian Institute of Neutron Scattering (CINS) II Chair: Lynann Clapham (Queen's Univ.) NC: Single Crystal Diffractometer IAT Chair: Christine Hoffman (SNS) ND: Data Storage using the NeXus Format Chair: Tom Worlton (Argonne National Lab.)	Tennessee Ballroom A Tennessee Ballroom B Tennessee Ballroom C Cumberland Room

Conference Schedule

NE: Sample Environment Requirements for the
SNS Magnetism Reflectometer
Chair: Ivan Schuller (Univ. Calif. San Diego)
NF: The Future Relevance of Neutron Reflectometry to
Soft-Matter Science
Chair: John Ankner (SNS)

Summit Grand Ballroom I

Summit Grand Ballroom I

6:15 PM

Finished

Thursday Morning 6/27/02

Time	Session	Location
7:30 AM	Continental Breakfast	Summit Grand Ballroom I
8:30 AM	Tour of ORNL Facilities	
12:00 PM	Return to Hotel	

Monday, June 24, 2002

Mon. Morning, Plenary Session B

Chair: James Rhyne (University of Missouri and Neutron Scattering Society of America)
Tennessee Ballroom A, B, C

Mon. 11:30 a.m., Plenary, BA-02

Current Directions in New Materials Research

Robert Cava (Princeton University)

The fields of chemistry, materials science, and condensed matter physics are becoming more and more closely intertwined, resulting in one of the most dynamic branches of currently active interdisciplinary research. Without the continuing discovery, development, and understanding of new materials, progress in the development of future technological systems and research in new phenomena in condensed matter physics would slow down dramatically. In this talk I will present some examples from the materials chemistry community that illustrate the directions in which we are heading. Some trends in new materials research present significant challenges and opportunities for the types of characterization that interest the neutron-scattering community.

Mon. Afternoon, CA–Colloids, Micelles, and Biomolecules

Chair: Lee Magid (University of Tennessee)
Tennessee Ballroom A

Mon. 1:45 p.m., Keynote, CA-01

RHEO-SANS Nonequilibrium Microstructure of Shearing Colloidal Dispersions

Norman J. Wagner (University of Delaware)

The shear induced microstructure for electrostatic and Brownian suspensions are compared using in situ small-angle neutron scattering (SANS). The dispersions consist

of 75-nm Stober silica coated with TPM and have a zeta potential of $-42.6 + -4.7$ mV. Neutralizing the surface charge with 0.066 M nitric acid yields stable hard-sphere dispersions. SANS is conducted over a range of shear rates on the charge-stabilized and Brownian suspensions to test the order-disorder transition and hydrocluster mechanisms for shear thickening and to demonstrate the influence of stabilizing forces on the shear induced microstructure evolution. Through treatment of the colloidal micromechanics, shear induced changes in the microstructure are correlated to the hydrodynamic component of the shear stress and the thermodynamic component of the normal stress; that is, the method of “Rheo-SANS” is developed. The results demonstrate that hydrocluster formation drives the shear thickening transition.

Mon. 2:15 p.m., Invited, CA-02

Topological Relaxation in a Sheared Membrane Phase: Kinetics and Energetics of Handle Formation

Lionel Porcar, W. A. Hamilton, P. D. Butler (Oak Ridge National Laboratory), G. G. Warr (University of Sydney)

We recently demonstrated the scaling behavior of a shear-induced isotropic sponge to lamellar phase transformation by complementary rheological and structural measurements. Above a critical shear rate, this progressive process leads to the total transformation of a sponge phase into a lamellar phase with membranes aligned along the velocity direction. We now report the first time-resolved structural kinetic decay of this steady shear-induced lamellar phase into its equilibrium sponge phase using small-angle neutron scattering. The time constant for the structural relaxation process scales as f^3 , where f is the membrane volume fraction and is much longer than the slowest membrane diffusion process as determined by dynamic light scattering. According to Milner’s predictions, these observations are evidence for a thermally activated topological relaxation process with a sponge’s handle formation energy barrier of the order of 8 kBT.

Oak Ridge National Laboratory is managed by UT-Battelle, LLC, for the U.S. Department of Energy under contract No. DE-AC05-00OR22725.

Mon. 2:30 p.m., Invited, CA-03

SANS Investigation of Molecular Gels

Pierre Terech (Centre National de la Recherche Scientifique)

Molecular gels are composed of self-assembled fibrillar networks that reversibly form from low-mass molecules at low concentrations (ca. 1 wt %) in organic or aqueous liquids. Small-angle neutron scattering (SANS) is a powerful technique to study the morphology of the constitutive aggregates (rods, fibers, helices, or tubules). The structures, mechanisms of aggregation, as well as kinetics of formation or melting of the one-dimensional aggregates can be investigated by SANS. The orientation distribution of the rodlike structures can be probed for systems at rest or under in situ shearing stimuli. The scattering information is important in the field of equilibrium nano-objects exhibiting certain monodisperse structural features. Supported by SAXS, electron microscopy, and rheology experiments, the data provide significant insights in the field of molecular gels or more generally self-assembled fibrillar systems found in biology or synthetic chemistry.

Mon. 2:45 p.m., Talk, CA-04

Kinetics of Bicelle to Lamellae Phase Transition in Phospholipid Mixtures

Howard Wang (National Institute of Standards and Technology)

The kinetics of the bicelle to lamellae phase transition in phospholipid mixtures of DMPC/DHPC is investigated using time-resolved small-angle neutron scattering. The data suggest that ordering in these mixtures is a multi-stage process, initiated by the coalescence of bicelles into stacked membrane layers, and limited at late time by the coarsening and swelling of stacks and pinning due to defects. The time evolution of the ordering process is quantified via structural scaling of the nonequilibrium structure factor.

Mon. 3:00 p.m., Talk, CA-05

Controlling Structure and Solution Interactions in Block Polyelectrolyte Assemblies

Surita Rani Bhatia, Mark Crichton (University of Massachusetts)

We present results on poly(styrene)-poly(acrylic acid/ethyl acrylate) copolymers in aqueous solutions that self-assemble to form spherical micelles. Previous work has shown that these systems form strong gels in water and that the gel elastic modulus can be chemically tuned by varying the number of ethyl acrylate groups. SANS studies on both dilute and concentrated solutions indicate that the micelle size and aggregation number increase with the number of ethyl acrylate groups. Finally, we investigated the effect of added cationic and anionic surfactant, which is known to greatly influence the rheology. Although the addition of surfactant does not disrupt the micellar structure, our data indicate that it does modify the intermicellar interactions.

Mon. Afternoon, CB—Magnetism I

*Chair: Bruce Gaulin (McMaster University)
Tennessee Ballroom B*

Mon. 1:45 p.m., Keynote, CB-01

Tuning Antiferromagnetic Quantum Criticality in the Cuprates by a Magnetic Field

Subir Sachdev, Ying Zhang (Yale University), Eugene Demler (Harvard University)

Neutron-scattering experiments have shown that underdoped LSCO has long-range incommensurate spin density wave order coexisting with superconductivity (a SC+SDW state). At higher doping, the ground state is a superconductor (a SC state). We focus attention on the quantum critical point between the SC+SDW and SC states and show how a theory of its vicinity can provide a useful description of many experiments in the cuprates.

An applied magnetic field can “tune” the position of this quantum critical point, and this provides a natural explanation of a number of recent experiments.

Mon. 2:15 p.m., Invited, CB-02

Dual Life of a High- T_c Superconductor

Young S. Lee (Massachusetts Institute of Technology)

The complex physics of the high- T_c superconductors originate from the delicate balance between competing influences on the electrons of the CuO_2 plane. Magnetic order and superconductivity are the two most prominent features on the generic phase diagram. We have studied the magnetic behavior of superconducting $\text{La}_2\text{CuO}_{4+y}$ single crystals using neutron scattering. A remarkable discovery is the observation of spin-density wave (SDW) order, which coexists with the superconducting phase. By varying multiple parameters in the extended phase diagram, we have probed in detail the relationship between the SDW order and the superconductivity.

Mon. 2:30 p.m., Talk, CB-03

Magnetic Field-Induced Antiferromagnetism in the Cuprate High-Transition Temperature Superconductor $\text{La}_{2-x}\text{Sr}_x\text{CuO}_4$

Bella Lake (Oak Ridge National Laboratory and Oxford University), G. Aeppli (N. E. C. Research Institute), K. Lefmann, N. B. Christensen, D. F. McMorrow, K. N. Clausen (Risø National Lab), H. M. Rønnow (Commissariat à l’Energie Atomique-Grenoble and Institute Laue-Langevin), P. Vorderwisch, P. Smeibidl (Hahn-Meitner Institute), N. Mangkorntong, N. E. Hussey, T. Sasagawa, M. Nohara, H. Takagi (University of Tokyo), T. E. Mason (Oak Ridge National Laboratory)

We have done a series of neutron-scattering measurements on the cuprate, high-transition temperature superconductor $\text{La}_{2-x}\text{Sr}_x\text{CuO}_4$ (LSCO) in an applied magnetic field. For temperatures below T_c and fields less than H_{c2} , magnetic flux penetrates the superconductor via vortices that are cylindrical inclusions of resistive material embedded in the superconductor. Phase coherent superconductivity

characterized by zero resistance is suppressed to the lower field-dependent irreversibility temperature $T_{irr}(H)$ and occurs when the vortices freeze into a lattice. Because superconductivity is destroyed within the vortex cores, they can provide information about the ground state that would have appeared had superconductivity not intervened. Our measurements show that both optimally doped LSCO ($x = 0.16$, $T_c = 38.5$ K) and underdoped LSCO ($x = 0.10$, $T_c = 29$ K) have an enhanced antiferromagnetic response in an applied magnetic field. Measurements of the optimally doped system for $H = 7.5$ T show inelastic subgap spin fluctuations that first disappear with the loss of finite resistivity at T_{irr} but then reappear at a lower temperature with increased lifetime and correlation length compared to the normal state. In the underdoped system, elastic antiferromagnetism develops below T_c in zero field and is significantly enhanced by application of a magnetic field; phase coherent superconductivity is then established within the antiferromagnetic phase at T_{irr} . Ordinary quasiparticle pictures cannot account for the nearly field-independent antiferromagnetic transition temperature revealed by our measurements in the underdoped sample, and our results imply that the vortices nucleate large antiferromagnetic regions extending far beyond the vortex cores and possibly into the superconducting areas of the material.

Mon. 2:45 p.m., Talk, CB-04

Long-Lived Resonance, Stripes, and Spin Gaps in Ortho-II Ordered YBCO

C. Stock (University of Toronto), W. J. L. Buyers (National Research Council and Canadian Institute of Advanced Research), R. Liang, D. Bonn, W. N. Hardy (University of British Columbia and Canadian Institute of Advanced Research), D. Peets (University of British Columbia), Z. Tun (National Research Council), L. Taillefer, R. J. Birgeneau (University of Toronto and Canadian Institute of Advanced Research)

Recent theories of the high-temperature cuprate superconductors have made specific predictions for neutron-scattering experiments. In particular, models involving orbital currents predict the presence of a spin-gap in the normal state for underdoped materials. In response, we have made inelastic neutron-scattering experiments to characterize the low-energy spin fluctuations in the highly

ordered YBCO ortho-II superconductor, where structural disorder is largely absent. The normal state low-energy susceptibility is gapless down to an energy of 4 meV, with fluctuations incommensurate along the normal to the oxygen-filled chains. In the superconducting state, the low-energy susceptibility is suppressed consistent with the opening of a spin-gap. The resonance mode occurs at 33 meV, is well defined, and grows rapidly below a temperature of 120 K (or 2 T). This contrasts with the heavily damped resonance seen in systems with relatively less oxygen order, which may arise from spin scattering by structural disorder rather than from damping by charge carriers.

Mon. 3:00 p.m., Invited, CB-05

Novel Spin Reorientation and Weak Ferromagnetism in $K_2V_3O_8$

Mark D. Lumsden, B. C. Sales, S. E. Nagler (Oak Ridge National Laboratory), D. Mandrus, J. R. Thompson (Oak Ridge National Laboratory and University of Tennessee), D. A. Tennant (Clarendon Laboratory, Oxford, and Rutherford Appleton Laboratory), D. F. McMorrow (Risø National Laboratory)

The magnetic properties of the two-dimensional, spin-1/2 square lattice antiferromagnet, $K_2V_3O_8$, have been studied using a combination of bulk measurements, neutron diffraction, and inelastic neutron scattering. Magnetization studies indicate a phase transition to a long-range ordered state ($T_N = 4$ K), which is characterized by “weak ferromagnetism” and a peculiar field-induced phase transition in the presence of a basal plane magnetic field. Neutron diffraction experiments indicate a very simple zero-field antiferromagnetic spin arrangement with spins along the c-axis. Application of a basal plane magnetic field causes a dramatic rotation of the spins about the applied field direction from the c-axis into the tetragonal basal plane. This spin reorientation and the observed “weak ferromagnetism” can be explained with a Hamiltonian incorporating Heisenberg exchange, Dzyaloshinskii-Moriya interactions, and an additional c-axis anisotropy. The spectrum of magnetic excitations is consistent with this Hamiltonian with the exception of an additional inelastic feature, which only has intensity in the immediate vicinity of the antiferromagnetic zone-boundary.

Mon. Afternoon, CC—Materials Chemistry

*Chair: Josef Zwanziger (Indiana University)
Tennessee Ballroom C*

Mon. 1:45 p.m., Keynote, CC-01

Time-Resolved, In Situ Neutron Powder Diffraction Studies of Hydrothermal Reactions

Dermot O'Hare (University of Oxford)

In this paper I will demonstrate that in situ neutron diffraction is now a feasible way of performing time-resolved investigations of chemical reactions. We will discuss our recent experiments using in situ neutron powder diffraction to investigate the hydrothermal crystallization of inorganic materials. The hydrothermal method is used widely in preparative solid-state chemistry, but little information is available about the processes taking place inside the sealed reaction vessel once elevated temperature is applied and conditions of autogenous pressure are achieved. I will describe a study of the crystallization of two important inorganic materials: (1) the microporous solid, Zeolite A, and (2) a ferroelectric solid, $BaTiO_3$, using in situ, time-resolved neutron powder diffraction. These results were obtained using a specially designed hydrothermal autoclave and the new high-flux/high-counting-rate GEM diffractometer at the ISIS Facility, Rutherford Appleton Laboratory, United Kingdom. These in situ studies allow us to quantitatively determine the growth and decay of various crystalline phases in real time and under real operating conditions. These experiments yield unique information about transient intermediate phases and on the reaction kinetics.

Mon. 2:15 p.m., Invited, CC-02

Morphing the Amorphous: Designing Intermediate Range Order in Glasses and Liquids

James D. Martin (North Carolina State University)

Amorphous materials, key components of many current technologies, are commonly understood to consist of random organizations of molecular-type basic structural

units. However, diffraction studies indicate that structural organization over nanometer-length scales is present in amorphous materials. Such intermediate-length structural organizations differentiate amorphous materials from isolated molecules and crystalline materials and impart unique properties to glasses, amorphous metals, and amorphous semiconductors. Understanding and controlling structural features that give rise to intermediate range order (IRO) in amorphous materials remains a fundamental, yet presently unresolved, question. Historically, there has been considerable debate over random network and crystalline-type models to explain amorphous structural organizations. Here we show that it is possible to employ principles of crystal engineering to design specific patterns of IRO within amorphous zinc-chloride networks by using alkylammonium cationic templates. Crystal-lattice models account for complex neutron-scattering patterns and provide unprecedented insight into the IRO in a series of amorphous networks.

Mon. 2:30 p.m., Talk, CC-03

Hydration Structure of Metal Ions in Aqueous Solution: Some New Insights from Neutron Diffraction

Yaspal Singh Badyal, J. M. Simonson (Oak Ridge National Laboratory), A. C. Barnes (University of Bristol), J. L. Fulton (Pacific Northwest National Laboratory)

It is widely accepted that ion-water interactions play a crucial role in many chemical and biological processes. In order to relate such microscopic interactions to the macroscopic thermochemical and reaction properties of electrolyte solutions, particularly as they vary with changes in temperature, pressure, and composition, a detailed understanding of structural properties (e.g., hydration and inner-sphere complexation) is essential. The technique of neutron diffraction with isotope substitution (NDIS) is particularly well suited to this task and can provide unique and relatively unambiguous information on the hydration structure around ions in solution. The exciting results of a new NDIS investigation of ambient calcium (II) chloride aqueous solutions are discussed. Compelling evidence is presented of changes in the orientational distribution of water molecules around the Ca^{2+} aqua-ion with increasing concentration. From these

data, particularly when combined with the results of complementary EXAFS measurements, it is possible to envision a consistent picture of the subtle but distinctive changes in the Ca^{2+} hydration structure as the number of available water molecules is sharply reduced. Also presented are preliminary results from neutron-scattering studies of nickel (II) chloride aqueous solutions, which provide fresh insights into the role of (increased) temperature in perturbing the hydration structure around the cation.

Mon. 2:45 p.m., Talk, CC-04

Slowing Down of Water Dynamics in Low-Temperature Hydrated Cement Paste

Antonio Faraone, Sow-Hsin Chen, Li Liu, (Massachusetts Institute of Technology), Emiliano Fratini, Piero Baglioni (University of Florence), Craig Brown (University of Maryland and National Institute of Standards and Technology Center for Neutron Research)

Quasi-elastic neutron scattering has been used to investigate the single particle dynamics of interfacial water in dicalcium silicate/water paste in the temperature range from 263 to 303 K. The dicalcium silicate is one of the major components in ordinary portland cement. The data have been analyzed by models for translation and rotation we recently proposed for supercooled and interfacial water. It has already been shown that the translational dynamics of a water molecule shows a short-time Gaussian decay, followed by a long-time alpha relaxation. We have extended this picture to include the rotational dynamic as well. MD simulations of water at low temperatures show that the rotational correlation functions exhibit a two-step relaxation, where the long-time decay is nonexponential, similar to that found for the translation. Using this model we have analyzed our data at five temperature values in the supercooled and low-temperature region, up to the room temperature. We have obtained the parameters describing the relaxational dynamics of water embedded in the dicalcium silicate matrix. Both translational and rotational relaxation times slow down with temperature. Whereas the translational one obeys an Arrhenius law in the investigated temperature range, the rotational one does not. The former is more than three times longer at 263 K with respect to its room

temperature value. The rotational relaxation time also increases with decreasing temperature, even if its variation is less noticeable. However, the parameter beta, accounting for the nonexponentiality of the relaxation, is constant for the translational dynamics and decreases for the rotational one. This finding suggests that the reorientational dynamics becomes hindered, triggering an alpha-relaxation-like phenomenon. Our conclusion is that the coupling between translational and rotational motions becomes stronger on decreasing temperature.

Mon. 3:00 p.m., Talk, CC-05

Phase Separation and Crystallization in Potassium Niobate Tellurite Glass

Robert T. Hart, Matthew A. Anspach, Josef W. Zwanziger, Barry Stein (Indiana University), Peter J. DeSanto, W. M. Keck (University of Delaware), Jaby Jacob, Papannan Thiyagarajan (Argonne National Laboratory)

Glass ceramic of composition $(K_2O)_{15} (Nb_2O_5)_{15} (TeO_2)_{70}$ shows optical second harmonic generation (SHG). We find that this phenomenon follows from liquid-liquid phase separation of the melt and subsequent crystallization of the droplet phase above T_g . In contrast to previously published findings, the crystalline phase is not FCC, clarifying the origin of SHG. Since symmetry and conservation of momentum forbid SHG in phases with inversion symmetry, SHG in this material had been attributed to rather exotic mechanisms. We have now indexed the cell as orthorhombic with $a = 6.37 \text{ \AA}$, $b = 6.12 \text{ \AA}$, and $c = 2.53 \text{ \AA}$. This determination would have been impossible without the use of neutron diffraction to complement X-ray diffraction. Also, the phase separation behavior explains the small size of the particles and the large amount of strain present in them. This strain is found to be mostly in the anion positions, as revealed by combining neutron and X-ray scattering, SAXS, and TEM. Further, the low symmetry unit cell allows us to understand the SHG in terms of Lines's theories of d-metal oxide hyperpolarizability.

Mon. Afternoon, DA—Polymer Structure and Thermodynamics I

*Chair: Mark Dadmun (University of Tennessee)
Tennessee Ballroom A*

Mon. 3:45 p.m., Keynote, DA-01

Structure of Sphere-Forming Block Copolymers in Solutions and Melts

Timothy P. Lodge (University of Minnesota)

Block copolymers are well known to self-assemble into approximately spherical aggregates, or micelles, under at least two conditions: in selective solvents at low and moderate concentrations and in the bulk when the copolymer composition is strongly asymmetric. In both circumstances, interesting questions persist, particularly in the vicinity of the order-disorder transition (ODT). For several styrene-isoprene diblocks in solution we have found regions of concentration and temperature where a suspension of micelles orders on a lattice upon heating, before disordering again at higher temperatures. In other words, there is both a lower (LODT) and an upper (UODT) transition. Furthermore, the intervening ordered state symmetry is either fcc or bcc, and in some cases a thermotropic, reversible, epitaxial fcc/bcc transition is found. In the case of asymmetric molten copolymers, the ordered state symmetry is always bcc. Self-consistent mean-field (SCMF) theory anticipates a narrow window of fcc packing before the ODT, but this has never been seen experimentally. Rather, the ODT corresponds to a transition from a bcc lattice to a disordered array of micelles. SANS measurements on ethylenepropylene-dimethylsiloxane diblocks over a wide range of temperature indicate that the micelles may persist as much as 100 degrees above the ODT.

Mon. 4:15 p.m., Talk, DA-02

Construction of Micro- and Nanoporous Hydrogels Via Designed Diblock Copolypeptide Self-Assembly and Oligopeptide Self-Assembly

Darrin J. Pochan, Lisa Pakstis, Joel Schneider (University of Delaware), Andy Nowak, Tim Deming (University of California, Santa Barbara)

The design and self-assembly of polypeptides as synthetic materials that possess the ability to aggregate into specifically defined, a priori designed, functional nano- and microstructures is being pursued via two avenues. First, synthetic block copolypeptides will be discussed that are observed to form novel hydrogels with structural and biological properties tailorable by the choice of amino acid (and consequent secondary structure) in the respective blocks. Specifically ionic, amphiphilic diblocks have been designed for tissue engineering hydrogels on assembly in aqueous solution. Second, de novo designed oligopeptides that undergo specific folding and consequent self-assembly events triggered by pH will be discussed. Specifically, the ability of oligopeptides to produce pH-sensitive hydrogels via a hierarchical self-assembly process will be discussed. Both classes of peptide-based, self-assembled materials were characterized via small-angle neutron scattering in order to explore local, nanometer length scale gel scaffolding structure. In the diblock copolypeptide case, significant local structural changes were observed via small-angle neutron scattering by changing the molecular weight of the assembling molecules. These structural changes (20k g/mole to 10k g/mole) coincided with significant changes in the rheological properties of the gels (solid to liquid). In addition, all gels were studied with ultras-small-angle neutron scattering in order to probe the rich heterogeneous microstructure formed during the gel self-assembly process.

Mon. 4:30 p.m., Talk, DA-03

A SANS Investigation of the Structure and Interactions of Dendrimer-Like Star Copolymer Architectures in Solution

Cheryl Marie Stancik, John A. Pople (Stanford Synchrotron Radiation Laboratory), James L. Hedrick (Almaden Research Center), Alice P. Gast (Massachusetts Institute of Technology)

We present a small-angle neutron scattering (SANS) study of a series of dendrimer-like star copolymers investigated in solution. These studies allow us to assess the effects of architecture on the conformation of individual copolymer molecules in the dilute regime and interactions of these molecules near the overlap concentration. Each copolymer within the series consists of a highly branched core prepared from poly(ϵ -caprolactone) (PCL). Emanating from the outermost generation of the PCL cores, partially deuterated linear poly(methylmethacrylate) (PMMA) chains are attached to create a star-like copolymer. This series allows us to consider the effects of branching architecture within the PCL core and arm architecture of the PMMA star branches. Using dilute solution results, we fit the data to models to obtain expressions for the form factor and parameters that describe the single molecule conformations. These results are applied to the semi-dilute data in order to obtain experimental structure factors for each molecule. From the structure factors, we see evidence of liquid-like structuring in some copolymers. We find that these copolymers do not adopt a uniform distribution. Both the dilute and semi-dilute analyses show that the different architectural features of these isomeric copolymers have an impact on both the conformation and interactions of these molecules in solution.

Mon. 4:45 p.m., Talk, DA-04

Small-Angle Neutron Scattering of PS-P2VP Arborescent Graft Polymers

Robert M. Briber, S. I. Yun (University of Maryland), M. Gauthier (University of Waterloo)

Arborescent graft polymers synthesized using different polymers for successive generations allows for the potential tailoring of properties. The molecules discussed are synthesized by grafting poly(2-vinylpyridine) (P2VP) onto a poly(styrene) (PS) core. Small-angle neutron scattering (SANS) was performed on solutions of PS-P2VP in deuterated methanol as a function of generation and molecular weight of the shell. Various models for the radial density profile were examined to fit the SANS data of the polymers deuterated methanol. A peak in the SANS data appeared upon addition of HCl due to development of long-range electrostatic interactions. Grafting a higher molecular weight P2VP shell onto the PS core results in a change in the structure forming an ordered gel in acidic deuterated

methanol. SANS was performed on the gel as a function of concentration and amount of charge. The structure of gel is tentatively believed to be hexagonal.

Mon. 5:00 p.m., Talk, DA-05

SANS Verification of a Structural Model for Equilibrium Swollen Networks

Gregory Beaucage, Sathish Sukumaran (University of Cincinnati)

The tensile blob construction for a linear chain, first predicted by Pincus, has been extended for branched structures and is used to explain structures in the network with size scales significantly bigger than the strand length, as observed in neutron-scattering data from equilibrium swollen networks. Under this model, equilibrium swollen networks display a base structural size, the “gel tensile blob” size, ξ , that follows the scaling relationship $\xi \sim l/(1/2 - \chi)^P$, where l is the chain persistence length, χ is the Flory interaction parameter, and P is a power determined by the connectivity of the network. The gel tensile blobs compose a large-scale linear structure, whose length, L , follows the scaling relationship, $L \sim Q^{1/2} N_{\text{avg}}^{-2}$, where $N_{\text{avg}}^{-2} = (1/fN_c^2 + 1/4N_c^2)$, Q is the equilibrium swelling ratio, N_c is the molecular weight between cross links, N_e is the entanglement molecular weight, and f is the functionality of the cross-links. The variation of the swelling ratio with molecular weight can now be expressed as $Q \sim N_{\text{avg}}^{-3/5}$, which reduces to the correct expressions under the limits, $N_c \gg N_e$ and $N_e \gg N_c$. SANS data that support this model will be presented.

Mon. 5:15 p.m., Talk, DA-06

From Single Molecules to Aggregates to Gels in Dilute Solution: Self-Organization of Nanoscale Rodlike Molecules

Dvora Perahia, Rakchart Traiphol (Clemson University), Uwe H. F. Bunz (University of South Carolina)

A transition from a fluid to a constrained phase, in dilute solutions of a rodlike molecule, poly(2,5-dinonylparaphenylene ethynylene)s (PPE) in toluene has been studied, exploring the dynamics and the structure of the PPE

molecules and the solvent in both phases. The transition is characterized by visual changes in the viscosity of the system and in its color, where a transparent liquid transforms into a yellow glassy phase. NMR relaxation measurements indicated that significant restriction of motion of the solvent and of the polymeric molecule take place as the gel-like phase is formed. Small-angle neutron scattering studies (SANS) have shown that in the liquid phase, PPE forms molecular solutions where the molecules are fully extended. Upon transition into the constrained phase, aggregation of PPE molecules into large flat clusters occurs. When the aggregates are too large to freely move in the solution, a transition into a constrained phase takes place. The interaction between the highly conjugated PPE molecules and the solvent results in constrain of the motion of the solvent as well.

Mon. Afternoon, DB—Magnetism II

*Chair: John Tranquada (Brookhaven National Laboratory)
Tennessee Ballroom B*

Mon. 3:45 p.m., Invited, DB-01

Critical Scattering Line Shapes of the Random-Field Ising Model

Feng Ye, D. P. Belanger (University of California, Santa Cruz), M. Matsuda, S. Katano (Japan Atomic Energy Research Institute), H. Yoshizawa (University of Tokyo), J. A. Fernandez-Baca (Oak Ridge National Laboratory)

The critical behavior of the $d = 3$ random-field Ising antiferromagnet $\text{Fe}(0.87)\text{Zn}(0.13)\text{F}_2$, which has a magnetic concentration above the vacancy percolation threshold $x_p = 0.76$, has been studied using neutron-scattering techniques in fields up to 10T. In the absence of a theoretical prediction for the critical scattering line shapes of the random-field Ising model, we employed fitting procedures developed using very general scaling assumptions. This approach allows us to obtain universal critical behavior exponents and amplitude ratios as well as the line shapes. It has recently been shown in ground state calculations by E. Seppala and M. Alava (cond-mat/

0102098) that fractal domain structures form for the $d = 2$ RFIM for fields just above the phase boundary at $T = 0$. The line shapes we obtain above T_c in the scattering experiments for $d = 3$ show evidence for such structure, consistent with a fractal dimension $D_f = 2.53$. Below T_c , the line shapes do not appear to exhibit fractal structure, consistent with the calculations. Measurements were performed at the Japan Atomic Energy Research Institute reactor in Tokai, Japan.

Mon. 4:00 p.m., Invited, DB-02

Field-Induced Magnetic Phenomena in Molecule-Based Magnets

Carmen R. Kmetz (Argonne National Laboratory), Q. Huang, J. W. Lynn, R. W. Erwin (National Institute of Standards and Technology Center for Neutron Research), S. McCall, J. E. Crow (National High Magnetic Field Laboratory), K. L. Stevenson (Indiana-Purdue University, Fort Wayne), J. L. Manson, Joel S. Miller (University of Utah), A. J. Epstein (Ohio State University)

Understanding the relationship between the crystal structure and magnetic ordering is crucial for the design of three-dimensional, molecule-based magnets with high ordering temperatures. In this talk, we introduce a novel series of molecule-based magnets consisting of transition metal ions (Mn, Fe, Co, Ni, or Cu) coordinated with the organic ligand dicyanamide $[\text{N}(\text{CN})_2]^-$. The crystal structures for all compounds are isomorphous in the paramagnetic regime as well as in the ordered state. However, the compounds with transition metal ions having six or less electrons in the three-dimensional orbitals order as canted antiferromagnets (AFM), while the ones with seven or more electrons order as ferromagnets (FM). The spin orientation is nearly in perpendicular directions for the AFM versus FM systems. An external magnetic field induces a spin rotation transition in the Mn compound and an energy-level crossing for the Fe compound. The possible origins of the variability of the magnetic structure for the first row transition metal ions compounds will be discussed.

Mon. 4:15 p.m., Talk, DB-03

Scaling and the Magnetic Phase Diagram of a Quasi-One-Dimensional, Spin-1/2, Heisenberg Antiferromagnet

Stephen E. Nagler, D. A. Tennant, C. Frost (Rutherford Appleton Laboratory), B. Lake (Oak Ridge National Laboratory)

KCuF_3 is a quasi-one-dimensional, spin-1/2, Heisenberg antiferromagnet where the dominant exchange interactions couple the magnetic Cu^{2+} ions into antiferromagnetic chains and weak ferromagnetic exchange interactions act to couple these chains together leading to long-range antiferromagnetic order below the Néel temperature of $T_N = 39$ K. The suppressed ordering temperature and moment reduction of 50% (from Néel ordering) shows that in spite of the interchain coupling, KCuF_3 exhibits strong quantum fluctuations. Neutron-scattering measurements made using the HB1 triple-axis spectrometer (at the High Flux Isotope Reactor, Oak Ridge National Laboratory) show that the low-temperature, long-range ordered phase is characterized by spin-wave excitations and behaves according to the three-dimensional nonlinear sigma model. In contrast, neutron-scattering data collected using the MAPS time-of-flight spectrometer (at ISIS, Rutherford Appleton Laboratory) show that at higher temperatures and energies the basic excitations are spinon pairs and the spectrum displays the universal energy/temperature scaling of a system in the vicinity of a one-dimensional Luttinger liquid quantum critical point. In fact, by testing for scaling, the boundaries in energy and temperature of this phase can be found and the adjacent phases identified. The most interesting adjacent phase lies on the low-energy side between the one-dimensional Luttinger liquid phase and the three-dimensional nonlinear sigma model. A novel longitudinal mode has been observed in this region existing below the Néel temperature. This mode signals the crossover from one-dimensional to three-dimensional behavior, and the phase has been identified as a nonuniversal crossover region.

Mon. 4:30 p.m., Talk, DB-04

Quantum Spin Dynamics in One-Dimensional Antiferromagnets

Igor A. Zaliznyak, M. Enderle (Institut Laue-Langevin), C. Broholm, D. Reich (Johns Hopkins University), L.-P. Regnault (MDN/DRFMC/CEN-G), M. Sieling (Universität Frankfurt), K. Katsumata (RIKEN Harima Institute), P. Vorderwisch, M. Meissner (Hahn-Meitner Institut)

Low-dimensional quantum spin systems are invaluable sources of insight in physics of the cooperative quantum ground states and quantum-critical behavior. Instability of coherently propagating excitations in some part of the phase space appears to be a fundamental feature of quantum (spin) liquids close to the quantum phase transition. A similar phenomenon is observed in the superfluid ^4He , where “maxon” acquires width when increasing pressure drives it towards crystallization. Some very recent neutron experiments reveal similar excitation decoherence in one-dimensional spin systems close to quantum phase transition.

Mon. 4:45 p.m., Invited, DB-05

Quantum Impurities in the Two-Dimensional Spin One-Half Heisenberg Antiferromagnet

Owen Peter Vajk, P. K. Mang, M. Greven (Stanford University), P. M. Gehring, J. W. Lynn (National Institute of Standards and Technology Center for Neutron Research)

The study of randomness in low-dimensional quantum antiferromagnets is at the forefront of research in the field of strongly correlated electron systems, yet there have been relatively few experimental model systems. Complementary neutron-scattering and numerical experiments demonstrate that the spin-diluted Heisenberg antiferromagnet $\text{La}_2\text{Cu}(1-z)(\text{Zn},\text{Mg})z\text{O}_4$ is an excellent model material for square-lattice site percolation in the extreme quantum limit of spin one-half [1]. As dilution increases, quantum fluctuations decrease the strength of the antiferromagnetic order, but the system retains a long-range-ordered ground state up to the percolation thresh-

old. Above the percolation threshold, spins are separated into finite-sized clusters and the long-range order disappears. Neutron-scattering measurements of the ordered moment and spin correlations provide important quantitative information for tests of theories for this complex quantum-impurity problem. Complementary numerical work provides evidence that the finite-temperature properties of the system are governed by the proximity to a new quantum critical point in an extended phase space. This new critical point can be realized numerically by introducing a small antiferromagnetic bilayer coupling between two identically diluted square lattices. [1] O. P. Vajk, P. K. Mang, M. Greven, P. M. Gehring, and J. W. Lynn, *Science* 295, 1691 (2002).

Mon. 5:00 p.m., Keynote, DB-06

Magnetic Correlations and Quantum Critical Points

Meigan C. Aronson, Wouter Montfrooij (University of Michigan), Ray Osborn (Argonne National Laboratory), Brian Maple (University of California, San Diego), Brian Rainford (University of Southampton), Alexei Tsvetik (Brookhaven National Laboratory), Amir Murani (Institut Laue-Langevin), Pierre Haen (Centre de Recherche sur les Très Basses Températures)

Pressure, magnetic fields, and doping can be used to suppress a finite temperature magnetic transition to zero temperature in a number of metallic magnets. This quantum critical point is thought to be generated either by the quenching or decoupling of magnetic moments. Inelastic neutron-scattering measurements on the quantum critical systems $\text{UCu}_{5-x}\text{Pd}_x$ (Aronson 1995, 2001), $\text{CeCu}_{6-x}\text{Au}_x$ (Schroder 2000), and $\text{Ce}(\text{Ru}_{1-x}\text{Fe}_x)_2\text{Ge}_2$ (Montfrooij 2002) are compared. In each case, robust magnetic moments are observed at all temperatures, whose excitations display an anomalous E/T scaling. For $\text{UCu}_{5-x}\text{Pd}_x$, the moments are entirely decoupled, leading to a susceptibility that is almost wave vector independent. A greater degree of spatial delocalization is found in $\text{Ce}(\text{Ru}_{1-x}\text{Fe}_x)_2\text{Ge}_2$, where the nature of the E/T scaling depends only weakly on wave vector. In contrast to these two systems, where the dynamics are highly local, $\text{CeCu}_{6-x}\text{Au}_x$ has a susceptibility in which E, T, and wave vector jointly control proximity to the critical point.

Mon. Afternoon, DC-Materials I

*Chair: Xun-Li Wang (Spallation Neutron Source)
Tennessee Ballroom C*

Mon. 3:45 p.m., Keynote, DC-01

Finite-Element Modeling of Crystal Deformations In Neutron Diffraction Experiments

Paul Richard Dawson, Donald Boyce (Cornell University), Stuart MacEwen (Alcan International, Ltd.), Ronald Rogge (National Research Council Canada)

Modeling the evolution of structure and properties in materials undergoing large deformations is an active research focus. Critical features of the material state are the crystallographic texture, strength, and residual stress. Coordinated diffraction experiments offer the means to guide and assess model development by providing direct measures of the material response at the level of the atomic lattice. This presentation will address neutron diffraction experiments performed for this purpose in which aluminum and stainless steel specimens were tested in situ and lattice strains were measured at different levels of load and for increasing levels of plastic strain. The experiments were simulated using polycrystal elastoplasticity in conjunction with a parallel finite-element formulation in which each element represents a separate crystal. We will outline the simulation methodology and then compare the measured and computed lattice strains for several combinations of scattering vector and diffraction plane. We also will examine the ability of the finite-element simulations to predict the changing peak intensities and peak widths in terms of the evolving texture and crystal strain hardening, respectively. We will conclude with a discussion of a number of issues associated with obtaining accurate predictions, including the sensitivity of the results to the knowledge of the elastic and plastic single-crystal behavior and to the coupling between the crystal and macroscopic length scales.

Mon. 4:15 p.m., Invited, DC-02

Stress Measurements in Bulk Metallic Glass Composites

Bjørn Clausen, Ersan Üstündag, Seung-Yub Lee (California Institute of Technology), Mark A. M. Bourke (Los Alamos National Laboratory)

The unique properties of bulk metallic glasses (BMG) place them among potentially significant engineering materials: very high strength (about 2 GPa) and initiation fracture toughness (40-50 MPam^{1/2}), a near theoretical specific strength, excellent wear and corrosion resistance, and high elastic strain limit (up to 2%). However, when loaded in an unconstrained fashion, the BMGs fracture catastrophically due to formation of macroscopic shear bands, which has limited the use of BMGs as a structural material. BMG matrix composites have been shown to increase the ductility over that of monolithic BMG. However, the matrix-reinforcement interactions have not been fully understood. One important issue in such composites is the presence of internal stresses due to the mismatch in coefficients of thermal expansion between the matrix and the reinforcements, as well as their elastic and plastic incompatibility under loading. In the present study, we have used neutron diffraction on the SMARTS instrument at Los Alamos Neutron Science Center to measure the thermal residual strains as well as internal strains during compressive loading in a series of BMG matrix composites with varying volume fraction of tungsten fibers. As the neutron diffraction measurements only yield information about the elastic deformation of the fibers, finite-element modeling was employed to predict the strains and stresses in both the fibers and the BMG matrix.

Mon. 4:30 p.m., Invited, DC-03

In Situ Intergranular Strain Accumulation in a Titanium Alloy Polycrystal

Kelly Timothy Conlon, David Dye (National Research Council of Canada), J. R. Cho (Cambridge University), Roger Reed (University of British Columbia), Mark Daymond (Rutherford Appleton Laboratories)

The elastic response of individual crystallites in a plastically flowing polycrystal is strongly influenced by intrinsic elastic and plastic anisotropy of the lattice. Anisotropy results in the accumulation of residual elastic microstrains during plastic flow, owing to local misorientations at grain boundaries, and are commonly termed “intergranular” strains in the literature. Lattice planes that accumulate significant intergranular strains cause considerable difficulties in the interpretation of macroscopic residual stress fields in components and must be avoided [1]. On the other hand, the prediction of the correct sign and magnitude of these strains, versus data gathered by in situ neutron diffraction methods, represents a powerful test of polycrystal plasticity models that incorporate both elastic anisotropy and inelastic strain relaxation mechanisms. In situ measurements of intergranular strain accumulation by neutron diffraction have been performed in a titanium alloy polycrystal (IMI-834) during tensile deformation at Chalk River Laboratories and at ISIS (ENGIN). An elasto-plastic self-consistent model, incorporating both elastic anisotropy and the slip and mechanisms commonly observed in pure titanium single crystals, successfully reproduces the sign and magnitude of intergranular strains in the deformed polycrystal in the tensile and poisson orientations. [1] ISO/TTA3 “Polycrystalline materials—Determinations of Residual Stresses by Neutron Diffraction,” ISO, Geneva, Switzerland, Sept. 2001.

Mon. 4:45 p.m., Invited, DC-04

Neutron Diffraction and SANS Study of Plasma-Sprayed Coatings

Thomas H. Gnäupel-Herold (National Institute of Standards and Technology and University of Maryland), Frank S. Biancaniello, John Barker (National Institute of Standards and Technology), Jiri Matejicek (Institute of Plasma Physics)

In this work we investigate the correlation between the microstructure of plasma-sprayed coatings on one side and the residual stress state, the adhesion to the substrate, and the elastic properties on the other side. Plasma-sprayed coatings differ as widely as the materials that can be deposited using the plasma spray technique. The common ground for almost all plasma-sprayed coatings is the defect density, which is considerably higher than for bulk materials. The most important groups of defects are pores, cracks, and localized regions of imperfect contact between deposit layers. It is found that, through their effect on the elastic modulus, the pore structure often has a far more pronounced impact on the coating stress than thermal strains that arise from quenching and from differences between thermal expansion coefficients. The residual stress state of the coating is correlated with the substrate adhesion, which is sensitive to the surface roughness of the substrate. By means of controlling the coating microstructure, it is possible to control the residual stress as well as, to some extent, the adhesion and the strain tolerance of plasma-sprayed coatings. As a means for controlling both the microstructure and the substrate bonding, we used feed stock powders with different particle sizes. Furthermore, different surface treatments of the substrate were used to investigate the influence of the surface roughness on residual stress and coating adhesion. The pore structure was characterized by means of small-angle neutron scattering. The residual stress measurements were performed using neutron diffraction, which proved to be superior to X-ray diffraction due to its depth scanning capability and the better volume averaging. The coating elastic properties were measured using neutron diffraction and mechanical testing. This was accompanied by a finite-element analysis of the stress distribution in the microstructure.

Mon. 5:00 p.m., Talk, DC-05

Neutron Diffraction Measurements During Loading In Shape Memory Alloys

Raj Vaidyanathan (University of Central Florida), David C. Dunand (Northwestern University), Mark A. M. Bourke (Los Alamos National Laboratory)

The stress-induced transformation of NiTi from an austenitic cubic phase to a martensitic monoclinic phase

can result in tensile strains as high as 8% under applied stress. On unloading, the martensitic phase becomes unstable and transforms back to the parent austenitic phase, with a concomitant macroscopic strain recovery that constitutes the superelastic effect. By recording neutron diffraction spectra during mechanical loading, such reversible stress-induced transformations can be investigated as they occur. We summarize and synthesize here a systematic study of superelastic NiTi subjected to monotonic and cyclic loading and NiTi–TiC subjected to monotonic, quasi-static loading, while neutron diffraction spectra are simultaneously acquired. The spectra were recorded while interrupting the cycle (but continuing to apply a constant load) during loading and unloading portions of the stress-strain curve. A Rietveld refinement methodology was established to obtain phase-specific quantitative strain, texture, and phase volume fraction information during the forward and reverse stress-induced martensitic transformation. The diffraction experiments allowed for a comparison between the microstructural texture, phase volume fraction, and strain changes during the stress-induced austenite to martensite transformation and the macroscopic stress-strain response. Associated with this superelastic behavior is the shape-memory effect wherein large strains are generated in the martensite phase (through deformation twinning) and then fully recovered by a temperature-induced transformation of martensite to austenite. Results from recent in situ neutron diffraction measurements during tensile and compressive loading of shape-memory martensitic NiTi will also be presented.

Mon. 5:15 p.m., Talk, DC-06

Measurement of Grain-Orientation-Dependent Stress Using a Pulsed Neutron Source

Yandong Wang, X.-L. Wang, A. D. Stoica (Oak Ridge National Laboratory), J. W. Richardson (Argonne National Laboratory)

The grain-orientation-dependent stress, or intergranular stress, has been a focus in the study of materials deformation behaviors. Grain-orientation-dependent stress is caused by stress or strain incompatibility between grains having different crystallographic orientations. Studies of the grain-orientation-dependent stress therefore give insights into some of the fundamental questions such as

how the grain-to-grain interactions occur in a polycrystalline material during and after deformation. The stress orientation distribution function (SODF), a new concept introduced by the authors recently, provides a statistical means to describe grain-orientation-dependent stress. A method was developed to construct the SODF from the lattice strains measured along various crystallographic and sample directions. Experiments on reactor neutron sources have proven the validity of the method. However, the measurement is slow, inhibiting comprehensive studies of the grain-orientation-dependent stress due to different deformation processes. Pulsed neutron sources, on the other hand, are more adapted for the determination of SODF since multiple reflections can be measured simultaneously with comparable precision. In this paper, the SODF determined with a pulsed neutron source is reported. The sample is cold-rolled, interstitial-free steel subjected to 78% reduction. The experimental results compared well with those measured with a reactor-based, constant-wavelength diffractometer. It is shown that on a pulsed neutron source, the increased measurement speed and the access to a large number of reflections (especially the low index ones) improve the precision of the experimental SODF and facilitate in situ studies of the evolution of grain-orientation-dependent stress during deformation and annealing.

Mon. Afternoon, DD–Neutron Optics

*Chair: Ian Anderson (Spallation Neutron Source)
Cumberland Room*

Mon. 3:45 p.m., Talk, DD-01

Design of the Incident Optics of the Spallation Neutron Source Liquids Reflectometer

John F. Ankner (Oak Ridge National Laboratory)

A liquids reflectometer presents distinct design challenges. Since the surface of the sample cannot be inclined, to measure a broad Q range one must either vary the inclination of the incident beam or include a broad range of wavelengths in it. Instruments at pulsed sources and chopper-based instruments at reactors intrinsically feature a range of wavelengths that are separable by time

of flight. Wavelength bandwidth for instruments at pulsed sources varies inversely with the source frequency. Generally, the source frequency is too high to allow one to measure the desired Q range at a single angle of incidence. Existing pulsed-source reflectometers either reject neutron pulses to increase bandwidth or employ a mirror to deflect the incident beam downward at a different angle. We propose an alternative concept that utilizes angular variation as well as a moderate wavelength bandwidth. The 60-Hz Spallation Neutron Source will provide a 3.75-Å wavelength bandwidth at our detector position. We will employ a tapered guide in the vertical direction as a nozzle to produce a continuous range of possible incident angles over 0 to 5°. Slits select the desired angle from that range. A multichannel bender eliminates moderator line of sight, reduces background, and features a short-wavelength cutoff of 1.75 Å. With this arrangement we will be able to measure liquid reflectivities out to $Q = 0.5 \text{ \AA}^{-1}$. We will describe the optical design and present its expected performance (both signal and background).

Mon. 4:00 p.m., Talk, DD-02

Solid-State Elements for Neutron Optics

Thomas Krist, F. Mezei (Hahn-Meitner Institut)

In the last years, solid-state neutron optical devices have been developed, especially polarizers and collimators. Such devices are smaller and lighter than their conventional counterparts and have very well defined channels. In this presentation, mainly results for radial elements are shown. A solid-state radial bender for the polarization analysis of neutrons over a wide angular range was built and tested at V6 and V14 at the Berlin Neutron Scattering Center. It consists of a bent stack of silicon wafers, each coated with a polarizing supermirror and an absorbing layer. The stack consisted of 19 channels, which were tilted against each other by 0.19 Grad, thus a total angular interval of 3.8 Grad could be analyzed. In another development, a radial collimator was built and tested at V14. Here a 75-mm-long collimator channel covered by a supermirror and an absorbing layer was opened at the downstream end by inserting a thin slab of a silicon wafer. It was measured that the angular range of the transmitted intensity could be doubled. Also, results for a collimator

with straight channels and a collimation angle of 7 minutes are shown.

Mon. 4:15 p.m., Talk, DD-03

Using Multiple Refractive Optics for Focusing and Gravity Cancellation on a SANS Instrument

Charles Joseph Glinka, S.-M. Choi (Korea Advanced Institute of Science and Technology), B. Hammouda, S. R. Kline, J. G. Barker (National Institute of Standards and Technology Center for Neutron Research)

Focusing a cold neutron beam with multiple biconcave lenses has been shown [1] to be a practical means of improving the resolution (i.e., reducing the low-Q limit) of conventional, long-flight-path, small-angle neutron scattering (SANS) instruments. The implementation and performance of lens systems now in routine use on two 30-m SANS instruments at the National Institute of Standards Technology's Center for Neutron Research will be described and compared with Monte Carlo calculations of expected performance. A recent development has been to add a stack of large-apex-angle prisms in series with the biconcave lenses to correct for the spreading of the focal spot in the vertical direction due to gravity. The combination of lenses and prisms enables SANS measurements to be made at Q-values as low as 0.005 nm^{-1} . [1] S.-M. Choi, J. G. Barker, C. J. Glinka, Y. T. Cheng, P. L. Gammel, *J. Appl. Cryst.* 33, 793-796 (2000).

Mon. 4:30 p.m., Talk, DD-04

Multiwafer Focusing Monochromators for Neutron Scattering

Mihai P. Popovici, (University of Missouri Research Reactor), Alexandru Stoica (Oak Ridge National Laboratory)

Neutron monochromators made of bent packets of silicon wafers have been developed at the University of Missouri Research Reactor. The initial aim was to use them in stress mapping by neutron diffraction, but theory has revealed an array of other possible applications. Computations and experimental checks have confirmed the

theory. The concept of imaging was developed. Neutron images from many wafers are put together so that a thick packet looks in scattering like a single thin wafer. Intense beams can be focused into spots of millimeter size. This is quite useful when small samples are used—a current tendency in neutron-scattering studies—and especially in combination with position-sensitive detection. Multiwafer packets were found to be useful in conventional Soller instruments too. In high-resolution neutron diffraction they offer good reflectivity and give additional flexibility, as focusing in diffraction may still transpire through Sollers. Imaging and nonimaging applications of bent packets of thin silicon wafers are reviewed. Results of test experiments for several applications are presented.

Mon. 4:45 p.m., Invited, DD-05

Doubly Focusing Neutron Monochromator for MACS

Collin Leslie Broholm (Johns Hopkins University), Stephen A. Smee, Dave K. Anand (University of Maryland), Paul C. Brand, Dwight D. Barry (National Institute of Standards and Technology Center for Neutron Research), Joseph D. Orndorff, Gregory Scharfstein, Yiming Qiu (Johns Hopkins University)

A doubly focusing neutron monochromator has been built for a new cold neutron spectrometer at the National Institute of Standards and Technology (NIST). It consists of 21 thin aluminum blades each holding 17 pyrolytic graphite (PG) platelets. The total reflecting area is 1428 cm². The blade thickness varies along the blades so that when they are compressed by a vertically moving bar, the attached PG platelets form the arc of a circle to focus the neutron beam in a vertical plane. Versatile focusing in the horizontal plane is enabled by stepping motor controlled rotation of the individual blades about vertical axes. The platelet positioning accuracy is 0.15 degrees, and the whole device is controlled by a rack of electronics that will respond to high-level commands from a serial communication port. The doubly focusing mono-

chromator has been built for a new high-intensity cold neutron spectrometer called MACS (Multi-Axis Crystal Spectrometer) that will be completed at the NIST Center for Neutron Research in the fall of 2006. By fully utilizing the large solid angle access to the NBSR cold source, MACS will have a neutron flux on the sample position in excess of 10⁸ n/cm²/s at an energy resolution of 0.2 meV. The MACS instrument also features a 21-channel analyzer system to enable ultrahigh-efficiency surveys of Q-dependent elastic and inelastic neutron scattering from condensed matter.

Work supported by the National Science Foundation through DMR-0116585.

Mon. 5:00 p.m., Keynote, DD-06

Free Lunch Theorem in Pulsed Source Instrument Optimization

Ferenc Mezei (Los Alamos National Laboratory and Hahn-Meitner Institute)

In current instrument design practice on pulsed sources, one of the often invoked guiding principles is to make the instrument as short as possible in order to maximize the flux on the sample. Two new developments, improved supermirror neutron optical beam delivery and beam extraction and repetition rate multiplication, make this paradigm counterproductive, with the exception of electron volt spectroscopy. Using one or both of these new techniques and increasing the source to sample distance (within certain limits, of course) enables us to improve the resolution without loss in neutron beam intensity on the sample or to increase the intensity without loss of resolution, or a combination of both. This is the “Free Lunch Theorem,” which only applies to pulsed sources and has no equivalent for steady-state sources. It is, of course, in no contradiction with the Liouville theorem. The main consequence of the theorem is that the optimal length of many pulsed source instruments will be found considerably longer than what is customary today.

Mon. Evening, EP—Instrumentation

Summit Grand Ballroom II

Mon. 8:00–9:30 p.m., Poster, EP-01

Design of a Dedicated High-Pressure Diffractometer for the Spallation Neutron Source

Chris A. Tulk (Oak Ridge National Laboratory)

Here we present the conceptual design and some performance details of the high-pressure diffractometer proposed for construction at the Spallation Neutron Source. This will include an overview of the general instrument layout; designs of several next-generation, large-volume, high-pressure cells; various neutron beam line components (such as choice of detectors and a novel neutron focusing scheme with its simulated performance); flux on sample requirements/estimates; and calculations of the instruments resolution performance.

Mon. 8:00–9:30 p.m., Poster, EP-02

MACS—A High-Intensity Cold Neutron Spectrometer for NIST

C. Broholm (John Hopkins University and NIST Center for Neutron Research), P. C. Brand, C. Brocker, J. W. Lynn (NIST Center for Neutron Research), R. Barkhouser, J. D. Orndorff, T. D. Pike, Y. Qiu, T. Reeves, and G. Scharfstein (Johns Hopkins University), S. A. Smee (Jefferson Laboratory)

A new high-intensity cold neutron spectrometer called MACS (Multi-Axis Crystal Spectrometer) is being built at the National Institute of Science and Technology (NIST) Center for Neutron Research. The instrument is funded jointly by NIST, the National Science Foundation (through DMR-0116585), and Johns Hopkins University and is scheduled to be completed in the fall of 2006. By fully utilizing the large solid angle access to the NBSR cold source, MACS will have a neutron flux on the sample position in excess of 10^8 n/cm²/s at an energy resolution of 0.2 meV. The detection system consists of 21 identical channels, each equipped with a double crystal analyzer

system. There are two detectors in each channel, one energy integrating and one spectroscopic detector. While the instrument will be a general purpose spectrometer for the energy range from 0 to 20 meV, it will be particularly efficient for surveys of Q-dependent elastic and inelastic scattering from condensed matter with static or dynamic short range order.

Mon. 8:00–9:30 p.m., Poster, EP-03

High-Resolution Fermi Chopper Spectrometer for the Spallation Neutron Source

Garrett Earl Granroth, Doug L. Abernathy, Stephen E. Nagler (Oak Ridge National Laboratory)

To enhance the suite of inelastic instruments to be built at the Spallation Neutron Source (SNS) in Oak Ridge, Tennessee, a high-resolution Fermi chopper spectrometer is under study. The proposed instrument will cover an incident energy range of 10 to 1000 meV, with a minimum energy resolution of 1%. Another aspect of this instrument is that it should provide a Q resolution over a low-angle range that complements the ARCS instrument (a wide-angle coverage direct geometry chopper spectrometer) currently under construction at SNS. This study discusses Q resolution considerations and provides an overview of the instrument concept.

Mon. 8:00–9:30 p.m., Poster, EP-04

New High Flux SANS Instrumentation and the Center for Structural and Molecular Biology at Oak Ridge National Laboratory

Gary W. Lynn, George Wignall, Paul Butler, Michelle Buchannan (Oak Ridge National Laboratory)

A number of projects are currently being undertaken at the High Flux Isotope Reactor (HFIR), including the installation of a supercritical hydrogen moderator (T ~20 K) on horizontal beam no. 4 (HB4) that will rival the “brightest” long-wavelength cold sources currently available. It will feed four neutron guides with new instrumentation, including a 35-m small-angle neutron scattering (SANS) facility, optimized for the study of biological systems as part of a Center for Structural and

Molecular Biology (CSMB), funded by the Office of Biological and Environmental Research. The CSMB will integrate existing Oak Ridge National Laboratory strengths in neutron sciences, mass spectrometry, and computational biology and make them available to a broad user community. In addition, there will be suite of instruments funded by the Office of Basic Energy Sciences, including a 40-m SANS instrument and reflectometer. The 40-m and 35-m SANS instruments will have variable wavelength and large area ($1 \text{ m} \times 1 \text{ m}$) high count-rate detectors that can translate 45 cm off axis to increase the dynamic Q-range (0.0008 to 1.0 \AA^{-1}). As the HFIR is one of only two high flux reactors worldwide, the beam intensities will be comparable to the best current facilities worldwide (e.g., at the Institut Laue-Langevin). This will enhance our ability to collect data from biological macromolecules more quickly and to study smaller sample quantities. The HB4 beam line and SANS instrumentation should be operational in late 2003 to early 2004.

Mon. 8:00–9:30 p.m., Poster, EP-05

Extended Q-Range Small Angle Diffractometer

Jinkui Zhao (Oak Ridge National Laboratory)

The extended Q-range small-angle scattering diffractometer is described. This instrument is one of the five funded instruments at the Spallation Neutron Source. It is designed to have wide Q coverage and high intensity. The primary flight path is designed at 14 m. A curved beam bender is used to avoid the direct line of sight from the moderator. Three bandwidth choppers are used to eliminate frame overlaps. The 1×1 -m area detector is located in an evacuated scattering tank.

Mon. 8:00–9:30 p.m., Poster, EP-06

High-Resolution NSE Spectrometer for Spallation Sources: A Feasibility Study

Michael Ohl, Michael Monkenbusch, Dieter Richter (Forschungszentrum Jülich), Catherine Pappas, Klaus Lieutenant, Ferenc Mezei (Hahn-Meitner Institut)

Neutron spin-echo (NSE) spectrometers reach the highest available energy resolution by encoding the

neutron velocity changes into changes of the neutrons spin precession angle. The spin echo condition does not depend on the wavelength, and it is possible—without affecting the high resolution—to operate the NSE spectrometers with a very broad wavelength (velocity) spread and therefore maximize neutron counting rates. The resulting signal is, however, not the spectral scattering function $S(Q, \omega)$ but its Fourier transformed function $S(Q, t)$, the intermediate scattering function. Given the utilization of a broad wavelength band at the existing spectrometers at reactor sources, the expected gain factors at spallation sources are smaller than, for example, time-of-flight spectrometers but will still be one order of magnitude. The special problems to be solved for a “next generation” NSE spectrometer for the Spallation Neutron Source (SNS) may be grouped as follows: (1) operation of the flippers (= localized spin rotations) for all incoming wavelengths; (2) software development for the extraction of $S(Q, t)$ from the raw counts; (3) design of neutron optics with appropriate polarizers and choppers (especially for highest wavelength); and (4) optimization of the magnetics to improve the resolution and/or the solid angle. While (1) and (2) are specific to the pulsed operation and (3) to the special properties of high-power spallation sources, (4) is a common problem of NSE spectrometers at continuous as well as pulsed sources. Point (4) is, however, the key for building beyond-state-of-the-art NSE instruments. We report on the progress of a feasibility study necessary to propose a design for an advanced high-resolution NSE spectrometer at the SNS, the first source to become operational from the next-generation spallation sources.

Mon. 8:00–9:30 p.m., Poster, EP-07

Building a High-Resolution Total Scattering Powder Diffractometer—Upgrade of NPD at LANSCE

Thomas E. Proffen (Los Alamos National Laboratory)

The Neutron Powder Diffractometer (NPD) at the Lujan Neutron Scattering Center at Los Alamos National Laboratory is the highest resolution neutron powder diffractometer in the United States. We are currently upgrading NPD by adding a large number of position-sensitive detectors in the backscattering position. This will optimize the instrument for total scattering measurements. The upgraded instruments will make it possible to collect

data from a powder sample over a wide range in Q , as well as with very good Q resolution. The total scattering includes Bragg as well as diffuse scattering and holds the key to determining the crystallographic average structure as well as the local structure, often responsible for the properties of complex materials.

Mon. 8:00–9:30 p.m., Poster, EP-08

A Flexible Representation for Time-of-Flight Neutron-Scattering Data

Dennis Mikkelson, R. Mikkelson (University of Wisconsin-Stout), T. Worlton, P. F. Peterson, A. Chatterjee, J. Hammonds, C.-K. Loong (Argonne National Laboratory)

The Integrated Spectral Analysis Workbench (ISAW) being developed at the Intense Pulsed Neutron Source at Argonne National Laboratory provides local and remote access to data, data visualization, reduction, and analysis for neutron-scattering instruments. ISAW is currently being extended to deal with data represented as a sequence of events and with model functions in a unified way. A Java class hierarchy has been defined for representing histograms, event data, tabulated functions, and model functions that allows the higher level ISAW tools to deal with data objects of any of these categories in the same way.

Mon. 8:00–9:30 p.m., Poster, EP-09

Data Collection Strategies and Data Evaluation Techniques for Next-Generation Neutron Spectrometers

Ferenc Mezei (Hahn-Meitner Institute and Los Alamos National Laboratory), Margarita Russina, Ron O. Nelson (Los Alamos National Laboratory)

State-of-the-art neutron-scattering spectroscopy on spallation sources implies data collection in histograms typically containing 50 million bins. In a typical spectrum, much fewer than 10 million events will be sorted into these bins, leaving most locations empty. A key development in progress at the Los Alamos Neutron Science Center, the prototype implementation of the method of

Repetition Rate Multiplication, will enhance the number of necessary bins to 500 million, while the number of events will stay in the 10-million range. Here we present the new strategy for data collection and evaluation using the event recording technique. The new approach will vastly reduce the primary raw data record size, give a complete history of the experiment, provide unprecedented fault tracking capability, and eliminate the need for a substantial part of the currently indispensable error interception hardware. Recording the time each chopper passes its top-dead-center position event recording technique will allow us to correct for the jitter with respect to the source firing and will solve a long-standing problem of the chopper instruments at pulsed sources. As this capability will be first developed and later maintained at the Lujan Center, the event recording will be developed as a user selectable alternative to conventional histogramming, and thus will be fully integrated into the data acquisition architecture. This proposed work nicely matches the recent data acquisition developments for new instruments.

Mon. 8:00–9:30 p.m., Poster, EP-10

Maximum Likelihood Method in Operation at the Scintillation Detector of the SANS Instrument at FRJ-2

Guenter Kemmerling (Forschungszentrum Jülich GmbH)

A completely new detector electronic is tested by taking the signals from the 15-year-old, two-dimensional scintillation detector, which is routinely operating for small-angle neutron scattering (SANS) studies at the research reactor FRJ-2. The detector consist of a 65- x 65-cm 6Li glass scintillator, a 7-cm-thick glass plate working as a light disperser, and 8 x 8 photomultipliers (PM) with 70-mm diameter and 83-mm spacing. The 64 preamplifier output signals are also fed into the new detector electronic so that scattering experiments and test measurements can be done simultaneously without any interference. The new detector electronic consists of 64 main amplifiers with free-running ADC and field programmable gate arrays for determining the pulse amplitudes of a captured neutron. This information is transferred to digital signal processors (DSPs) for further data evaluation. The most advanced method for determining the x and y coordinates of a captured neutron from the PM signals is the maximum

likelihood method. This method is based on the PM signal amplitude as a function of distance between neutron capture position and PM center. An iterative and adaptive method has been developed to determine this information during SANS measurement. For determining positions of captured neutrons, the box of 3 x 3 PMs with the largest signals is selected, the x and y coordinates are estimated by pulse height division with these four or nine signals, and then, iteratively, the most likely coordinates are determined. Very few iterations are needed. With one DSP the mean processing time is currently 30 μ s. SANS patterns are presented that are accumulated with various reconstruction methods, for example, center of gravity and maximum likelihood. The results show differences in linearity, homogeneity, usable detection area, spatial resolution, etc.

Mon. 8:00–9:30 p.m., Poster, EP-11

Development of a Flexible Data Acquisition System Upgrade for IPNS

John P. Hammonds, Alok Chatterjee, Rodney Porter, Peter Peterson, Thomas Worlton, Patrick De Lurgio, Istvan Naday, John Weizeoric (Argonne National Laboratory), Dennis Mikkelson, Ruth Mikkelson (University of Wisconsin–Stout)

The Intense Pulsed Neutron Source (IPNS) is in the process of updating its data acquisition system. A flexible set of hardware/software components has been developed or adopted. These components include time-of-flight modules that are configurable, pluggable, analog-to-digital conversion modules (also configurable); control software (EPICS) that is used at over 100 laboratories worldwide; and setup and analysis software that can be used with a variety of data types. These components are being installed on all instruments at IPNS, allowing ease of maintenance while allowing experiments flexibility.

Work performed at Argonne National Laboratory is supported by the U.S. Department of Energy Office of Basic Energy Sciences under contract W-31-109-ENG-38.

Mon. 8:00–9:30 p.m., Poster, EP-12

Modular, Pixel-Cell Neutron Detectors Meeting Requirements of Neutron-Scattering Facilities

Manfred K. Kopp, Daniel M. Kopp (ORDELA, Inc.)

Ongoing research has shown the feasibility of a new generation of position-sensitive neutron detector systems capable of meeting detector specifications for the U.S. Spallation Neutron Source (SNS) and similar installations now under construction or being upgraded. Such neutron detectors are needed to greatly enhance utilization of power and resolution capabilities at these neutron-scattering facilities. Advanced gas-proportional counter technology was applied to develop pixel cells having a millimeter-size active area, each having an independent output channel and count-rate capability >100,000 neutrons per second per pixel. Arrays of these pixel cells are enclosed in detector modules, which also contain the common counter gas and the front-end electronics. Standard 61-pixel-cell detector modules are configured to be plugged into support frames for assembly as multimodule, large-area detectors of customized size and shape. The honeycomb design of these standard modules allows detector assemblies having minimum dead spaces between pixel cells and no tiling artifacts between adjacent modules. Demonstration modules having pixel-cell areas of 1 and 5 mm² were successfully fabricated and tested. A special, ~1-m-long linear detector module having 36 pixel cells of ~2.5 x 2.5 cm² and a flat window was also designed. Its timing resolution for 1-meV neutrons is ~4 microseconds. Based on the successful test results reported in this paper, work is progressing to develop assembly facilities that enable mass production of standardized pixel-cell detector modules and to make these modules and detector systems available to scientists in neutron-scattering research.

Mon. 8:00–9:30 p.m., Poster, EP-13

Advances in Scintillation Neutron Detectors

Ralf Engels (Forschungszentrum Jülich GmbH)

Position-sensitive neutron scintillation detectors suffer from the poor reputation that is derived from the early gamma Anger cameras, that is, moderate spatial resolution, poor long-time stability, limited count rate capabilities, inhomogeneous detection efficiency, large background, and nonlinear detector response. The purpose of this presentation is to demonstrate that neutron scintillation detectors of today have almost nothing in common with Anger cameras and that enormous progress has been made because of a variety of means: (1) The detector has long-time stability because of automatic controls and adjustments of the photo multiplier (PM) gains. Formerly, the PM gain was measured with light pulses applied in separate calibration modes. In the new concept, one measures the PM gain with neutrons during the normal measurements. (2) Nonlinearities in the detector response disappeared almost completely because of pulse height division with not all photomultiplier lines and columns but by selecting the most significant three lines and columns closest to the captured neutron. (3) With a position-dependent pulse height discrimination, the rejection of pulses, which are likely being caused by high-energy gammas, improved the gamma insensitivity considerably, which means less background in scattering patterns, particularly where the neutron intensity is weak. More recently, it was demonstrated that both higher spatial resolution and better gamma discrimination were achieved with the new scintillator ${}^6\text{Li} {}_{160}\text{Gd B}_2\text{O}_3$ developed by Photogenics. (4) With free-running analog-to-digital converters, field programmable gate array data acquisition, and DSP data evaluation, the pulse processing becomes faster. A temporal component can easily be implemented as needed for time-of-flight experiments, rejection of pile-up effected pulses becomes possible (which further reduces the background level), and even more efficient gamma discrimination caused by pulse height and pulse shape can be investigated. Experimental and theoretical results are presented.

Mon. 8:00–9:30 p.m., Poster, EP-14

Remote Access and Display of Neutron Data

Thomas G. Worlton, P. F. Peterson, A. Chatterjee, J. Hammonds, C.-K. Loong (Argonne National Laboratory), D. Mikkelson, R. Mikkelson (University of Wisconsin-Stout)

With the proliferation of high-intensity neutron spallation sources and involvement of scientists from diverse areas, it is important to provide methods for remote access and display of data. We have developed Integrated Spectral Analysis Workbench software (ISAW) that can read, combine, operate on, and visualize large arrays of data from a variety of instruments. ISAW is written in a general, modular fashion that facilitates adaptation to different types of instruments and different analysis requirements. ISAW now supports reading NeXus and Intense Pulsed Neutron Source (IPNS) run files to be used with data from instruments at both the Los Alamos Neutron Science Center and IPNS.

Work performed at Argonne National Laboratory is supported by the U.S. Department of Energy Office of Basic Energy Sciences under contract W-31-109-ENG-38.

Mon. 8:00–9:30 p.m., Poster, EP-15

Personal Computer-Based Timing Reference Generator

Chris R. Rose, M. Stettler, P. D. Lara (Los Alamos National Laboratory)

This paper describes a timing-reference generator built on the personal computer platform. The device is used to phase-lock an accelerator-wide timing or reference signal to the phase and frequency of the AC-power grid. The timing-reference generator uses two PCI-compatible plug-in cards: one is a PCI DSP card from a commercial vendor that uses the TI 'C67 DSP, and the other is a PCI-interface card designed by Los Alamos National Laboratory. By using the PCI bus as a system platform, custom software has been written that allows the user to monitor the performance of the grid, the timing output pulse

stream, and various error signals in real time. Additionally, links can be made to other control systems, such as EPICs, via an Ethernet connection and software links.

Mon. 8:00–9:30 p.m., Poster, EP-16

The Lujan VME Phase Controller

Robert B. Merl, Ronald O. Nelson (Los Alamos National Laboratory)

The Lujan VME Phase Controller is a 6U VME board that synchronizes the position (phase) of rotating neutron choppers to the quasi-periodic production of neutrons at the Los Alamos Neutron Science Center (LANSCE). This VME board uses an embedded digital signal processor (DSP) to implement the active phase control system for choppers with large moments of inertia. Since the timing of the production of neutrons at LANSCE is tightly coupled to the instantaneous phase of the local commercial power grid, active control is required in order to keep the rotating choppers in phase with the grid. This system has the ability to maintain rotor phase control within 162 ns (σ) of the coupled power grid when used with optical feedback and within 329 ns when used with magnetic feedback. An EPICS driver has been written for the PHASE controller card, and an MEDM graphical user interface has been developed. Three of these systems are currently in use at LANSCE, and four more are in the process of being installed. The design and performance of the phase controller will be discussed.

Mon. 8:00–9:30 p.m., Poster, EP-17

Dynamic Theory of the Neutron Spin Pendellösung Resonance in the Spherical Wave Approximation

Eugene M. Iolin (Institute of Physical Energetics), Samuel A. Werner (National Institute of Standards and Technology)

Neutron Spin-Pendellösung Resonance, NSPR, is the resonance enhancement effect of the small neutron Spin Orbit (SO, Schwinger) interaction in the perfect, nonmagnetic crystal placed in the external magnetic field. NSPR was predicted by Horne, M. A., Finkelstein, K.D., Shull, C. G., Zeilinger, A., and Bernstein, H. J. (*Physica B*, 151,

189-192, 1988) and was observed by K. D. Finkelstein in Silicon [reflection (111), Laue geometry]. The experimental result was positive (without a doubt). However, Finkelstein underlined that the observed parameter of SO interaction was larger than predicted at 17%. Cadmium slits were used in the experiment in order to extract the central part of the Borrmann fan. The observed results were compared with the plane wave contribution to the central part of the Borrmann fan. We calculated NSPR in the Spherical Wave, SW, approximation and found that NSPR is stronger than predicted by the plane wave formulae. The difference between two calculations is explained as follows. Geometry of the neutron Dispersion Surface, DS, is changed by SO interaction in the condition of the NSPR (flat part of the DS and crossing between DS branches are created in this case). This effect is taken into account in the SP approximation but ignored in the used plane wave approximation. The whole picture of NSPR is more complicated than predicted before (maximum of the NSPR curve is displaced from the condition corresponding plane wave approach, intensity is different and so on). We calculated NSPR for the case when neutrons are spreading inside the silicon plate. Almost all neutrons will leave the plate due to the multiply reflections at the plate surface. Only the neutrons corresponded to the Darwin tableside will remain inside of the plate. This stayed neutron polarization is strongly perturbed by SO interaction in the condition of the NSPR.

Mon. Evening, EQ-Chemistry

Summit Grand Ballroom II

Mon. 8:00–9:30 p.m., Poster, EQ-01

Investigation of Catalytic Reaction Intermediates by Neutron Vibrational Spectroscopy

Sivadinarayana Chinta (Texas A&M University), T. V. Choudhary, J. Eckert, L. L. Daemen, D. W. Goodman (Los Alamos National Laboratory)

Neutron vibrational spectroscopy (NVS), which can be employed for investigating supported catalysts at industrially relevant pressure/temperature conditions, is highly

sensitive towards hydrogenous species, is not limited by selection rules, and allows accurate quantitative estimations. These attributes make NVS an ideal technique for characterizing surface hydrocarbonaceous species on supported catalysts. In this work, NVS is employed to investigate two technologically very important reactions: methane activation and propylene epoxidation. Methane conversion to higher hydrocarbons is an extremely challenging process and will therefore greatly benefit from an enhanced understanding of surface species formed on the catalyst. This NVS investigation provides the first experimental evidence for the formation of methylidyne (CH), vinylidene (CCH₂), and ethylidyne (CCH₃) species from methane on supported metal catalysts. The studies also reveal that the vinylidene species were more stable at higher reaction temperatures. Interestingly, similar species (to that observed on supported ruthenium catalysts) were also observed on supported nickel catalysts. Similarly, key intermediates like acroline, allylic species along with other products, were also observed during propylene oxidation over highly dispersed gold-based catalysts. This information is very important to understanding catalytic reaction mechanisms and for subsequent development of superior catalysts. Our work clearly shows the effectiveness of exploiting NVS for catalytic studies.

Mon. 8:00–9:30 p.m., Poster, EQ-02

Inelastic Neutron Scattering on Co-Crystals

Jennifer A. Ciezak, Bruce Hudson, Chris Middleton, Timothy Jenkins, Yanmei Lan, Hegui Hu, Gavin Jones, Nathan Hoteling (Syracuse University)

Systems that form co-crystals provide interesting cases for studies of the solid state vibrational patterns at both an empirical and ab initio level because they provide opportunity for the analysis of the individual components of the co-crystal. Many of these crystals tend to form planar hydrogen-bonding networks, thus simplifying simulations. Deuteration is often easily achieved in one component, which permits studies with selective amounts of deuteration. Two classes of co-crystal hydrogen-bonded structures have been chosen, and various representative compounds from each have been studied by inelastic neutron scattering. These are co-crystals of dicarboxylic acids with simple amides and co-crystals of dicarboxylic

acids with imidazole. Most of these systems have moderate to weak hydrogen bonds, yet they form unique one-dimensional and two-dimensional hydrogen-bonding arrays. In acetamide:oxalic acid complex, the acetamide forms a cyclic dimer and the oxalic acid acts as both a donor and acceptor to the acetamide dimer, forming hydrogen-bonding interactions with other oxalic acid units to form an infinite chain. Imidazolium Hydrogen Succinate forms unique hydrogen dicarboxylate chains in an anti-anti linkage. Imidazolium Hydrogen Adipate forms a structure with both imidazolium protons donated to the two carboxylate oxygens. This molecule also forms a similar structure in which an acetonitrile molecule is inserted between each imidazolium cation. Spectral data will be presented and compared to ab initio calculations to examine accuracy of theoretical methods. Ab-initio methods used include Hartree-Fock (HF) and Density Functional Theory. Experimental data were obtained from FANS at the National Institute of Standards and Technology Center for Neutron Research and TOSCA at ISIS Pulsed Neutron and Muon Source.

Mon. 8:00–9:30 p.m., Poster, EQ-03

Short, Strong, Low-Barrier Hydrogen Bonds

Timothy A. Jenkins, Bruce Hudson, Chris Middleton, Jenn Ciezak, Damian Allis, Yanmei Lan, Hegui Hu (Syracuse University), Dale Braden (Schrödinger Inc.)

Symmetric hydrogen bonds (e.g., O-H . . . O) have equivalent local minima for the H atom positions separated by a barrier at the position of equal O-H-O lengths. This barrier decreases in height as the O-O distances and apparently vanishes for sufficiently short distances. The short, strong hydrogen bonds that occur for small O-O distances are also known as “low barrier” hydrogen bonds. These systems were expected to display a failure of the harmonic dynamical treatment due to the anharmonic nature of the short, strong hydrogen bonds. We examined several co-crystals of varying O-O distances and both intermolecular and intramolecular hydrogen bonds by vibrational spectroscopy to provide a high-resolution basis calculation comparison. Selective deuteration of the molecule allowed the examination of specific vibrations related to hydrogen bonding. We will present our findings and examine the simulation of spectral

properties by ab initio and density functional methods. Vibrational spectrums were determined using FANS at the National Institute of Standards and Technology and TOSCA at ISIS, RAL.

Mon. 8:00–9:30 p.m., Poster, EQ-04

Neutron Scattering Study of 1,3-Cyclohexanedione and Its Benzene Complex

Yanmei Lan, Jenn Ciezak, Hegui Hu, Bruce Hudson, Tim Jenkins, Chris Middleton (Syracuse University)

1,3-Cyclohexanedione (CHD) exists in its crystal structures in the enol form in linear hydrogen-bonded arrays, which provides interesting aspects for hydrogen-bonding research. We have obtained the inelastic neutron scattering (INS) spectrum of CHD and compared it with a DFT/B3LYP/6-31G** calculation with constraints imposed. The degree of agreement is sufficiently good. Besides forming a one-dimensional chain, CHD forms an interesting “clathrate”-type structure with benzene. We will show the INS spectrum and its simulation calculation. Meanwhile, we prepared CHD species with additional sites of deuteration, changed back the H-bonded site for hydrogen, and took INS spectrum and compared it with the calculated data. The procedure used for deuterium substitution will be discussed.

Mon. 8:00–9:30 p.m., Poster, EQ-05

Inelastic Neutron Scattering Studies of Hydrocarbons

Chris Middleton, Damian G. Allis, Jenn Ciezak, Hegui Hu, Bruce Hudson, Tim Jenkins, Yanmei Lan (Syracuse University), Taner Yildirim (National Institute of Science and Technology)

Results of inelastic neutron-scattering (INS) spectroscopy studies of the vibrational dynamics of solid-state hydrocarbons will be presented. Comparisons with ab initio calculations will be used to examine the applicability of theoretical methods and the approximations used therein. The combination of INS studies and ab initio studies provide unique insight into both molecular properties and the crystalline environment. Compounds studied include

dodecahedrane, pagodane, and [2.2]paracyclophane. Ab initio methods used include Hartree-Fock (HF), Density Function Theory (DFT), and Møller-Plesset perturbation theory of order 2 for electron correlation (MP2). Periodic DFT methods may also be discussed. Experimental data were obtained from the FANS spectrometer at the National Institute of Standards and Technology (NIST) Center for Neutron Research and from the TOCSA spectrometer at the ISIS Pulsed Neutron & Muon Source. Dodecahedrane is a highly symmetric molecular cage compound. Because the isolate molecule has icosahedral-h symmetry, very few vibrational transitions are allowed under infrared and Raman selection rules. With INS studies, there are no selection rules and all transitions in the range of study are seen. Ab initio methods are highly successful at predicting the INS spectrum of dodecahedrane and give evidence of a lower symmetry in the crystal site. Pagodane is an isomer of dodecahedrane, which is also a highly symmetric cage compound. Most interesting is the failure of ab initio methods to adequately describe the INS properties of this relatively simple hydrocarbon, which lacks intermolecular interactions. [2.2]Paracyclophane is a highly strained hydrocarbon with two bent benzene rings connected by sterically strained ethano bridges in the para positions. While the crystal structure was resolved with the ethano hydrogens in an eclipsed position, ab initio studies in the literature have begun to suggest a staggered geometry to be the global minimum. INS, infrared, far-infrared, and Raman data, as well as calculations, will all be combined to resolve this question.

Mon. 8:00–9:30 p.m., Poster, EQ-06

INS Study of Solid Methanol and DFT Modeling of Differently Deuterated Molecular Clusters

Ireneusz Natkaniec (Frank Laboratory of Neutron Physics and H. Niewodniczanski Institute of Nuclear Physics), K. Holderna-Natkaniec (Mickiewicz University), I. Majerz (University of Wroclaw)

Methanol, CH₃OH, is an interesting example of a simple hydrogen-bonded substance. It is known to exist in at least three solid modifications: the ordered phase stable below 160 K, the disordered phase stable between 160 K and melting at 175 K, and the amorphous phase transforming into the ordered phase at about 130 K. We have

studied four isotope modifications of methanol: CH₃OH, CH₃OD, CD₃OH, and CD₃OD using the NERA time-of-flight inverted geometry spectrometer at the IBR-2 high flux pulsed reactor in Dubna. Glass samples were prepared by fast quenching of liquid samples in a liquid nitrogen bath. The measurements were performed over the temperature range from 20 to 180 K for a wide range of momentum and energy transfers. This allowed us to investigate vibrational spectra up to 2000 cm⁻¹ for all solid phases of methanol whose structures were simultaneously controlled by the NPD method. The different isotope modifications of methanol molecules allow us to study the contribution of methyl group rotations and hydrogen bond dynamics to lattice dynamics. A wide energy transfer range allows displaying of the effects of disorder over the whole frequency range of lattice dynamics (up to 350 cm⁻¹), as well as its effect on hydrogen vibrations perpendicular to hydrogen bonds in the frequency range 700 to 950 cm⁻¹. At low frequencies, the vibrational density of states (VDOS) of glassy methanol clearly show an enhancement in comparison with the reference VDOS of the ordered phase. The origin and the microscopic mechanism of low-frequency excitations in molecular glass formers have not yet been satisfactorily explained. We have compared the experimental VDOS with the vibrational spectra calculated for small methanol clusters by the DFT quantum chemistry method. The frequencies of the experimental bands and the H-D isotope effects observed in the VDOS spectra are well reproduced by clusters of 4 to 8 molecules kept together with hydrogen bonds.

Mon. 8:00–9:30 p.m., Poster, EQ-07

Intermediate Density Amorphous Ices

Jacob Urquidi, C. J. Benmore, J. Neuefeind (Argonne National Laboratory), C. A. Tulk (Oak Ridge National Laboratory), D. D. Klug (National Research Council of Canada), B. Tomberli, P. A. Egelstaff (University of Guelph)

Ice is known to have at least two reproducible amorphous phases produced by compression of crystalline ice Ih: high-density amorphous (HDA) ice and low-density amorphous (LDA) ice. Here we report the discovery of several intermediate amorphous ice phases obtained by

annealing HDA ice at different temperatures for several hours. Structural measurements were performed using pulsed neutron and high-energy X-ray diffraction techniques. Five amorphous phases were characterized by the position of the first peak in the static structure factor, $S(Q)$, at temperatures between 40 and 115 K. The new structures could not be reproduced by any combination of the known HDA and LDA ice phases. The results suggest that a continuum of metastable ices exist between the widely accepted HDA and LDA states.

Mon. 8:00–9:30 p.m., Poster, EQ-08

Formation and Gas Exchange in Methane Hydrate

Arthur J. Schultz, Xiaoping Wang (Argonne National Laboratory)

The kinetics, phase transformations, and structures of gas hydrates have been studied in situ using time-of-flight powder diffraction at the Intense Pulsed Neutron Source. These have included the formation of sI (CO₂, methane) and sII (argon) hydrates from D₂O ice. In addition, we have observed the transformation of sII argon hydrate to a mixed gas argon/CO₂ sI hydrate by immersing the argon hydrate in liquid CO₂. For methane, the conversion of ice particles to methane hydrate follows Arrhenius behavior, from which an activation energy for the diffusion-controlled of 14.7(5) kcal/mole was derived. Complete transformation of ice to methane hydrate was achieved through temperature ramping, which is a nonisothermal procedure that involves slowly increasing the sample temperature through the ice melting point. Temperature ramping is shown to be a reliable method for the synthesis of methane hydrate that can be used for other studies. We also have obtained direct structural evidence from time-of-flight neutron diffraction data that methane is partially replaced by CO₂ when methane hydrate is immersed in liquid CO₂. Furthermore, our data clearly show that only methane molecules in the large 14-hedra cavities exchange, whereas the methane in the smaller 12-hedra cavities remain unaffected.

This work was supported by the U.S. Department of Energy, Basic Energy Sciences—Materials Sciences, under contract W-31-109-ENG-38.

Mon. 8:00–9:30 p.m., Poster, EQ-09

Inelastic Neutron Scattering from NH₃ Rotors in Hofmann Clathrates

Peter W. Vorderwisch (Hahn-Meitner Institut)

Hofmann clathrates Ni(NH₃)₂ Ni(CN)₄, 2G with guest molecules G=C₆D₆, C₆H₆ (benzene), and C₁₂H₁₀ (biphenyl) are among the rare examples where nearly free uniaxial quantum NH₃ rotations have been observed by inelastic neutron scattering. We have performed an extensive study on the biphenyl clathrate using neutron time-of-flight and triple-axis spectroscopy to investigate the temperature dependence of both the line positions and line widths for transitions between rotational levels. Observed line shifts are in agreement with expectations from a known model based on rotation-translation coupling. Observed line widths are explained by a new model based on phonon-rotor coupling. Intensities of rotational transition lines as a function of momentum transfer and temperature agree with calculations for a free NH₃ rotor.

Mon. 8:00–9:30 p.m., Poster, EQ-10

Measuring D₂O Nucleation Rates in Supersonic Nozzles

Barbara E. Wyslouzil, Kiral A. Streletzky, Christopher H. Heath, Amjad Khan, Yury Zvinevich (Worcester Polytechnic Institute), Judith Wölk, Kristina Iland, Reinhard Strey (Universität zu Köln)

Nanodroplet aerosols form in supersonic expansions of a condensable vapor. The process is usually studied by measuring the pressure trace along the length of the nozzle to determine the onset of condensation. Alternatively, onset is found by locating the point in the nozzle where light is first scattered by the rapidly growing droplets. These conventional techniques do not, however, directly determine the nucleation rate in the nozzle because it is not possible to determine the number density of the aerosol without a strong assumption regarding the shape and width of the droplet size distribution. In our work, we use small-angle neutron scattering experiments to determine the number density of the aerosol, assuming that the droplets follow a log-normal size distribution. We use pressure measurements to determine the characteris-

tic time associated with the peak nucleation rate and the corresponding supersaturation and temperature. From the number density and characteristic time we can directly estimate the peak nucleation rate. We will summarize our D₂O nucleation rate measurements made using both conventional and specially shaped nozzles designed to decouple nucleation from droplet growth. In the latter case, the nucleation rates are lower and the droplets are both larger and more monodisperse.

Mon. Evening, ER-Materials

Summit Grand Ballroom II

Mon. 8:00–9:30 p.m., Poster, ER-01

Neutron Scattering of Nanofoams

Bryan Spraul, D. W. Smith, R. Traiphol, X. Jiao, D. Perahia (Clemson University)

Small-angle neutron scattering (SANS) has been used to study the pore shape and dimensions in new porous silicates. Nanofoams or controlled-pore media are a uniquely important class of materials. They consist of either organic or inorganic relatively rigid networks with large vacancies. The voids may assume different shapes from isolated cavities to interconnected channels. The shape, dimensions, and size distribution of the vacancies determine the properties of these materials. The control over pore size and shape is central in the wide spread of applications of nanofoams, from separation processes to making low dielectric materials. Forming different organic-inorganic hybrid composite materials as means to form porous media controlling pore distribution in silica by organic templating is a widely used technique. In this process, organic templates are dispersed via sol-gel methods followed by removal of the template by thermal and/or chemical steps to obtain precise pore sizes. However, current processes typically generate a wide distribution of pore sizes. Recently we used condensation of tetrahydroxy terminated tetrayne monomers with sol-gel precursors to form a homogeneous distribution of reactive monomer nano-domains capable of thermal polymerization, pyrolysis to glassy carbon, followed by oxidative elimination. Tunneling electron microscopy has

shown the formation of relatively monodispersed 20-30 nm holes that are equally distributed at the surface of the glass. SANS measurements have shown that this glass consists of relatively monodispersed spherical pores. Some are isolated and some are interconnected. Further studies are currently on the way to explore the factors that affect the size, shape, and distribution of the pores in this nanofoam and correlate them with the properties of the material.

Mon. 8:00–9:30 p.m., Poster, ER-02

Thermal Expansion of Structure I and Structure II Clathrate Hydrates Determined by In Situ Neutron Scattering

Claudia J. Rawn, Bryan C. Chakoumakos, Adam J. Rondinone (Oak Ridge National Laboratory), Laura A. Stern, Susan Circone, Stephen H. Kirby (U.S. Geological Survey), Yoshinobu Ishii (Japan Atomic Energy Research Institute), Camille Y. Jones, Brian H. Toby (National Institute of Standards and Technology)

Clathrate hydrates or “guest-host” inclusion compounds consist of a “host” lattice formed from an ice-like hydrogen-bonded network of water molecules with polyhedral cavities large enough to accommodate a variety of “guest” molecules. Most clathrate hydrates crystallize in one of two cubic structures. The unit cell of structure I contains 46 water molecules comprising 2 pentagonal dodecahedra, polyhedra with 12 pentagonal faces, and 6 tetrakaidecahedra, polyhedra with 12 pentagonal faces and 2 hexagonal faces. The unit cell of the structure II contains 136 water molecules forming 16 pentagonal dodecahedra and 8 tetrakaidecahedra. Structure I has a lattice parameter of approximately 12 Å; structure II has a lattice parameter of approximately 17 Å. The lattice parameter depends on the kind of guest molecule, the hydration number, or the amount of gas filling the polyhedra, as well as the structure type. We have collected neutron powder diffraction data as a function of temperature (between 5 and 265 K depending on the guest molecule) for hydrates containing carbon dioxide, tetrahydrofuran, trimethylene oxide (which can form structure I or II depending on the composition), propane, methane, and mixed methane-ethane as the guest molecules. For each case the host lattice was deuterated. From the

lattice parameter data as a function of temperature, we have calculated the thermal expansion, $\Delta L/L_0$ and fit a third-order polynomial to the results. The instantaneous coefficient of thermal expansion (CTE) for each of the clathrate hydrates studied has been calculated by differentiating the resulting third-order polynomial equations with respect to temperature. Our results indicate that structure I has a greater thermal expansion than structure II and that both are greater than values for D₂O ice found in the literature.

Research sponsored by the Laboratory Directed Research and Development Program of Oak Ridge National Laboratory (ORNL). ORNL is managed by UT-Battelle, LLC, for the U.S. Department of Energy under contract DE-AC05-00OR22725.

Mon. 8:00–9:30 p.m., Poster, ER-03

Neutron Diffraction for Liquids Under Extreme Conditions

Richard Weber, Jean Tangeman (Containerless Research, Inc.), Christopher Benmore, Joan Siewenie (Argonne National Laboratory)

Containerless techniques and neutron diffraction were combined to study the structure of molten oxides at temperatures up to ~2000 K. Experiments were performed at the Glass Liquids and Amorphous Diffractometer (GLAD) at the Intense Pulsed Neutron Source (IPNS) at Argonne National Laboratory using an aerodynamic levitator with a pure vanadium nozzle and a 30-W CO₂ heating laser integrated with the beam line. Samples of 3.5-mm-diameter 64:36 mol % CaO:Al₂O₃ (eutectic) were levitated in pure argon and melted with the laser beam. Progress of the experiments was followed with a video camera and an optical pyrometer focused on the sample. Scattered neutrons were detected with a bank of ³He detectors. This poster presents results of the study and discusses designs for an advanced instrument to investigate the structures of liquids under extreme conditions.

Work supported by the U.S. Department of Energy under contracts DE-FG02-01ER86121 (CRI) and W-31-109-ENG-38 (IPNS).

Mon. 8:00–9:30 p.m., Poster, ER-04**Residual Stress Measurement in a Co-based Haynes-25 Cylinder**

Cecilia Larsson (Linköping University), T. M. Holden, M. A. M. Bourke, M. Stout (Los Alamos National Laboratory)

A tubular container for a satellite application was fabricated from a Co-based Haynes-25 alloy by welding two hemispherical end caps to either end of a cylinder. The wall thickness was approximately 3 mm, and the tube length was 74 mm. Concerns relating to precipitation aging following long-term exposure to heat in the application lead us to assess the fabrication induced residual stress profile. Spatially resolved measurements were made using the Spectrometer for Materials Research at Temperature and Stress (SMARTS) at Los Alamos National Laboratory. Axial, hoop, and radial strain measurements were performed in and within approximately 30 mm of the weld. Strains were determined by fitting single peaks in the spectra as well as by using entire spectra in Rietveld refinements. Subject to assumptions concerning the principal stress directions, residual stresses were computed and conclusions drawn on their possible ramifications. This work also demonstrates the capabilities of the newly commissioned third-generation neutron diffractometer, SMARTS.

Mon. 8:00–9:30 p.m., Poster, ER-05**Anisotropic Thermal Expansion Behavior of a Ti-6Al-4V/SiC Composite**

Hahn Choo (University of Tennessee), Partha Rangaswamy, Mark A. M. Bourke (Los Alamos National Laboratory)

We studied thermal expansion anisotropy in a Ti-6Al-4V alloy reinforced with 35 vol % SiC continuous fibers. The lattice expansion of the matrix and fibers within the composite was monitored from axial (parallel to the unidirectionally aligned fibers) and transverse (perpendicular to the fibers) directions during heating from room temperature to 1170 K using in situ high-temperature neutron diffraction. The results show that, in the axial direction, the matrix and the fiber in the composite co-

expand up to about 800 to 900 K. Above 900 K, the matrix and fiber strains diverge and approach the expansion behavior of their respective monolithics. In the transverse direction, the phase-specific expansion is quite different as both phases in the composite expand independently over the whole temperature range with behavior almost identical to their monolithic expansion. The anisotropic thermal expansion behavior of the constituent phases in the composite will be discussed in terms of the thermal residual stress and its inelastic relaxation at elevated temperatures. The neutron diffraction result, coupled with a finite-element analysis, will provide insights to the micromechanics of the thermal expansion behavior of a continuous fiber-reinforced composite.

Mon. 8:00–9:30 p.m., Poster, ER-06**Structural Characterization of Near Frictionless Carbon (NFC) Films for Tribological Applications**

Jacqueline Anne Johnson, John Woodford (Argonne National Laboratory)

Carbon-based coatings exhibit many attractive properties that make them good candidates for a wide range of engineering applications. Several coatings have been deposited on silicon wafers in a plasma-enhanced chemical vapor deposition (CVD) system that uses high proportions of gaseous hydrogen in addition to hydrocarbon source gases such as methane and acetylene. Tribological studies of the films revealed a close correlation between the chemistry of the hydrocarbon source gases and the friction and wear coefficients of the diamond-like carbon (DLC) films. Those films grown in source gases with higher hydrogen-to-carbon ratios had much lower friction and wear coefficients than did films derived from source gases with lower hydrogen-to-carbon ratios. Neutron reflectivity was used to characterize these films, giving the scattering length density and information on the quantity, position, and uniformity of the hydrogen contained in them. Experiments were performed on a series of films deposited with 0, 50, and 75% hydrogen in the source gas. For comparison, the experiments were repeated with deuterated films. Deuterium is not in the films in the same proportion as the hydrogen because differences in pumping dynamics between hydrogen and deuterium bring about differences in plasma composition for the same nominal gas flow rates. However, because

the contrast in scattering length between carbon and deuterium is very small, these experiments revealed the carbon density changes as a function of deuterium content.

Mon. 8:00–9:30 p.m., Poster, ER-07

Neutron Irradiation of Boron-10 Isotope-Doped Diamond

Jag Kasichainula K. Verghese, A. Smirnov (North Carolina State University), M. J. Lance, T. E. Haynes (Oak Ridge National Laboratory), J. Butler (Naval Research Laboratory)

Diamond films prepared by chemical vapor deposition and doped with boron-10 isotope to a concentration of $1.0 \times 10^{19} \text{ cm}^{-3}$ have been irradiated under a thermal neutron flux of $5.0 \times 10^{13} \text{ cm}^{-2}/\text{s}$. Continuous cooling of diamond samples was provided during irradiation. Transmutation of boron-10 to the lithium-7 isotope after 100, 200, and 400 hours of irradiation is followed by characterization using secondary ion mass spectrometry. Formation of different types of defects in the diamond films because of neutron irradiation is investigated by Raman, photoluminescence, and electron paramagnetic resonance spectroscopy. The advantage of continuous cooling in preventing amorphization or graphitization of diamond by the high energy released during the transmutation reaction is studied in these experiments. The significance of these results to achieve n-type doped diamond films for applications in radiation-resistant detectors and electronic devices will be presented.

Mon. 8:00–9:30 p.m., Poster, ER-08

Neutron Diffraction Study of Phase Evolution of Ball-Milled Fe-Zn Alloys

Oswald N. C. Uwakweh, Zhentong Liu (University of Puerto Rico), Aszetta Jordan (Raytheon), Bryan Chakoumakos, Steve Spooner, Philip Maziasz (Oak Ridge National Laboratory)

High-energy ball milling with subsequent annealing is used to synthesize Fe-Zn alloys from elemental powders. The thermodynamic state of the milled materials and their

structural evolution are characterized. Neutron diffraction, electron microscopy, and differential scanning calorimetry (DSC) measurements are used to monitor the phase evolution. The case of (zeta-phase) ζ -FeZn₁₃ intermetallic with three characteristic stages corresponding to activation energies of 128, 202, and 737 kJ/mole, respectively, with increasing temperatures are determined and will be presented. These stages are related to limited atomic diffusion/rearrangements, recovery/recrystallization long-range diffusion leading to stable phase formation, and structural decomposition due to phase transition. Structural determination confirming C₂/m with lattice parameters of $a = 13.40995 \text{ \AA}$, $b = 7.60586 \text{ \AA}$, $c = 5.07629 \text{ \AA}$, and $\beta = 127^\circ 18'$ based on neutron diffraction studies will be presented.

Mon. 8:00–9:30 p.m., Poster, ER-09

Review of Some New Investigations on Different Oxide-Based Advanced Materials

Udayan De (VEC Centre)

Our application of various modern techniques to a wide range of materials has led to interesting and new observations. Positron lifetime spectroscopy (PLS) and doppler broadening of positron annihilation radiation lineshape (DBPARL) experiments probe electron density and electron momentum distribution, respectively, in the region of the electron-positron annihilation sites within the samples. These two electronic properties greatly govern electrical conductivity, s , perhaps the most well studied bulk property. Intriguing variations observed in s with defect concentration for originally insulating, mullites (${}^3\text{Al}_2\text{O}_3$, ${}^2\text{SiO}_2$ type), II-VI compounds, and Polyethylene oxide or PEO will be reported along with the matching signatures observed in PLS and DBPARL investigations. Electrical conductivity of the mullites increased up to 90 times due to addition (a kind of “defect”) of a transition metal, TM, (done for five TMs) with a peak at about 1 wt % addition. Positron lifetime and S-parameter data for up to 2 wt % TM “doping” will be shown to support this peaking of s . Neutron diffraction can pinpoint the sites of added TM and help explain the results. We also observed minima at $\sim T_c$ and $\sim 0.95 T_c$ (for Y-123 crystals and (Bi,Pb)-2223 pellets) and a minimum at $\sim T_c$ (for Bi-2212 pellets) in S vs T graphs where S-parameter, determined from the “shape” of Doppler Broadened

annihilation gamma-line, gives the fraction of “low” momentum electrons at the annihilating sites. These minima in the fraction of low-momentum electrons, on cooling or heating across the superconducting transition region, have not been observed for the metallic conventional superconductors. This makes it more interesting. Pair distribution function derived from neutron diffraction for Tl-2212 and other HTSC showed a complex but similar maximum at T_c . Since an anomalous lattice distortion across T_c has the potential to explain the minimum we observe for S, neutron diffraction and S-parameter measurements across T_c on the same set of HTSC-samples are proposed. We are concentrating on developing newer or more effective catalysts based on micro- and meso-porous zeolites or similar compounds with various TM substitutions. The scope of neutron diffraction in understanding some of these materials will be discussed.

Mon. 8:00–9:30 p.m., Poster, ER-10

In Situ Neutron Diffraction Study of High-Temperature Intermetallic Composites

Xun-Li Wang, Y. D. Wang, J. H. Schneibel (Oak Ridge National Laboratory), J. W. Richardson (Argonne National Laboratory)

Cast Mo-Mo₃Si intermetallic composites crack after annealing at high temperature. This phenomenon is difficult to understand from the point of view of thermal residual stress that develops during cooling, as the thermal expansion mismatch between the two phases is very small. Indeed, analysis of the crack morphology suggests that the cracks are initiated at high temperature. In situ neutron diffraction experiments revealed subtle phase changes during annealing. At $T > 1200^\circ\text{C}$, silicon atoms diffuse from the silicon-enriched molybdenum phase to the silicon-depleted Mo₃Si phase. In addition, a small fraction of the silicon-containing molybdenum transforms into Mo₃Si. These experimental results provided new insights into the processing of Mo-Mo₃Si intermetallic composites.

Research sponsored by the Division of Materials Sciences and Engineering, Office of Basic Energy Sciences, U.S. Department of Energy, under contract DE-AC05-00OR22725 with UT-Battelle, LLC.

Mon. 8:00–9:30 p.m., Poster, ER-11

Residual Strain Distribution in a Bent Composite Boiler Tube

Edward Andrew Payzant, C. R. Hubbard, S. Spooner, T. M. Ely (Oak Ridge National Laboratory), T. M. Holden, S. C. Vogel (Los Alamos National Laboratory)

Kraft recovery boilers are an essential component of modern pulp and paper mills. These boilers are constructed of carbon steel tubes, with an extremely chemically aggressive environment on the fire side. Cladding with a more corrosion-resistant material such as stainless steel generally protects the carbon-steel core of the tube. The resulting composite tubes are subsequently welded together to manufacture the boiler. Stress corrosion cracking of the boiler tubes is a serious concern and has prompted a series of investigations into the residual stress distribution in such structures. One location where cracking has been observed after service is in tubes bent to create an opening for insertion of a port to allow air to enter the boiler. For this reason, the residual stresses caused by the superposition of coextrusion and forming processes in a bent composite (304L on SA210) tube were examined using X-ray and neutron strain mapping. Since the mechanical properties of the two alloys are quite different, this is potentially a much more complex problem than that of a simple bent tube. X-ray stress mapping was carried out on the 304L cladding material. Neutron diffraction strain mapping was undertaken using the SMARTS beam line at the Los Alamos Neutron Science Center. Axial and radial strain components were determined at selected locations in both the carbon steel core and stainless steel cladding. It was found that, at the locations examined, the core and cladding layers had opposite strains (i.e., tension versus compression) of significant magnitude and that these strains changed sign going through the bend. These preliminary results may have implications for resistance to stress corrosion cracking.

Research sponsored by the U.S. Department of Energy, Assistant Secretary for Energy Efficiency and Renewable Energy, Office of Industrial Technologies, Advanced Industrial Materials Program, Oak Ridge National Laboratory, managed by UT-Battelle, LLC, for the U.S. Department of Energy under contract DE-AC05-00OR22725. This work has benefited from the use of the

Los Alamos Neutron Science Center at Los Alamos National Laboratory; this facility is funded by the U.S. Department of Energy under contract W-7405-ENG-36.

Mon. Evening, ES–Soft Condensed Matter

Summit Grand Ballroom II

Mon. 8:00–9:30 p.m., Poster, ES-01

Study of the Dicephalic Sugar Surfactant C12-DLA (N-alkyl-N, N'-bis [(3-lactabionylamido)propyl]amine with the SANS Method

Aldona Rajewska (Institute of Atomic Energy and Joint Institute for Nuclear Research), K. A. Wilk, L. Syper (Wroclaw University of Technology), A. H. Islamov, A. I. Kuklin (Joint Institute for Nuclear Research)

The new nonionic dicephalic surfactant N-alkyl-N, N'-bis [(lactabionylamido)propyl]amine was investigated by the small-angle neutron scattering (SANS) method. The water solutions (in D₂O) of this rare nonionic surfactant (C12-DLA) were investigated for temperatures 20, 40, and 60°C and for eight concentrations: $c = 4.08 \times 10^{-3} \text{ mol/dm}^3$, $1.64 \times 10^{-2} \text{ mol/dm}^3$, $3.87 \times 10^{-2} \text{ mol/dm}^3$, $6.32 \times 10^{-2} \text{ mol/dm}^3$, $8.59 \times 10^{-2} \text{ mol/dm}^3$, $2.38 \times 10^{-1} \text{ mol/dm}^3$, $3.09 \times 10^{-1} \text{ mol/dm}^3$, and $4.76 \times 10^{-1} \text{ mol/dm}^3$, with the time-of-flight (TOF) SANS spectrometer (“YuMO”) of the IBR-2 on the pulsed neutron source at FLNP, JINR in Dubna, Russia. Measurements have covered Q ranges from 0.01 to 0.15 Å⁻¹. It was observed that when the concentration of the solution increased, the intensity of the neutron scattering increased too. For the temperature of 40°C, intensity quickly increased compared with the intensity for 20°C; but for the temperature 60°C, the intensity increased very slowly in comparison with 40°C. In the presence of the nonorganic salt NaCl, the sample $1.63 \times 10^{-2} \text{ mol/dm}^3$ was investigated for the few concentrations of the salt at 20°C. The intensity of the scattering neutrons increased for the first two concentrations (0.0412 mol/dm³ and 0.1800 mol/dm³) of the salt and became constant for the 0.4116 mol/dm³ and 1.0334 mol/

dm³ concentrations. The shape and size of micelles was obtained from our experimental results, too.

Mon. 8:00–9:30 p.m., Poster, ES-02

Supramolecular Structure of Gemini Surfactants with Flexible and Rigid Spacers

Vinod Kumar Aswal (Paul Scherrer Institut), P. S. Goyal (Bhabha Atomic Research Centre), S. Bhattacharya (Indian Institute of Science)

Gemini surfactants consist of two hydrophobic chains and two hydrophilic head groups covalently connected by a spacer. These surfactants are referred to as the surfactant of next generation because of the number of exceptional properties that they manifest. Gemini surfactants have very low critical micelle concentration (CMC) and are very efficient to lower the oil-water interfacial tension in comparison to single-chain counterparts. Another property for which Gemini surfactants differ from simple surfactants is aggregation morphology. These surfactants form the large structures, while corresponding conventional surfactants form only spherical micelles. It has also been found that the oil solubilization is significantly better for Gemini surfactants, and it has been attributed to the propensity of formation of large structures by these surfactants. We report herewith the comparison of structure of Gemini surfactants with flexible and rigid spacers in aqueous solution as studied by small-angle neutron scattering. It was found in earlier studies that micelles of Gemini surfactants with flexible spacers form different shapes of micelles such as disklike, rodlike, and spherical depending on the spacer length [*Phys. Rev. E* **57**, 776 (1998)]. On the other hand, recent experiments show that Gemini surfactants with rigid head groups consisting of different aromatic groups form the large multilamellar vesicles. The conformation of the hydrophobic tails inside the above structures also depends on the nature and the length of the spacer.

Mon. 8:00–9:30 p.m., Poster, ES-03

Membrane Ordering of Sponge Phases at a Solid-Solution Interface

William Anthony Hamilton, L. Porcar, P. D. Butler (Oak Ridge National Laboratory), G. G. Warr (University of Sydney)

The intriguing convoluted membranes of bicontinuous surfactant sponges are manifestly isotropic bulk phases. Recently we have used neutron scattering to address the question of how bulk sponge phases accommodate themselves structurally to the semi-infinite: the ordering potential exerted by a quartz surface. In particular, to what extent does the proximate surface drive the obvious transition of the system to the adjacent lamellar phase domain. This work, carried out on instruments on the High Flux Isotope Reactor at Oak Ridge National Laboratory, involves a combination of conventional bulk small-angle neutron scattering (SANS) and simultaneous neutron reflectivity and “Near-Surface SANS” (NS-SANS) from sponge solutions in reflection geometry cells.

Mon. 8:00–9:30 p.m., Poster, ES-04

Solvent Diffusion into Complex Perfluorinated Ionomer Thin Films

Teresa Anne Hill, Dvora Perahia (Clemson University)

The diffusion into complex polymer thin films of perfluorinated ionomers has been studied. These polymers consist of two non-compatible components: a perfluorinated hydrophobic backbone and a hydrophilic pendant side chain terminated by a sulfonic ionic group. The type of diffusion (Fickian versus non-Fickian) depends on the polymer structure and the interaction of its different segments with the solvent. As films become thinner, swelling may differ from that of the bulk and interfacial characteristics become critical. Neutron reflectometry has been used to study the interfacial structure of spin cast polymer films ~ 1000 Å dry and in direct contact with liquid and in the presence of saturated vapor. Butanol and Octanol liquid and saturated Octanol vapor were used. Dry films consist of three distinct regions: a region of high density at the interface with silicon oxide, intermediate density, and an air interface

layer where the density decreases. Films in direct contact with solvents show changes within the first four hours, and the extent of swelling varies with each solvent. At room temperature the films in contact with Octanol swell by 29% and with Butanol swell by 13%. Swelling of the films in direct contact with solvent was different from films in contact with saturated vapor. This indicates that wetting of the film by the solvent may play an important role in the diffusion into a complex polymer film.

Mon. 8:00–9:30 p.m., Poster, ES-05

Bulk Thermodynamics of Blends of Linear and Branched Functionalized Polymers

Jonghwi Hwang, Teresa D. Martter, Mark D. Foster, Roderic P. Quirk, Maurice Morton (University of Akron)

We have investigated the effect of architecture and chain-end functionalization on bulk thermodynamics of linear/linear and star/linear blends of polybutadiene (PB) with four different chain ends. Star-branched PBs with chain ends of 3-(tert-butyl)dimethylsiloxy-1-propyl (SO), hydroxypropyl (OH), and 2,2,2-trifluoroethanesulfonyloxy propyl (CF) chain ends have essentially the same overall molecular weight (MW) since only the chain end was modified. Conventional butyl (Bu) chain-ended PBs have also been synthesized using sec-butyllithium as an initiator instead of 3-(tert-butyl)dimethylsiloxy-1-propyllithium. The components of linear/linear and star/linear blends have about the same overall MW. Small-angle neutron scattering (SANS) was used to estimate the value of an overall thermodynamic interaction parameter, χ , for the blends. The value of χ in the star/linear blends increases as the functional group at the chain ends of the star is varied in the order of Bu, SO, OH, and CF. Blends of 12-arm stars with OH and CF chain ends show bulk phase separation. A blend of 8-arm star with CF chain ends also shows phase separation. In general, as the number of arms is increased, the value of χ increases. In the blend of 12-arm star with OH end groups, about two-thirds of the value of χ can be attributed to chain-end/branching effects. Changing the functionality of one chain end has a stronger impact on the value of χ for linear/linear blends in which both components have low molecular weights (9 k) comparable to that of an arm of the 12-arm star.

Research funding from an Ohio Board of Regents Challenge Grant and access to SANS facilities at the National Institute of Standards and Technology supported through NSF-DMR-9423101 are gratefully acknowledged.

Mon. 8:00–9:30 p.m., Poster, ES-06

Effect of a Triblock Copolymer on the Structure of a Water-in-Oil Microemulsion

Xuesong Jiao, Dvora Perahia (Clemson University), Liora Shmueli, Moshe Gottlieb (Ben Gurion University)

The effect of the addition of a polyethylene oxide (PEO) - poly-dimethyl siloxane (PDMS)-PEO triblock copolymer on the structure of the water/sodium di-2-ethylsulfosuccinate (AOT)/decane microemulsion system has been investigated by small-angle neutron scattering. The water-to-surfactant molar ratio was kept constant at 38/1 in order to control the dispersed water droplet size in the initial three-component microemulsion. The previous study shows that the copolymer enhances the viscosity, and both droplet and polymer concentration affect the viscosity. Upon adding the copolymer, the neutron-scattering pattern changes from that of isolated spherical droplets to that of an interacting system. As the copolymer concentration and/or the volume fraction of the aqueous phase are increased, the interaction peak develops and shifts toward larger wave vector Q . The fitting analysis suggests that a bicontinuous structure exists in the complex system with additional triblock copolymer. Based on the bicontinuous structure, we proposed an explanation to the viscosity anomaly that the more viscous aqueous phase and the local ordering dominate the overall viscosity.

Mon. 8:00–9:30 p.m., Poster, ES-07

Using Small-Angle Neutron Scattering to Study the Conformation of Polyions in Aqueous Solutions

Yue Shen, Lee Magid (University of Tennessee), Paul D. Butler (Oak Ridge National Laboratory)

Aliphatic ionenes are strong charged cationic polyelectrolytes whose charge groups are located on the polymer main chain. The charge density can be changed by changing the methylene groups between the quaternized nitrogen atoms. Small-angle neutron scattering can be used to study the structure of ionenes in aqueous solutions. By changing the ionene charge density, ionene concentration, counterions, or ionic strength in the solutions, the conformation of the polyions can be changed. In our systems, we choose [3,3], [6,6], and [8,8] ionenes to produce different charge density parameters, x , and we choose chloride and 2,6-dichlorobenzoate as counterions for the reason of difference of counterion binding.

Mon. 8:00–9:30 p.m., Poster, ES-08

Neutron Reflectivity Study of Layer-by-Layer Processing of Polyelectrolyte Multilayer Films

Stella Yoon-Sun Park, Juan Gonzalez, You-Yeon Won, Jonas Mendelsohn, Michael F. Rubner, Anne M. Mayes (Massachusetts Institute of Technology)

The interface and top-layer effects of polyelectrolyte multilayers formed through layer-by-layer assembly—alternate polyanion and polycation adsorption—are investigated by neutron reflectivity at the solid/liquid interface. Although polyelectrolyte multilayers have been previously investigated using X-ray and neutron reflectivity [1], there exists no systematic study near known morphological transition points. For example, post-assembly processing, such as introduction of the films to acidic solutions [2], or assembly processing, such as addition of salt to polyelectrolyte solutions [3], are known to cause dramatic changes in the multilayer film morphology. Here, we present the in situ multilayer structure near a transition acidic condition. We also present a comparison of cell-resistant and non-resistant film profiles. [1] See for example, Steitz, R., Jaeger, W., and v. Klitzing, R., *Langmuir* **17**, 4471 (2001). [2] Mendelsohn, J. D.,

Barrett, C. J., Chan, V. V., Pal, A. J., Mayes, A. M., and Rubner, M. F., *Langmuir* **16**, 5017 (2000). [3] McAloney, R. A., Sinyor, M., Dudnik, V., and Goh, M. C., *Langmuir* **17**, 6655 (2001).

Mon. 8:00–9:30 p.m., Poster, ES-09

Phase Behavior in Thin Polymer Blend Films

Ananth Indrakanti, Sanat K. Kumar (Pennsylvania State University), Ronald L. Jones (National Institute of Standards and Technology), Robert M. Briber (University of Maryland)

The phase behavior of confined polymer mixtures has been of continuing theoretical interest for the last 30 years since critical properties such as film roughness, gloss, and adhesion can be qualitatively altered by phase separation. However, little reliable experimental data exist because of the extremely small sample volumes in films with thickness of $D \sim 0.01$ -1 micron. To our knowledge, the only other attempt to study the phase behavior in thin polymer blend films was made by Reich and Cohen in 1981. They

performed light scattering in transmission on the thin films of PS/PVME. Their results were qualitatively consistent with theory. These results must be viewed with caution since light scattering is sensitive to domains only as large as the wavelength of light (0.5 micron). Neutron scattering would be a more appropriate technique to study concentration fluctuations in the miscible regime of a polymer blend, thus providing a better insight into this problem. Our novel neutron-scattering measurements suggest that, consistent with the earlier work, the magnitude of the spatial correlation length of concentration fluctuations in the single phase decreases strongly with D , with this effect manifesting itself even for films as thick as 1 micron. Extrapolating these results suggests dramatic confinement effects on phase boundaries, and we predict critical temperature shifts as big as ~ 250 K for $D = 60$ nm. In sharp contrast, the measured phase separation temperature, or the cloud point, is found to be unperturbed relative to its bulk value for $60 \text{ nm} < D < 1$ micron. These apparently contradictory results are conjectured to be driven by the flexibility of the air surface of the film, which plays no role in the single phase state but results in new physics when the bulk binodal of the film is accessed.

Tuesday, June 25, 2002

Tuesday Morning, FA–Soft Matter Dynamics

Chair: Darrin Pochan (University of Delaware)
Tennessee Ballroom A

Tues. 8:30 a.m., Keynote, FA-01

Polymer Dynamics from the Global to the Local Scale as Revealed by High-Resolution Neutron Spectroscopy

Dieter Oswald Richter, M. Monkenbusch, L. Willner,
A. Wischnewski (Institut für Festkörperforschung),
A. Arbe, J. Colmenero (Universidad del Pais Vasco)

Neutron scattering accesses the space time evolution of molecular motion and atomic length and time scales covering all dynamic processes from local relaxation to the overall chain diffusion. Using the dynamics of a chain in a melt as an example, we review results obtained by various high-resolution neutron-scattering techniques. Starting from the entropy-driven Rouse dynamics, we address its limitation to large and small scales. On the large scale side, neutron spin echo spectroscopy revealed the dynamic structure factor of a spatially confined chain in accordance with the reptation concept. Recently, for the first time it has become possible also to study the self correlation function of a reptating chain by NSE. The data corroborates the crossover from the Rouse to local reptation dynamic at an entanglement time t_e . Towards smaller scales, the influence of the local chain structure causes deviations from the Rouse dynamics. A comparative study on polydimethylsiloxane (PDMS) and polyisobutylene (PIB), two polymers exhibiting the same static rigidity but very different orientational barriers, showed that the Rouse dynamics is limited by intrachain viscosity effect arising from jump motion across rotational barriers. These result are corroborated by studies in dilute solution. Finally, results on the α - and β - relaxations are displayed, which emphasizes the capability of neutron scattering in this range of length and time scales also.

Tues. 9:00 a.m., Invited, FA-02

Self-Motion and the Alpha Relaxation in Glass-Forming Polymers; MD-Simulation by Molecular Dynamics Simulations

Juan Colmenero (Universidad Del Pais Vasco)

Neutron-scattering results of many different polymers show that in the time and Q -range where the segmental alpha-relaxation is observed by these techniques (typically: $5 \text{ ps} < t < 2 \text{ ns}$; $0.2 \text{ \AA}^{-1} < Q < 1.5 \text{ \AA}^{-1}$), the incoherent intermediate scattering function $F_s(Q,t)$ shows an approximate Gaussian behavior, that is, the corresponding Van Hove correlation $G_s(r,t)$ is a Gaussian function. This result, together with the nonexponential time dependence of $F_s(Q,t)$, suggests that sublinear diffusion processes drive the alpha relaxation in glass-forming polymers. Recently, we have carried out fully atomistic MD-simulation in two different glass-forming polymers—polyisoprene and polyvinylethylene—in a wide time range extending until 20 ns. From the atomic trajectories obtained by MD-simulation, we have calculated the Van Hove correlation function and the atomic mean squared displacements, as well as the magnitudes measured in neutron-scattering experiments. The results obtained agree with the neutron-scattering results in the Q -range just mentioned. However, at higher Q -values, MD-data show a crossover from Gaussian to non-Gaussian taking place in the Q -range of the first maximum of the static structure factor $S(Q)$. The existence of such a crossover in real samples would have some implications concerning the possible theoretical scenarios for the alpha-relaxation. The experimental observation of this crossover is a very difficult task because the Q -range is in the limit of the most common neutron backscattering instruments. We have recently investigated this crossover in polyisoprene by means of neutron spin echo and a backscattering (IN13, ILL, Grenoble, France) instrument extending the Q -range until about 5 \AA^{-1} . The results obtained seem to confirm the crossover found by MD-simulations.

Tues. 9:15 a.m., Invited, FA-03

Nanoscale Dynamic Correlations Near the Glass Transition

Margarita Russina (Los Alamos Neutron Science Center)

More than ten years ago an unexpected microscopic process in the picosecond time range was discovered by neutron inelastic scattering in supercooled liquids near the glass transitions. This process appears in addition to atomic vibrations and the global, viscous flow. Since then it has been found not only in ionic melts but also in polymers and biological systems, such as hydrated myoglobin. However, the nature of this process, often referred to as beta-process, remained controversial until now. Using coherent and incoherent neutron scattering to explore the dynamic behavior at the length scale of the intermediate range order in an archetypal fragile glass Ca-K-NO₃, we were able to analyze the collective aspects of this microscopic process. We found that the beta-process originates from correlated displacements of groups of atoms. This motion is highly heterogeneous on the nanoscopic scale: while a small fraction of atoms moves in the form of correlated, presumably string-like motion of 6 to 10 Å size groups, the bulk follows the much slower viscous flow. Remarkably, the nanoscale dynamic heterogeneity of the picosecond process appears spontaneously in an otherwise (e.g., at other temperatures or on average on longer time scales) homogeneous system. The discovery of this motion helps to understand the global mechanism of the glass transition.

Tues. 9:30 a.m., Talk, FA-04

Dynamics and Structure of Interacting Rodlike Particles Revealed by Neutron Spin Echo Spectroscopy

Steven R. Kline, Sung-Min Choi (Korea Advanced Institute of Science and Technology), Nicholas Rosov (National Institute of Standards and Technology Center for Neutron Research)

Polymerized rodlike micelles with controllable surface chemistry have been prepared, providing a model system to study the structure and dynamics in dispersions of

charged, anisotropic particles. Micelles have been polymerized with two different surface charge densities and measured with and without screening electrolyte. Small-angle neutron scattering (SANS) measurements can yield the structure factor, $S(q)$, but only if the form factor, $P(q)$, is accurately measured. The coherent dynamics of the micelles have been measured using neutron spin-echo spectroscopy (NSE). NSE measurements, coupled only with a high- q measurement of the free diffusion coefficient of the micelles, also yield the structure factor, $S(q)$. SANS-derived $S(q)$ compare favorably to the NSE-derived $S(q)$, where the peak visible in the SANS data is a result of the electrostatic interactions between the rodlike micelles and is reflected as a minimum in the diffusion coefficient measured by NSE. The addition of a simple salt or a reduction of the surface charge density eliminates the interparticle interaction peak in the SANS spectra. NSE measurements reveal that screening does not completely eliminate the interparticle interactions. In the absence of the NSE measurements, the SANS data could easily be misinterpreted, yielding an incorrect micelle length.

Tues. 9:45 a.m., Talk, FA-05

Interaction between Hydrophobically Modified Polymer and Surfactant Mesophases

Jyotsana Lal (Argonne National Laboratory)

We investigate the effect of polysoaps on the phase behavior and membrane elastic properties of the lyotropic lamellar (La) phase of the nonionic surfactant penta(ethylene glycol) dodecyl ether (C₁₂E₅) and hexanol. The polysoap is a hydrophobically modified polymer (hm-polymer) with n-alkyl sidegroups randomly grafted to a polyacrylate (PAA) backbone. The membrane properties are extracted from small-angle neutron scattering (SANS) data through on a model due Nallet et al. and the excess area method developed by Roux et al. The phase behavior, membrane rigidity, compression modulus, and bilayer mean bending modulus are independent of molecular weight, polydispersity, and hydrophobe length of hm-polymers. The rigidity and compression moduli of membranes increase with increasing polymer concentration and hydrophobe substitution level. A new scaling model delineates the domain of compatibility for hydrophobically modified polymers and surfactant lamellar phase on the

basis of two criteria: (1) the surface coverage of chain segments between hydrophobes (i.e., blobs) being less than the available membrane area and (2) the interlamellar spacing being larger than the blob size. This simple model captures the essential features of the phase diagrams. The effect of adsorbed hydrophobically modified polymers (hm-polymers) on the dynamics of surfactant bilayers was investigated using neutron spin-echo (NSE) spectroscopy. The range covered by the static and dynamic measurements coincide with the slowest relaxation coinciding with the diffraction peak. The quality of the NSE data invites the development of new theories of the dynamics of lamellar phase liquid crystalline fluids.

Tues. 10:00 a.m., Talk, FA-06

Neutron Spin-Echo Study on the Modification of Surfactant Membrane Properties Due to Polymer Addition

Michael Monkenbusch, Mihaela Mihailescu, Jürgen Allgaier, Henrich Frielinghaus, Dieter Richter (Forschungszentrum Jülich), Britta Jakobs, Thomas Sottmann (Universität zu Köln), Bing-Shiou Yang, Robert K. Prud'homme (Princeton University), Jyotsana Lal (Argonne National Laboratory)

Microemulsions consisting of a mixture of water, “oil,” and a surfactant form a variety of thermodynamically stable phases where oil and water domains with a typical dimension of some nanometers are separated by a surfactant-rich interface. The mechanical properties (bending moduli) of these surfactant membranes determine the phase behavior and the fluctuation dynamics. Incorporation and association of amphiphilic polymers change these membrane properties. Macroscopically this results in—sometimes significantly—modified phase behavior. Here we report on the effect on the membrane fluctuation dynamics as observed by neutron spectroscopy. Combination of small-angle neutron scattering and neutron-spin echo is used to assess the validity of theoretical concepts to describe the dynamics and the role of friction. The effect of different types of polymers on bicontinuous and oriented lamellar nonionic microemulsion systems is discussed.

Tues. Morning, FB—Neutron Techniques

Chair: Patrick Gallagher (National Institute of Standards and Technology)
Tennessee Ballroom B

Tues. 8:30 a.m., Invited, FB-01

University-Based Pulsed Neutron Sources: the LENS Project

David V. Baxter, J. M. Cameron, H. Nann, W. M. Snow, J. W. Zwanziger (Indiana University)

A pulsed neutron source based on low-energy (p,n) reactions on beryllium and lithium has been proposed for construction at Indiana University: the Low Energy Neutron Source, or LENS. We describe the pivotal roles that such a source will play in support of the Spallation Neutron Source through the education of an expanding user base, the testing of new moderator designs, and the development of new instrumentation. For suitable applications such as small-angle neutron scattering (SANS), LENS will provide a cold neutron intensity that is at least as great as that from the Intense Pulsed Neutron Source C-moderator; therefore, it will also serve as a regional SANS user facility. LENS will have variable neutron pulse widths of 1 ms or less, in contrast to the fixed short-pulse time structure used at existing spallation sources. Therefore, the facility will also be ideal for developing new instrumentation suitable for the next generation of long-pulse spallation sources. The development of a spin-echo SANS instrument for pulsed sources will be discussed as one example. This instrument will provide structural information on length scales as large as a few microns but will use neutrons with an efficiency that is some four orders of magnitude greater than conventional ultrasmall-angle neutron scattering instruments.

Tues. 8:45 a.m., Talk, FB-02

Deep Inelastic Neutron Scattering as a Probe of Hydrogen Bonded Systems

George F. Reiter (University of Houston), J. Mayers (Rutherford Appleton Laboratory), Phil Platzman (Lucent Technologies)

Recent progress in analyzing deep inelastic neutron-scattering data on Vesuvio at the Rutherford Laboratory demonstrates that this technique is capable of highly refined characterization of the hydrogen bond in crystals, easily resolving the effects of surrounding ligands, and in cases of a symmetric bond, a direct measurement of the effective Born-Oppenheimer potential. We present data for KHC_2O_4 , a salt of oxalic acid, where the accuracy of the data allows more than a dozen anharmonic coefficients describing the momentum distribution of the bond to be determined, and for KH_2PO_4 (KDP), where an unambiguous observation of tunneling in the bond has been made and the first Born-Oppenheimer potential has been reconstructed directly from data. In liquids or powder samples, where the data must be fit with models, it is possible to measure five or six parameters characterizing the average bond. Preliminary measurements on polycrystalline ice and water will be presented.

Tues. 9:00 a.m., Invited, FB-03

Atomic Resolution Holography Using Thermal Neutrons

R. B. Rogge, R. L. Hammond, J. Katsaras, B. Sur, V. N. P. Anghel (Chalk River Laboratories)

Recently, there have been a number of publications demonstrating that atomic resolution holograms can be created using various forms of electromagnetic radiation (e.g., [1] and [2]). It has been predicted that the signal would be too weak to observe with neutrons. We have demonstrated for the first time that atomic resolution holography using thermal neutrons is feasible [3]. Central to the technique is the so-called inside source concept [4], where atoms of the material act as internal sources of spherical wave fronts. The hologram is produced by the interference between the noninteracting reference waves from the internal source and the wave fronts that have

interacted with other atoms. The characteristic signal is similar to what are known as Kossel and Kickuchi lines (*K*-lines collectively). This secondary scattering is expected to give rise to a relatively weak signal. We have demonstrated, through the first observation of *K*-lines using thermal neutrons [5], that the rather strong incoherent scattering cross section of hydrogen atoms provides a sufficiently intense internal source. Spence has summarized the potential of atomic resolution holograms in general [6]. Of particular note is that holograms contain phase information, the structure is reconstructed directly from the data (without recourse to a model system), and only orientational order is required (translational order is not necessary). As such, noncrystalline materials can also be imaged. It is self-evident that the complementarity of neutrons with forms of electromagnetic radiation will result in thermal neutron holography having its own unique place among holographic techniques. Given the sensitivity of neutrons to hydrogen and that hydrogen is abundant in organic systems, it is expected that neutron holography will be of particular importance to the studies of biologically relevant and polymeric materials. [1] G. R. Harp, D. K. Saldin, and B. P. Tonner, *Phys. Rev. Lett.* **65**, 1012-1015 (1990). [2] M. Tegze, and G. Faigel, *Europhys. Lett.* **16**, 41-46 (1991). [3] B. Sur, R. B. Rogge, R. P. Hammond, V. N. P. Anghel, and J. Katsaras, *Nature* **414**, 525 (2001). [4] A. Szöke, "In Short Wavelength Coherent Radiation: Generation and Applications," edited by T. Attwood and J. Boker, *AIP Conf. Proc.* No. **147** (AIP, New York, 1986). [5] B. Sur, R. B. Rogge, R. P. Hammond, V. N. P. Anghel, and J. Katsaras, *Phys. Rev. Lett.* **88**(6) 065505 (2001). [6] J. Spence, *Nature* **410**, 1037-1040 (2001).

Tues. 9:15 a.m., Talk, FB-04

Monte Carlo Simulation of a Prototype Time Focused Crystal Analyzer Spectrometer for IPNS

John Marland Carpenter (Argonne National Laboratory), Géza Zsigmond, Ferenc Mezei (Hahn-Meitner Institut)

We report Monte Carlo simulations of a prototype time-focused pulsed-source crystal analyzer (inverse geometry). The configuration of the instrument is one suggested by the recently reported general theory of this class of instrument [1,2]. That theory provides the basis

for design to accomplish high resolution while allowing other than backscattering geometry and more flexibility in choices of the type of analyzer crystal and the detector location. We used the VITESS code [3], which has all the capabilities needed to treat this type of spectrometer: three-dimensional generality, time-of-flight, off-cut mosaic crystal reflection, and high computational efficiency, all of which we exercised. Parameters in the simulation are ones roughly appropriate for a test installation at the Intense Pulsed Neutron Source (IPNS). The goals of the prototype operation are to provide an implementation of a time-focused CAS in which practical considerations come into full play and to provide a benchmark from which to scale performance to more elaborate instruments and larger installations. Space downstream from the GPPD powder diffractometer allows installation of the prototype approximately 30 m from the moderator, an aggressively poisoned 100 K liquid methane system for which the shape of the emitted neutron pulses is well known (about 25 μs FWHM for 5.7- \AA neutrons). Although this moderator with the available length of flight path will not provide the prototype with raw resolution to approach its ultimate possibilities, deconvolution of the pulse, which has an exceedingly fast rising edge, will provide a test of the geometric focusing of the instrument. We conclude that the test will demonstrate the potential high resolution of the time-focused CAS. [1] J. M. Carpenter, "Time Focusing of Pulsed-Source Crystal Analyzer Spectrometers I. General Analysis," In press at *Nucl. Instr. & Meth. in Phys. Res.* (2001). [2] J. M. Carpenter et al., "Time Focusing of Pulsed-Source Crystal Analyzer Spectrometers II. Practical Expressions," In press at *Nucl. Instr. & Meth. in Phys. Res.* (2001). [3] G. Zsigmond et al., Monte Carlo Simulation of Crystal Monochromators/Analysers—Applications for the Crystal-Analyzer Neutron Spectrometer IRIS, *Nucl. Instr. and Meth. in Phys. Res. A*, **457**(2001) 299-308.

Tues. 9:30 a.m., Talk, FB-05

Time-of-Flight Ultrasmall-Angle Neutron-Scattering Instrument for SNS

Michael Agamalian, J. M. Carpenter, K. C. Littrell, P. Thiyagarajan (Argonne National Laboratory), Ch. Rehm (Oak Ridge National Laboratory)

We present a preliminary concept of a Bonse-Hart-type time-of-flight ultrasmall-angle neutron-scattering (TOF-USANS) double-crystal diffractometer (DCD) adapted for use at pulsed neutron sources. The experimental setup for this instrument is in principle similar to that designed for the conventional ultrasmall-angle neutron-scattering (C-USANS) instruments with triple-bounce channel-cut crystals; however, usage of the TOF technique allows separating of several higher order Bragg-reflected wavelengths arriving at the detector. This gives an opportunity to obtain several USANS data simultaneously, which gives significant intensity gain and makes the instrument competitive with the best conventional USANS instruments now in use at steady operational reactor sources. Besides, the proposed instrument allows working simultaneously with different Q-resolution at each separated wavelength using the fact that the Darwin width is proportional to the square of wavelength. This effect makes it possible to increase the real space upper resolution limit of the instrument compared to conventional USANS cameras, as well as extend the USANS Q-range to the larger Q values. Silicon, which is mostly in use for the dynamical diffraction studies, is chosen as a material of channel-cut crystals for the first variant of TOF-USANS mockup, which we plan to design and test at Argonne's Intense Pulsed Neutron Source. The further development in this field will be connected with an attempt to replace silicon with other single crystals with larger d-spacing. The latter allows the further increase of the Darwin width, which leads to increase of the number of useful high order Bragg reflections and as a result to the effectiveness of the proposed instrument.

Tues. 9:45 a.m., Keynote, FB-06

Enhancing Reflectometry and SANS using Neutron Spin Echo

Roger Pynn (Los Alamos National Laboratory and University of California, Santa Barbara)

Although neutron spin echo (NSE) has been used for a quarter of a century to achieve very high-energy resolution in neutron-scattering experiments, the method has the potential for wider applicability. In principle, it can be used to achieve good (or even very good) resolution along any desired direction in (Q,E) space. In contrast with conventional methods of improving resolution, NSE does not

require highly monochromatic beams or tight beam collimation. It therefore has the potential to achieve good resolution without the normal intensity penalties. The method should also be combinable with real-space focusing techniques that can further enhance signal intensity without degrading the resolution. In this talk I will describe methods by which NSE can be used to enhance both reflectivity and small-angle neutron scattering (SANS) measurements. The methods use thin magnetic films deposited on silicon substrates to manipulate the neutron spins. A sequence of eight such films suitably oriented and spaced can be used to increase the length scales accessible to SANS, to separate diffuse from specular reflection, and to probe structure within the plane of thin reflecting samples. For monochromatic-beam instruments, the apparatus needed is inexpensive and can be added easily to existing spectrometers that already produce polarized neutrons.

Tues. Morning, FC–Materials II

*Chair: Arthur Schultz (Argonne National Laboratory)
Tennessee Ballroom C*

Tues. 8:30 a.m., Talk, FC-01

High-Resolution Study of Roton Excitations in Superfluid ⁴He

Géza Zsigmond (Hahn-Meitner Institut)

High-energy-resolution spectra (15 to 40 μeV) of superfluid ⁴He were measured at constant low pressure (0.4 bar) on the time-of-flight backscattering spectrometer IRIS at ISIS. The combination of high resolution and wide dynamic range allowed for a nonconventionally detailed line-shape analysis of the roton excitations and made possible the better separation of the roton and the multiphonon components. It was shown that the spectral weight of the rotors and the shape of the multiphonon “background” remains nearly constant with changing the liquid temperature. The roton can be identified above the lambda transition point. The T dependence of roton energy and line width is well described by the BPZ-theory. The measured high-resolution spectra made possible a direct comparison of the GG parametrisation

with a model of two (non-)coupled DHOs by introducing a generalized dielectric formalism.

Tues. 8:45 a.m., Talk, FC-02

Layer Excitations of Superfluid Helium-4 in Confined Geometries

Jonathan Vaughan Pearce, Richard Azuah (University of Liverpool), Mark Adams (ISIS), William Stirling (European Synchrotron Radiation Facility), Paul Sokol (Pennsylvania State University)

Detailed analysis of new inelastic neutron-scattering data has yielded a rigorous model of the dynamic structure factor of superfluid helium-4 confined in porous glasses such as MCM-48, aerogel, xerogel, and SBA-15. These types of silica glass are ideal environments for studying the effects of confinement on the superfluid. Aerogel and xerogel are tenuous glass structures containing pores of random dimension, while MCM-48 consists of a system of highly regular pores. SBA-15 is composed of very narrow, parallel “one-dimensional pores.” The fitting model employed enables the resolution of the different components of the neutron-scattering spectra and confirms the results of previous measurements, the two main results of which are that while the bulk-like phonon-maxon-roton (pmr) excitation appears unchanged, an additional layer pmr mode is also present in the confined superfluid. This layer mode is thought to arise from 2 or 3 layers of high-density helium absorbed onto the walls of the pores. We present neutron-scattering data of high statistical quality and the detailed fitting model developed to account for the manifold components of the data in a consistent way.

Tues. 9:00 a.m., Talk, FC-03

Characterization of Nanophases of Lanthanides in Vitreous Silica

P. Thiyagarajan, James V. Beitz, S. Skanthakumar (Argonne National Laboratory)

We used Diphosil, an ion-exchange porous silica, to sorb lanthanide ions from an aqueous solution and heated the powders to collapse the pores in silica to encapsulate

them in vitreous silica. While encapsulation of certain lanthanides provides materials with unique photo-physical properties, this single materials approach also enables encapsulation of actinides for potential applications in nuclear waste storage. Determination of the optimal temperature for proper encapsulation through pore-collapse required systematic investigation of metal ion-loaded Diphosil that has been heated in air to a series of temperatures that ranged from 700 to 1200°C. This series of Diphosil powder samples, each loaded with a single lanthanide element as trivalent ions, were investigated to characterize their pore structures using small-angle neutron scattering (SANS). These studies showed that pore collapse occurred above 1000°C for these elements. We also determined the size of the resulting nanophases that varied for different lanthanides. To validate that the nanophases embedded in vitreous silica are inaccessible to water, we carried out contrast-match SANS experiments on these powders imbibed in 58% D₂O. Details of the results from a systematic SANS study of encapsulated lanthanides and actinides will be presented.

This work benefited from the use of the Intense Pulsed Neutron Source at Argonne National Laboratory, both of which are funded by the U.S. Department of Energy Office of Basic Energy Sciences, and was carried out under the auspices of the Nuclear Energy Research Initiative of the U.S. Department of Energy under contract W-31-109-ENG-38.

Tues. 9:15 a.m., Talk, FC-04

High-Pressure Neutron-Scattering Study of Cerium Gamma-Alpha Phase Transition

Il-Kyoung Jeong, T. Darling, A. C. Lawson, Th. Proffen, M. J. Graf, R. H. Heffner (Los Alamos National Laboratory)

The gamma-alpha phase transition of cerium is quite interesting in two respects: (1) huge volume collapse (~17%) at the transition and (2) iso-structural phase transition. We studied the gamma-alpha phase transition of cerium using high-pressure, high-resolution neutron scattering. From the pressure dependence of the lattice parameter, we calculated the gamma and alpha phases compressibility of cerium. These results are compared with those of the "piston displacement" method. We also

obtained the thermal parameters of cerium as a function of pressure using the Rietveld refinement. As the pressure increases in gamma-phase, the thermal parameter decreases slowly and shows a sudden drop of about 40% at the phase transition to alpha-phase. Finally, based on our high-pressure alpha-phase cerium measurement, we discussed the distorted-FCC structure in alpha-phase cerium, which was recently proposed by Eliashberg et al. [1]. [1] G. Eliashberg and H. Capellmann, *JETP Letters*, **67**, 25 (1998).

Tues. 9:30 a.m., Invited, FC-05

Physical and Thermodynamic Properties of Gas Clathrate Hydrates Determined by In Situ Neutron Scattering

Bryan C. Chakoumakos, C. J. Rawn, A. J. Rondinone (Oak Ridge National Laboratory), L. A. Stern, S. Circone, S. H. Kirby (U.S. Geological Survey), Yoshinobu Ishii (Japan Atomic Energy Research Institute), B. H. Toby, C. Y. Jones (National Institute of Standards and Technology)

The structure and dynamics of technologically and environmentally important gas clathrate hydrates are being determined by neutron-scattering methods. Clathrate hydrates consist of an ice-like, hydrogen-bonded network of water molecules with polyhedral cavities occupied by various guest molecules. They are stable at low temperatures and modest pressures. Natural gas hydrate deposits are widespread in the seafloor of the continental margins and in permafrost regions. By any estimate, natural gas hydrates constitute an immense, untapped supply of fossil fuel. Research in this area is motivated by specific practical interests: (1) exploration for concentrated natural-gas hydrates in marine sediments and arctic permafrost, (2) natural-gas production by thermal stimulation of natural hydrates, (3) storage and transport of natural gas using hydrocarbon gas hydrates as compact and safe storage media, and (4) carbon dioxide sequestration by exchange of carbon dioxide for methane in natural deposits. Neutron scattering is well suited for the study of hydrates because it is sensitive to the hydrogen atoms and the neutron's large penetration depth provides a bulk probe for large and complex sample environments. At the Japan Atomic Energy Research Institute, temperature-dependent neutron powder diffrac-

tion data were collected on hydrates containing carbon dioxide, tetrahydrofuran, trimethylene oxide, propane, and mixed methane-ethane. At the National Institute of Standards and Technology, similar data were collected on hydrates containing carbon dioxide, methane, and mixed methane-ethane. In Rietveld refinements, the rotationally disordered guest molecules are modeled with disordered rigid bodies, which allows the temperature dependence of the mean-square-displacement of each guest molecule to be determined and provides a means of evaluating the positional disorder of the guest molecules within the oversized cages. In subsequent work, the dynamics of the guest molecules will be directly probed using quasi-elastic neutron scattering. High-pressure cells for in situ neutron scattering and Raman spectroscopy studies, and for low-temperature (ambient pressure) X-ray diffraction, have been constructed and are being tested.

Tues. 9:45 a.m., Keynote, FC-06

Chemistry and Structural Properties of the Superconductor MgB₂

James D. Jorgensen, David G. Hinks (Argonne National Laboratory)

The discovery of superconductivity at 39 K in MgB₂ was an unexpected surprise. Hexagonal diboride compounds were examined for superconductivity over 30 years ago, but MgB₂ was somehow overlooked; the previous studies were focused on transition-metal diborides. In the work on transition-metal diborides, T_c was optimized by chemical substitutions and the creation of vacancy defects on the metal site. Similar approaches to raising T_c in MgB₂ have not been fruitful. For example, our recent work has shown that vacancy defects do not form in MgB₂. Most attempts at chemical substitution have failed. The remarkably high T_c in MgB₂ appears to result from features of its two-dimensional structure, which lead to unusually strong electron-phonon coupling. This gives rise to an anisotropic lattice anomaly at T_c that is much larger than predicted by simple thermodynamics for a second-order phase transition. The strong anisotropy is also manifest in the response of T_c to lattice compression. As a result, measurements of T_c and structure vs pressure have yielded a wide range of results, depending on the choice of pressure

fluid. These special features of MgB₂ provide guidance to the search for other high-T_c materials with the hexagonal diboride structure.

This work is supported by the U.S. Department of Energy, Office of Science, under contract W-31-109-ENG-38.

Tues. Morning, FD–Nuclear/Particle/Astrophysics with Neutrons I

Chair: Michael Snow (Indiana University)
Cumberland Room

Tues. 8:30 a.m., Keynote, FD-01

The Neutron as a Fundamental Physics Laboratory

Fred E. Wietfeldt (Tulane University)

The decay of the free neutron is the simplest nuclear beta-decay and the prototype charged current semi-leptonic weak interaction. Cold and ultracold neutron experiments can make precise measurements of the neutron decay lifetime and angular correlations. These results are used to test the completeness and self-consistency of the standard model of particle physics and could indicate the presence of new physics, such as right-handed weak currents, scalar and tensor weak forces, and new sources of CP-violation in nature. Neutron decay was an important process in the early universe; it played a controlling role in light element nucleosynthesis. The neutron decay lifetime determines the abundance of primordial helium. Parity-violating interactions of cold neutrons with light nuclei provide a means to study the role of the neutral current weak interaction at the hadronic level. Cold and ultracold neutron experiments comprise a key sector of the “low-energy frontier” of nuclear and particle physics. I will review the current theoretical and experimental situation.

Tues. 9:00 a.m., Invited, FD-02

Parity Violation in the n-p System: An Update from the Collaboration

Mark Leuschner (University of New Hampshire)

The NPDGamma collaboration plans to measure $A\gamma$, the directional asymmetry of gamma rays emitted in the reaction $n + p \rightarrow d + \gamma$, to a precision of 5×10^{-9} . This asymmetry is directly related to H_π^1 , the weak pion-nucleon coupling constant. A non-null measurement of this parameter would provide information about the longest-range component of the nuclear weak force. Despite many years of effort, the value of H_π^1 remains uncertain. Measurements of parity violation in the ^{18}F and ^{133}Cs systems have yielded contradictory results. A new measurement of a fundamental nuclear reaction is needed to distinguish between the existing values without adding to the difficulty of the interpretation due to nuclear structure uncertainties. A previous measurement of the $\bar{n} + p \rightarrow d + \gamma$ asymmetry produced a result of $A\gamma = -1.5 \pm 4.7 \times 10^{-8}$, insufficient to test the range predicted by modern theories. The NPDGamma experiment is currently under construction at the Los Alamos Neutron Science Center (LANSCE). A neutron beam from the LANSCE pulsed spallation source will be transmitted through a polarized- ^3He spin filter and directed onto a liquid hydrogen target. Gamma rays emitted from the capture of neutrons on protons will be detected in an array of CsI crystals surrounding the target. The commissioning of the completed beam line and experimental apparatus is expected to commence in the fall of 2003. Progress and results from recent test runs will be presented.

Tues. 9:15 a.m., Invited, FD-03

Using Magnetically Trapped Ultracold Neutrons (UCN) to Measure the Neutron Lifetime

Paul R. Huffman, A. K. Thompson, G. L. Yang, K. J. Coakley (National Institute of Standards and Technology), S. N. Dzhosyuk, C. E. H. Mattoni, S. Maxwell, D. N. McKinsey, L. Yang, J. M. Doyle (Harvard University), R. Golub, E. I. Korobkina (Hahn-Meitner Institut), S. K. Lamoreaux (Los Alamos National Laboratory)

Magnetic confinement of UCN in an Ioffe-type superconducting magnetic trap should lead to an improved measurement of the neutron lifetime τ_n . The trap is loaded through inelastic scattering of 0.89-nm neutrons with phonons in superfluid He-4 cooled to 150 mK. When trapped neutrons decay, energetic decay electrons ionize helium atoms, resulting in efficient conversion of electron kinetic energy into light (scintillation), which is then detected by photomultiplier tubes. The advantages of this technique over previous experiments are continuous detection of scintillations from decay electrons and the elimination of wall losses and betatron oscillations. Analysis indicates that systematic errors due to neutron losses should be controllable to $10^{-5}\tau_n$. We have upgraded our apparatus by constructing a larger, deeper magnetic trap and are implementing techniques to substantially reduce backgrounds. The experiment is conducted at the National Institute of Standards and Technology Gaithersburg facility, and we will report its current status.

Tues. 9:30 a.m., Invited, FD-04

High-Energy Physics with Ultra-Cold Neutrons

Albert R. Young (North Carolina State University)

The UCNA collaboration is preparing to measure angular correlations in the decay of polarized neutrons using a spallation source of ultra-cold neutrons at Los Alamos Neutron Science Center. These measurements provide fundamental information on the form factors for the semileptonic charged weak current for the nucleon and can be used in unitarity tests of the CKM matrix.

Tues. 9:45 a.m., Talk, FD-05

Measurement of the Free Neutron Lifetime

Jeffrey S. Nico, M. S. Dewey, D. M. Gilliam (National Institute of Standards and Technology), F. E. Wietfeldt (Tulane University), W. M. Snow (Indiana University), G. L. Greene (Los Alamos National Laboratory)

An accurate determination of the neutron lifetime is important in testing the standard V-A theory of weak interactions and in addressing fundamental questions in astrophysics and cosmology. A new measurement of the lifetime was recently completed at the National Institute of Standards and Technology Center for Neutron Research. The lifetime was determined by simultaneously measuring the fluence of a cold neutron beam and counting the decay protons. The protons were stored in a Penning trap until being released and accelerated into a silicon detector held at a high negative potential. A description of the measurement technique, a discussion of systematic effects, and the results from the data runs will be presented.

Tues. 10:00 a.m., Talk, FD-06

Testing Time Reversal in Neutron Beta Decay—the emiT Experiment

Kevin Patrick Coulter (emiT Collaboration)

The emiT experiment searches for time reversal violation in polarized neutron decay in the form of the angular correlation $D \langle \mathbf{J} \rangle \cdot \mathbf{p}$ using a novel octagonal detector that optimizes electron-proton coincidence rates. The first run of emiT set measured $D = [-0.6 \pm 1.2(\text{stat}) \pm 0.5(\text{syst.})] \times 10^{-3}$, improving constraints on the phase of g_a/g_v and limits contributions to T violation due to leptoquarks. Upgrades to the detector have been made, including the replacement of PIN diodes with surface barrier detectors for proton detection and improvements in high-voltage stability, which should improve both the statistical and systematic uncertainties. Additionally, there has been an increase in the cold neutron flux at the National Institute of Standards and Technology reactor. A second run has begun in the spring of 2002 with the expectation of reaching the emiT design goal of $D < 3 \times 10^{-4}$.

Tuesday Morning, GP–Instrumentation

Summit Grand Ballroom II

Tues. 10:30 a.m.–12:00 p.m., Poster, GP-01

U.S.-Japan Triple-Axis Spectrometer: HFIR's TAS on Cold Guide 4

Barry L. Winn, S. Shapiro (Brookhaven National Laboratory), S. Nagler (Oak Ridge National Laboratory), H. Yoshizawa, N. Aso (University of Tokyo), H. Kadowaki (Tokyo Metropolitan University)

A new cold triple-axis spectrometer (TAS) will be installed on the High Flux Isotope Reactor's (HFIR's) Cold Guide 4. The U.S.-Japan Cooperative Research Program on Neutron Scattering supplies preexisting sample and analyzer air-pad tables that had been part of the High Flux Beam Reactor's H4M spectrometer. We anticipate an intensity at the sample comparable with the highest intensity cold TAS in the world, Institut Laue-Langevin's IN14. We are designing the vertical focusing monochromator and its shield to be compatible with Brookhaven's 13-T magnet, which produces the highest available field in the United States for neutron-scattering experiments.

Tues. 10:30 a.m.–12:00 p.m., Poster, GP-02

Design of a Disordered Materials Diffractometer for the Spallation Neutron Source

Chris A. Tulk (Oak Ridge National Laboratory)

The disordered materials diffractometer proposed for construction at the Spallation Neutron Source will be a high-flux, medium-resolution diffractometer with a short incident flight path. This instrument will be used primarily for diffuse scattering studies from liquids, glasses, and amorphous solids with significantly higher resolution capabilities for total scattering measurements from disorder in crystals. This presentation provides a general overview of the instrument concept, including calculations and simulations of instrument performance.

Tues. 10:30 a.m.–12:00 p.m., Poster, GP-03**Neutron Optics Test Station**

*Christine Rehm, Michael Agamalian, Frank Klose
(Oak Ridge National Laboratory)*

The Neutron Optics Test Station (NOTS) is designed for precise, comprehensive studies of any contemporary wide-bandwidth neutron optical devices and components to be used by the experimental facilities of the Spallation Neutron Source (SNS). NOTS will have the capability to obtain reflectivity and polarizing efficiency, as well as wavelength-dependence of these parameters, in a wide range of wavelengths, $2 \text{ \AA} \leq \lambda \leq 20 \text{ \AA}$, and scattering vectors, $2.4 \cdot 10^{-4} \text{ \AA}^{-1} \leq q \leq 6 \text{ \AA}^{-1}$. The maximum cross section of the beam is 0.019 m wide and 0.15 m high. Spatial resolution of mechanical components is 0.01 mm. NOTS will be accommodated at the High Flux Isotope Reactor (HFIR) at Oak Ridge National Laboratory. Since HFIR delivers a white neutron beam, a pulse chopper system will be used to allow time-of-flight neutron experiments. In addition, NOTS will consist of a silicon-based multislit neutron guide polarizer, spin-flipper, sample stage, and two-dimensional position/time sensitive detector. The pulse chopper, polarizer, and spin-flipper are easily removable, which allows fine alignment and measurements of integrated reflectivity of the optical component under study at a chosen angle. When the polarizer and spin-flipper are added, the integrated polarizing efficiency can be obtained. The pulse chopper allows for spectral measurements to determine the wavelength-dependence of these parameters. The two-dimensional detector is particularly useful for alignment and testing of focusing devices. Thus, NOTS should give complete information about the quality of any kind of wide-bandwidth neutron optical components. Objects to be tested at NOTS include, but are not limited to, supermirrors, neutron guide segments, (remanent) polarizers, polarization analyzers, beam benders, band pass filters, focusing devices, focusing monochromators, multilayer monochromators, fiber lenses, toroidal mirrors, and spin-flippers.

Tues. 10:30 a.m.–12:00 p.m., Poster, GP-04**Conceptual Design for the Small-Angle Neutron Scattering Instrument at the Australian Replacement Research Reactor**

Elliot Paul Gilbert (Australian Nuclear Science and Technology Organisation)

A small-angle neutron scattering (SANS) instrument is being designed as part of the initial instrument suite for the 20-MW Australian Replacement Research Reactor. The new instrument, receiving neutrons from a large liquid-D₂ cold source, will be in the spirit of the world's best facilities and will greatly build upon the Australian Nuclear Science and Technology Organisation's existing expertise and facilities. Scheduled for completion in January 2006, it will provide Australian and international researchers with opportunities to access state-of-the-art SANS instrumentation. The conceptual details of the new SANS will be presented.

Tues. 10:30 a.m.–12:00 p.m., Poster, GP-05**New Paradigm in Pulsed Source Cold Neutron Spectroscopy**

Ferenc Mezei (Los Alamos National Laboratory and Hahn-Meitner Institute), Margarita Russina (Los Alamos National Laboratory)

Neutron scattering is used by a worldwide scientific community as a most important tool in condensed matter research. As of today, the large majority of this work is performed on research reactors as neutron sources. Spallation sources play a complementary role, with reactors offering superior neutron beam performance in some 70% of the experiments. Further progress in neutron-scattering research depends on our capability of making spallation sources first competitive and ultimately superior to reactors in those majority of core applications in which reactors currently provide much superior performance than spallation sources. This revolution in neutron-scattering science is the challenge of the next decade. The Los Alamos Neutron Science Center (LANSCE) made the first major step in realizing this revolution by installing at Lujan center the first so-called coupled moderators, which can produce up to 6 to 8 times more

useful neutrons for the same driving proton beam power than those used at other leading spallation sources, such as ISIS in the United Kingdom. This high neutron intensity comes in long pulses compared to the ones only used now, with significant intensities up to 3 to 4 ms from the beginning of the pulse. The IN500 LDRD project at LANSCE is developing a series of novel approaches specifically conceived to establish the use of these long pulses (mechanical pulse shaping, repetition rate multiplication, and enhanced neutron optical beam extraction and delivery system). Implemented on the novel coupled H₂ moderator at Lujan center, these will for the first time open up the way for spallation sources to surpass the capabilities of the most advanced reactor facilities in one of their core competence, cold neutron spectroscopy. This is a crucial research tool for the study of soft and complex matter.

Tues. 10:30 a.m.–12:00 p.m., Poster, GP-06

Low-Q Time-of-Flight Neutron Diffraction on a Partially Coupled Cold Moderator: The Use of Choppers and Gravity Correction

Rex Paul Hjelm, Loren I. Espada, Kevin Kupcho (Los Alamos National Laboratory)

Low-Q time-of-flight (TOF) neutron diffractometers at pulsed sources are designed to make long length scale measurement at low-to-moderate precision, $*Q$, in momentum transfer, Q . Such instruments are best placed on a cold moderator source with a pulsed neutron response matching the TOF resolution of the experiment. This strategy optimizes the conflicting requirements of count rate and $*Q$. A new liquid hydrogen cold moderator, partially coupled to a beryllium-lead reflector in flux trap geometry, was installed as a source for the low-Q, TOF diffractometer, LQD, at the Lujan Neutron Scattering Center. Measurements show overall increases in the neutron flux by a factor of 2.5 over the previous decoupled cold moderator. TOF measurements indicate that this factor increases with TOF and that there is a significant increase of flux for neutrons that contribute to subsequent frames, leading to a significant increase in sample-dependent background. We have implemented a frame-overlap chopper that, together with a t-zero chopper to handle prompt background, significantly reduces the sample dependent background. We will also

describe implementation of a new design of a device for LQD to correct for the drop of the neutron beam caused by gravity.

Tues. 10:30 a.m.–12:00 p.m., Poster, GP-07

The New QENS: A successful upgrade of the Quasi-Elastic Neutron Spectrometer of IPNS

Robert W. Connatser, Jr. (Argonne National Laboratory)

Recently, the quasi-elastic Neutron Spectrometer (QENS) at the Intense Pulsed Neutron Source (IPNS) was upgraded. Over the old QENS instrument, an inverse geometry crystal analyzer instrument, the new QENS significantly increases the data rate (by about one order of magnitude) for both quasi-elastic and inelastic neutron-scattering measurements on all the available energy transfer ranges from -2.5 to 200 meV. The original three analyzer arms mounted on a rotating table have been replaced by 22 stationary analyzer arms. Data are now simultaneously collected over the whole available Q range, from 0.3 up to 2.6 Å⁻¹, with an energy resolution of 90 μeV. Moreover, compared to more classical instruments, this new design makes it possible to override the “slab sample shadow” problem that usually dramatically reduces the scattered intensity onto the detectors placed in the sample plane. Additionally, two banks of detectors have been placed for diffraction measurements at high and low Q , covering a global Q range from 0.1 to 25.0 Å⁻¹. This new feature will considerably improve the amount and the quality of physical information collected, particularly for coherent samples where phase transitions are expected. This poster gives details of the improvements and the technical specifications of the new instrument.

The submitted manuscript has been created by the University of Chicago as Operator of Argonne National Laboratory (“Argonne”) under contract W-31-109-ENG-38 with the U.S. Department of Energy. The U.S. Government retains for itself, and others acting on its behalf, a paid-up, nonexclusive, irrevocable worldwide license in said article to reproduce, prepare derivative works, distribute copies to the public, and perform publicly and display publicly, by or on behalf of the government.

Tues. 10:30 a.m.–12:00 p.m., Poster, GP-08

A High-Resolution Neutron Powder Diffractometer for the University of Michigan Ford Nuclear Reactor

Ronald R. Berliner, M. Hartman (University of Michigan), M. Popovici, W. B. Yelon (University of Missouri)

With the commissioning of high-flux neutron sources in the 1960s and continuing to the current time, neutron-scattering researchers have substantially abandoned university-based neutron sources. Nevertheless, research grade instruments can be constructed and operated at a low-flux source. We will describe the Phoenix Neutron Powder Diffractometer (PNPD) that is currently under construction at the 8 in. diameter Beamport-J of the University of Michigan Ford Nuclear Reactor (FNR). The FNR is a 2-MW, MTR-type, open-pool, research reactor with 10 beam ports, a peak beam-tube source flux of 5×10^{12} n/cm² and with full-power operation 10 days out of each 2-week cycle. The PNPD employs a vertically segmented, mechanically bent, silicon monochromator at a 90° takeoff angle, open neutron beam optics, and large-area position-sensitive neutron detector to compensate for the low neutron source flux. The 20×13 cm² monochromator is composed of nine $20 \times 1.5 \times 0.6$ cm³ silicon plates and can be used to obtain (at 90° takeoff angle) wavelengths of 1.48, 1.76, 2.30, and 1.17 Å from the (511), (331), (311), and (553) planes, respectively. The detector is composed of an array of 15 linear position-sensitive proportional counters clamped together to form a 60×38 cm² array. The detector plane can be placed at 1.6 m from the specimen position for high resolution: 20° two-theta detector span, 3-mm-diameter specimen, $dD/D = 1.8 \times 10^{-3}$ or 1.05 m for low resolution: 30° detector span, 5-mm-diameter specimen, $dD/D = 2.5 \times 10^{-3}$. The instrument will be able to obtain one to two high-resolution diffraction patterns with good statistics/day or four low-resolution patterns in the same time period. The characteristics of the PNPD will be presented in comparison to neutron powder diffraction instruments at HFBR, NIST, and MURR.

Tues. 10:30 a.m.–12:00 p.m., Poster, GP-09

Single-Crystal Sapphire Cell for In Situ Neutron Diffraction Study of Gas Hydrate

Adam Justin Rondinone, C. J. Rawn, B. C. Chakoumakos (Oak Ridge National Laboratory), C. Y. Jones (National Institute of Standards and Technology), S. L. Marshall (Electrochemical Systems Inc.)

A sapphire cell was constructed for in situ high-pressure (350 bar), low-temperature (10 to 300 K) neutron diffraction studies of gas hydrates. The cell was designed so that no metallic parts intercept the incident or diffracted beams. The cell is a 10×2.4 -cm cylinder with an internal diameter of 1.0 cm. Two 3.4-cm flanges were machined into the ends of the cell to provide a surface for unsupported sealing clamps that require no external pressure to seal the cell, which eliminated the need for bolts along the length of the cell. The size and shape of the cell allow it to be mounted on the cold-tip of a 10-K closed-cycle helium refrigeration stage. The cell was machined from a single crystal of sapphire, with the long axis of the cell 5° off from the C-axis of the sapphire in order to eliminate strong sapphire reflections from the scattering plane in Debye-Scherrer geometry. The combination of unsupported clamps and the off-axis cut provide a low background (elastic and inelastic) to the neutron-scattering experiment. The cell will be filled with liquid or solid D₂O and will be exposed to high-pressure hydrate-forming gases fed through the bottom of the cell. Pressure is built and maintained with a two-stage gas booster and electronic pressure controller. The cell will be a platform for a wide range of elastic and inelastic in situ neutron-scattering experiments that will observe hydrate growth under a variety of conditions. Fully formed hydrate also will be observed under high pressures and low temperatures to investigate polymorphism, thermal expansion, and compressibility and thermodynamic properties such as stability.

Research sponsored in part by the Laboratory Directed Research and Development Program of Oak Ridge National Laboratory, managed by UT-Battelle, LLC, for the U.S. Department of Energy under contract DE-AC05-00OR22725.

Tues. 10:30 a.m.–12:00 p.m., Poster, GP-10

Pressure and Temperature: Pushing the Limits of Sample Environments for Neutron-Scattering Experiments

Kenneth James Volin (Argonne National Laboratory)

Neutron diffraction is a powerful tool for structural studies of samples in special sample environments because of the high penetrating power of neutrons compared to X rays. The Intense Pulsed Neutron Source (IPNS) at Argonne National Laboratory offers its users a variety of sample environments for pulsed neutron-scattering and diffraction experiments. Included in these are numerous pressure cells that span a wide range of temperatures and pressures. Each has been designed to achieve the temperatures and pressures that the current science being investigated requires while operating within the constraints of the particular neutron-scattering instrument. Different scattering geometries for powder diffraction, single-crystal diffraction, and small-angle diffraction have led to a variety of innovative designs. Some experiments require the use of a pressure transmitting fluid, which may be an inert liquid or a gas, or require that the sample itself be used as the pressure transmitting fluid. The limits of temperature and pressure, as governed by the cell material and design, must be balanced by the contribution of the particular cell material to the neutron-scattering background. Several successful examples of how these requirements have been met and the respective pressure cell utilized at the IPNS will be presented.

Tues. 10:30 a.m.–12:00 p.m., Poster, GP-11

Stop Wasting Your Time on Sample Environments

Louis Joseph Santodonato (Oak Ridge National Laboratory)

Researchers are understandably frustrated when a large chunk of their neutron beam time is lost because of equipment trouble. Sample environment devices are often the culprit here, so we must place a high priority on improving their reliability and ease of use. This will have a direct impact on the strength of our scientific programs and help attract new users to the neutron community. The strategy being pursued at the Spallation Neutron Source

involves site-wide support infrastructure, systematic diagnostic testing, emphasis on accessory development, and thorough market research to select the best products.

Tues. 10:30 a.m.–12:00 p.m., Poster, GP-12

Neutron Diffraction from Levitated Liquids—A Technique for Measurements Under Extreme Conditions

Richard Weber, Jean Tangeman (Containerless Research, Inc.), Christopher Benmore, Joan Siewenie (Argonne National Laboratory)

Combining neutron diffraction and containerless techniques enables the structure of liquid oxides to be studied at extreme temperatures and under highly non-equilibrium conditions. Results complement data obtained by X-ray techniques and permit a detailed understanding of the relaxation of liquid structures. This paper will describe the implementation of experiments on molten group II metal oxide aluminates under containerless conditions. Data were obtained at the Glass Liquids and Amorphous Diffractometer at the Intense Pulsed Neutron Source using aerodynamic levitation and CO₂ laser beam heating of 3- to 3.5-mm-diameter liquid samples. Levitation was performed in argon gas and using pure vanadium nozzles. Structure factors were measured for liquids with the compositions CaAl₂O₄, Ca₆₇Al₆₆O₁₆₆, and Sr₆₇Al₆₆O₁₆₆ at temperatures up to 2100 K. Results will be compared to data for glasses with the same chemical compositions.

Work supported by the U.S. Department of Energy under contracts DE-FG02-01ER86121 (CRI) and W-31-109-ENG-38 (IPNS).

Tues. 10:30 a.m.–12:00 p.m., Poster, GP-13

Polarization System of the SNS Magnetism Reflectometer

Frank Klose, Andre Parizzi, Wai Tung Lee (Argonne National Laboratory)

In this contribution, we describe the expected performance of the polarization system of the magnetism reflectometer designed for the Spallation Neutron Source.

The polarizing optical elements consist of bender-type polarizers and analyzers. Mezei-type spin flippers are compared with radio-frequency and spatial spin-resonance flippers. The outcome of a set of polarized Monte Carlo simulations will be presented. Realistic reflectivity/spin-flip spectra are used to model the polarizing optical elements and the spin-flippers. The moderator spectrum is modeled with data obtained from Monte Carlo simulations as well. The detailed pulse shape (i.e., the time structure of the source) and the intensity profile are taken into account. Based on the results, we discuss some important features of the instrument, such as (1) usable wavelength range, (2) angular divergence of the beam that can be handled by the setup, (3) evaluations of typical measurement times, (4) achievable resolution, etc. Although the details of the (nonpolarizing) neutron guide system and other elements are included in the model, the focus is kept on the performance of the polarizing and analyzing elements and on simulating magnetic reflectivity measurements performed on typical samples, using a pulsed source.

Tues. 10:30 a.m.–12:00 p.m., Poster, GP-14

X-Y-Z Magnet for Polarized Neutron Reflectometry

Gian P. Felcher, R. J. Goyette, H. Belch, K. Volin, S. G. E. te Velthuis (Argonne National Laboratory), M. N. Jirmanus (Janis Research Company)

The polarized neutron reflectometer POSYI at the Intense Pulsed Neutron Source has been equipped with a magnet composed of three mutually perpendicular pairs of superconducting coils. The pairs provide magnetic fields on the sample up to 8 and 20 kOe in the horizontal plane (which is also the scattering plane) and 8 kOe in the vertical direction. The coils are independently controlled. The sample—with a maximum diameter of 2.5 cm—is temperature controlled between 1.6 and 300 K. Clear passages are provided for neutrons transmitted through the major axes of the two horizontal fields, with only 2 mm of aluminum along the neutron flight path. An automated horizontal motion allows precise positioning of the magnet in the neutron beam, and a jack lifts the magnet out of the way when not needed. The X-Y-Z magnet provides a new degree of flexibility in reflectivity experiments. The magnetic state of a sample is dependent on its history, and the combination of fields and tempera-

ture control allows virtually all kinds of magnetic and cooling cycles. The 20 kOe field, when applied perpendicularly to the surface, is larger than the shape anisotropy for most magnetic systems and is therefore sufficient to pull the magnetization perpendicular to the surface, thereby nullifying the magnetic scattering. The applied field can orient the polarization of the neutron beam in any direction. These features will greatly increase the usefulness of polarized neutron reflectometry in studying the magnetic phenomenology of thin films and multilayers.

This work was supported by the U.S. Department of Energy Office of Science under contract W-31-109-ENG-38.

Tues. 10:30 a.m.–12:00 p.m., Poster, GP-15

Dynamic Neutron Energy Filter for Spallation Sources

Andre de Azevedo Parizzi (Argonne National Laboratory and Federal University of Rio Grande do Sul), Frank Klose, Wai-Tung Lee (Oak Ridge National Laboratory)

We present a new approach for dynamic neutron energy filtering at pulsed sources, based on the original concept of the Drabkin spin-resonance flipper. The apparatus utilizes the neutron magnetic moment and consists of a wavelength-selective magnetic resonator and a supermirror polarizer/analyzer system. In this contribution, we present a design for a prototype spin-resonator that can be operated in conjunction with the 60-Hz Spallation Neutron Source for wavelengths larger than 2 Å. Descriptions of key design features and solutions to overcome practical problems are discussed. The performance of the proposed design is calculated. A computer program for modeling the spin-flip process inside the energy filter has been developed, in which the spin state along the flight path through spin resonance flipper is calculated using a quantum mechanics approach. Using the program, we have evaluated the effects of different time-dependent magnetic field profiles along the flipper. The results are combined with the performance estimated for other optical elements and polarization devices of the SNS magnetism reflectometer, at which we will eventually install the resonator. The impact of the energy filter on the

instrument performance will be illustrated by comparing results of simulated reflectivity measurements with and without using the device.

Tues. 10:30 a.m.–12:00 p.m., Poster, GP-16

Spallation Neutron Source Neutron Chopper Systems

David B. Chojnowski (Oak Ridge National Laboratory and Argonne National Laboratory), Ralph Niemann, Michael Molitsky (Argonne National Laboratory), Doug Abernathy (Oak Ridge National Laboratory)

Spallation Neutron Source (SNS) instrument beam lines will use neutron choppers to modify the neutron beams along their paths from the target/moderator to the instrument sample volumes. Three functional classes of neutron choppers will be employed: (1) T_0 choppers—block fast neutrons from the prompt pulse; (2) bandwidth-limiting choppers—block all neutrons except those in the bandwidth of interest; (3) E_0 choppers—transmit only a very narrow bandwidth of neutrons. The status of the SNS chopper construction program will be presented. Progress to date includes design, construction, and operation of two prototype T_0 choppers; procurement and operation of a prototype E_0 chopper; and the procurement of low-speed bandwidth choppers.

Tues. 10:30 a.m.–12:00 p.m., Poster, GP-17

Performance of the PHAROS T-Zero Chopper with DSP Control

Chris R. Rose, Patrick D. Lara (Los Alamos National Laboratory)

The PHAROS T-zero chopper at Los Alamos National Laboratory's neutron-scattering facility is controlled by a DSP-based speed and phase controller. This paper supplements and updates previously published methods and data regarding the control and performance of the chopper. The PHAROS chopper has a moment of inertia of about 17 kg-m² and weight of more than 800 lb. Using the controller, the user can operate the chopper at 20, 40, or 60 Hz and remain phase-locked to an AC-power-grid-

based reference signal. Built-in circuitry detects when the top-dead-center of the chopper falls outside a user-programmable window with respect to the timing reference pulse and generates veto events used by the data-acquisition system. This paper will present performance data taken in August 2001 that show the chopper tracking sigma to be about 350 ns at a 60 revolution speed as well as explain the hardware used to implement the control system, remote links, and methodologies used to implement a robust chopper control system.

Tues. 10:30 a.m.–12:00 p.m., Poster, GP-18

High-Resolution, Large-Aperture, High-Speed Fermi Chopper—Advancing Technology

Joseph S. Fieramosca (Argonne National Laboratory)

The Argonne Intense Pulsed Neutron Source (IPNS) has provided two chopper spectrometers, HRMECS and LRMECS, to users for spectroscopic investigations of materials for more than 20 years. The original chopper system—rotor, motors, bearings, phasing control, electronic system, etc.—is still in use today. An upgrade of the chopper system is under way to increase the resolving power of HRMECS from 4 to 1.5% of DE/E0 (where DE and E0 are the full-width-at-half-maximum of energy transfer E and the incident energy, respectively), resulting in better quality S(Q, E) measurements, matching those of the HET and MARI chopper spectrometers at ISIS. This will require the choppers to transmit a beam size of 7.62×10.16 cm for HRMECS at a rotational speed up to 600 Hz, making it the world's largest aperture high-speed chopper for pulsed-source neutron spectroscopy. Various materials, including monolithic metal-based and fiber-reinforced composite-based structures, were investigated for use in the construction of the rotor and slit-package housing. The chopper is to be mounted onto a magnetic-bearing/motor drive shaft system. The upgrade project is a collaboration of several teams, including engineers and scientists at IPNS, the Spallation Neutron Source, and the Materials Sciences Corporation in the United States and Forschungszentrum Jülich in Germany.

Work performed at Argonne National Laboratory is supported by the U.S. Department of Energy Office of Basic Energy Sciences under contract W-31-109-ENG-38.

Tues. Morning, GQ–Magnetism*Summit Grand Ballroom II***Tues. 10:30 a.m.–12:00 p.m., Poster, GQ-01****Antiferromagnetic Polaron Correlations in $\text{Nd}_{0.6}\text{Sr}_{1.4}\text{MnO}_4$**

Branton J. Campbell, R. Osborn, J. F. Mitchell, H. Zheng, E. Badica, S. Rosenkranz (Argonne National Laboratory), J. W. Lynn (National Institute of Standards and Technology Center for Neutron Research)

Magnetization and triple-axis neutron-scattering measurements have uncovered a low-temperature polaronic cluster-glass state in the single-layered perovskite manganite $\text{Nd}_{0.6}\text{Sr}_{1.4}\text{MnO}_4$, which simultaneously exhibits short-range charge/orbital and antiferromagnetic correlations.

Tues. 10:30 a.m.–12:00 p.m., Poster, GQ-02**Structural Order/Disorder and Properties of $\text{RE}_{1-x}\text{Ba}_x\text{MnO}_8$**

Omar Chmaissem, B. Dabrowski, J. Mais, S. Kolesnik, D. E. Brown (Northern Illinois University), J. D. Jorgensen, S. Short (Argonne National Laboratory)

We successfully synthesized $\text{RE}_{0.5}\text{Ba}_{0.5}\text{MnO}_8$ materials (RE = Y, Sm, Pr, Nd, La) with oxygen contents δ of 2.5 or 3 atoms per unit cell. Using a thermogravimetric balance to carefully monitor the synthesis conditions and the final oxygen content of the samples, we deliberately prepared disordered cubic Pm3m samples assuming the ABO_3 perovskite structure and ordered layered materials assuming the tetragonal P4/mmm structure in which lanthanum and barium atoms occupy independent layers in an orderly fashion. We investigated the temperature dependency of the structures of these materials using

neutron powder diffraction (Intense Pulsed Neutron Source) and synchrotron X rays (Advanced Photon Source). The properties of these materials were established from magnetization and resistivity measurements that show two distinct transitions at different temperatures corresponding to the ferromagnetic ordering of the samples at higher temperatures and the possible charge/orbital ordering and antiferromagnetic ordering at lower temperatures. We observe clear correlations between the structure and the magnetic resistive and charge ordering properties of the samples. Similar behavior also was observed for the oxygen deficient samples ($\delta = 2.5$).

Work at Northern Illinois University was supported by the DARPA/ONR and by the state of Illinois under HECA. At Argonne National Laboratory, this work was supported by the U.S. Department of Energy Office of Science under contract W-31-109-ENG-38.

Tues. 10:30 a.m.–12:00 p.m., Poster, GQ-03**Magnetic Coupling in the CMR Manganites**

Jaime A. Fernandez-Baca (Oak Ridge National Laboratory), Pengcheng Dai (University of Tennessee and Oak Ridge National Laboratory), H. Kawano-Furukawa (Ochanomizu University), H. Yoshizawa (University of Tokyo), Y. Tomioka (Joint Research Center for Atom Technology and Correlated Electron Research Center), Y. Tokura (Joint Research Center for Atom Technology, Correlated Electron Research Center, and University of Tokyo)

Inelastic neutron scattering has been utilized to study the spin excitations in ferromagnetic $\text{La}(1-x)\text{Ca}(x)\text{MnO}(3)$ (LCMO) as a function of the hole-doping x (0.2, 0.25, and 0.30) and in ferromagnetic $\text{Pr}(0.70)\text{Ca}(0.3)\text{MnO}(3)$ as a function of external magnetic field. The evolution of the magnetic coupling in these materials as they undergo a metal-to-insulator transition is both surprising and inconsistent with existing models for these materials such as Heisenberg ferromagnetism, double-exchange, or modified double-exchange. These results will be discussed.

Tues. 10:30 a.m.–12:00 p.m., Poster, GQ-04

Mode Splitting in Doped SmS

Randy Scott Fishman, Sam Liu (University of California, San Diego)

We show that the recently observed mode splitting in SmYS can be explained by a simple model which breaks the cubic environment of each samarium atom due to the Y impurities. It is well known that the dispersive mode observed in pure SmS is produced by the exchange interaction between samarium atoms with crystal field states of $J = 0$ and $J = 1$ (three-fold degenerate). Because of the broken symmetry in doped SmYS, the $J = 1$ crystal field state splits into a doublet and a singlet with energies Δ_1 and $\Delta_2 > \Delta_1$. Although the local quantization axis is randomly oriented, two well-defined modes are found. Along the (111) direction, the difference between the mode frequencies is approximately $\Delta_2 - \Delta_1$, which for small impurity concentrations x is a linearly increasing function of x . As expected, the fits to the experimental data also indicate that the exchange interactions are decreasing functions of doping.

Tues. 10:30 a.m.–12:00 p.m., Poster, GQ-05

Enhancement of Long-Range Magnetic Order by Magnetic Field in Superconducting $\text{La}_2\text{CuO}_{(4+y)}$

Boris Khaykovich (Massachusetts Institute of Technology)

We report a detailed study, using neutron scattering, transport, and magnetization measurements, of the interplay between superconducting (SC) and spin density wave (SDW) order in $\text{La}_2\text{CuO}_{(4+y)}$. Both kinds of order set in below the same critical temperature. However, the SDW order grows with applied magnetic field, whereas SC order is suppressed. Most importantly, the field dependence of the SDW Bragg peak intensity has a cusp at zero field, as predicted by a recent theory of competing SDW and SC order. This leads us to conclude that there is a repulsive coupling between the two order parameters. The question of whether the two kinds of order coexist or microscopically phase separate is discussed.

Tues. 10:30 a.m.–12:00 p.m., Poster, GQ-06

Longitudinal Mode in a Quasi-One-Dimensional, Spin-1/2, Heisenberg Antiferromagnet

Bella Lake (Oak Ridge National Laboratory and Oxford University), S. E. Nagler (Oak Ridge National Laboratory), D. A. Tennant (Rutherford Appleton Laboratory)

KCuF_3 is a quasi-one-dimensional, spin-1/2, Heisenberg antiferromagnet, where the dominant exchange interactions couple the magnetic Cu^{2+} ions into antiferromagnetic chains and weak ferromagnetic exchange interactions act to couple these chains together leading to long-range antiferromagnetic order below the Néel temperature of $T_N = 39$ K. The suppressed ordering temperature and moment reduction of 50% (from Néel ordering) show that in spite of the interchain coupling, KCuF_3 exhibits strong quantum fluctuations. Our measurements of the low-temperature phase reveal for the first time the existence of a longitudinal mode using the experimental technique of both polarized and unpolarized neutron scattering. This mode signals the crossover from one-dimensional to three-dimensional behavior and indicates a reduction of the ordered spin moment in the ground state of a spin-1/2 antiferromagnet. Low-temperature measurements ($T < 11$ K) are compared with recent quantum field theory results, and the data are found to be in excellent agreement with the predicted energy and intensity. One feature that was not predicted by theory is damping of the mode by decay processes to the transverse spin-wave branches. The temperature dependence of both the longitudinal mode and the zone-boundary spin-waves (in the direction perpendicular to the chain) were also measured. The data reveal that both modes broaden as temperature approaches T_N and their energy drops somewhat. Unexpectedly however, both features are still observable above T_N at finite energy transfer although with reduced amplitude. These results are discussed in the light of current models.

Tues. 10:30 a.m.–12:00 p.m., Poster, GQ-07

Is CaRuO₃ Antiferromagnetic?

Juscelino Batista Leao, J. J. Neumeier (Florida Atlantic University), D. N. Argyriou (Hahn-Meitner Institut), C. D. Ling (Institut Laue-Langevin)

Early reports [1, 2] of antiferromagnetism in CaRuO₃ will be discussed within the framework of our recent experiments. We have observed that slight ruthenium deficiency (~1 to 2%) leads to a weak feature in the magnetic susceptibility. Temperature-dependant time-of-flight neutron powder diffraction data revealed no long-range magnetic order in the ruthenium deficient CaRuO₃ sample. More careful analysis of magnetization data indicates that a weak ferromagnetic phase forms below an ordering temperature of $T = 147$ K. It was also observed that this feature is destroyed with lanthanum doping (~2%). Measurements of the magnetic susceptibility versus temperature of the series Ca(1-x)La(x)RuO₃ ($0 \leq x \leq 0.1$) led to further study of CaRuO₃ and SrRuO₃. The structural parameters of CaRuO₃ and SrRuO₃ powder samples, obtained from neutron time-of-flight data analysis via Rietveld refinement, will be compared. [1] J. B. Goodenough, *Progr. Solid-State Chem.* **5**(1971) 330. [2] J. M. Longo, P. M. Raccach, and J. B. Goodenough, *J. Appl. Phys.* **39**(1968) 1327.

Tues. 10:30 a.m.–12:00 p.m., Poster, GQ-08

Pressure Dependence of Magnetism and Dynamic Response in TbCu₂

Michael B. Loewenhaupt, M. Rotter, M. Doerr, A. Schneidewind (Technische Universität Dresden), R. I. Bewley, R. S. Eccleston, W. Kockelmann (Rutherford Appleton Laboratory), G. Behr (Leibniz-Institut für Festkörper- und Werkstoffforschung Dresden)

Some members of the RCu₂ (R = rare earth) series are known to show strong magnetostrictive effects (GMS = giant magnetostriction). Inelastic neutron-scattering experiments were performed at the HET spectrometer of ISIS in order to investigate the crystal electric field (CF) and magnetoelastic interactions in Tb_{1-x}Y_xCu₂ ($x = 0.05$ and $x = 1$) powder samples in detail. The CF excitation spectrum of TbCu₂ at 60 K indicates a ground state quasi

doublet (0 and 0.58 meV) and two levels at about 4.9 and 6.4 meV. At $T = 4$ K, well below $T_N = 54$ K, the level at 0.58 meV is shifted to an energy of about 8 meV above the ground state that can be attributed to the action of the molecular field. The experiments on TbCu₂ were repeated under an external pressure of 2 GPa and show a remarkable change of the spectra. Due to the magnetoelastic interaction, the excitations were shifted by 0.4 meV to higher energies. Neutron diffraction performed at 2 GPa on ROTAX did not show a significant change of the magnetic propagation vector. The experiments indicate a strong interaction between the lattice and the CF, which may be liable for the GMS effect.

Tues. 10:30 a.m.–12:00 p.m., Poster, GQ-9

Non-Fermi-Liquid Behavior in a Locally Disordered System

Wouter Montfrooij, M. C. Aronson (University of Michigan), B. D. Rainford (University of Southampton), J. Mydosh (University of Leiden), A. Murani (Institut Laue-Langevin), P. Haen (Centre de Recherche sur les Très Basses Températures)

Systems that order magnetically at $T = 0$ K, the quantum critical point (QCP), exhibit properties that are not described by Fermi-liquid theory. Most notable are the unusual temperature dependences of the resistivity, susceptibility, and the scaling behavior of the dynamic response function in terms of reduced variables $f(E/T)$ and $g(H/T)$. The latter scale invariance implies that there is no characteristic energy scale associated with the QCP, unlike the case for its classical counterpart. However, the underlying physics driving the QCP, and the origin of the non-Fermi-liquid (nFl) properties, remain mysterious. One of the more hotly debated issues is whether nFl behavior originates from the proximity to a magnetic instability or whether it originates in local disorder, as necessarily introduced by the doping of the sample in order to drive it through the QCP. To address this issue, we present dc susceptibility data and inelastic neutron-scattering experiments on a system that exhibits some degree of disorder, CeRuxFe_{2-x}Ge₂ ($x = 0.3, 0.5, \text{ and } 0.8$). Systems of this type are known to be able to support a well-defined magnetic phase, despite the presence of disorder. With increasing x , the compound goes from a heavy fermion system, through a QCP (at $x = 0.5$) into an antiferromag-

netic phase, and finally into a ferromagnetic phase. We observe nFI behavior near the QCP for $x = 0.5$, extending to temperatures as high as 20 K. We show that the QCP is characterized by correlations that are long ranged in time, yet remain practically localized in space. This is the opposite of what happens at a classical phase transition and is in qualitative agreement with recent theories on the role of disorder at a QCP.

Tues. 10:30 a.m.–12:00 p.m., Poster, GQ-10

Ilmenite-Hematite Ferromagnetic Semiconductors

Rainer Schad, P. Padmini, R. K. Pandey, W. Butler, H. Alouach (University of Alabama)

Conventional electronics makes use of the charge transfer property of electrons. On the other hand, spintronics takes advantage of spin direction and spin coupling leading to higher speed and very low power consumption. There has been much recent interest in the discovery or creation of magnetic semiconductors, with interest centered primarily on traditional semiconductors such as GaAs or GaN doped with 3-d atoms such as Mn or Co. However, ferromagnetic semiconductors studied so far often have low Curie temperatures, possibly consist of ferromagnetic precipitates in a semiconducting matrix, have small moments or form doping-bands resulting in a fixed carrier concentration and polarity (most often p-type). An alternative approach is to utilize nontraditional materials that are known to be magnetic and semiconducting. One such family of materials is the ilmenite-hematite (IH) solid solution system which have the chemical formula $(1-x)\text{FeTiO}_3 \times (x)\text{Fe}_2\text{O}_3$ and crystallize in a rhombohedral structure. The stoichiometric ilmenite is a p-type semiconductor and antiferromagnetic with the Néel point of 55 K. It is also one of the best known radiation resistant materials. The band gap of pure ilmenite is 2.58 eV and of hematite it is 2.0 eV. For 0.050.2, samples prepared by us show consistently higher Curie temperatures (about 150 K higher) than those reported in literature. From the measured Seebeck coefficient we found either p or n type semiconductor behavior depending on composition with a transition from p to n type as x increases around $x = 0.2$.

Tues. 10:30 a.m.–12:00 p.m., Poster, GQ-11

Stripe-Liquid Phase in Cuprates and Nickelates

John M. Tranquada, S.-H. Lee (National Institute of Standards and Technology), D. Buttrey (University of Delaware), M. Fujita, K. Yamada (Kyoto University), L. P. Regnault (Commissariat à l’Energie Atomique, Grenoble)

Hole-doped, two-dimensional antiferromagnets are known to frequently exhibit a phenomenon called stripe order, in which the holes segregate to antiphase domain walls of the magnetic background. In cuprate superconductors, stripe order tends to compete with superconductivity. An interesting question is whether a liquid phase of charge stripes can occur. To investigate this, we have studied the dynamical spin correlations in strontium-doped lanthanum nickelate and in (Ba,Sr)-doped lanthanum cuprate. In both cases we find evidence that the stripe solid melts into a stripe-liquid phase.

Tues. 10:30 a.m.–12:00 p.m., Poster, GQ-12

Longitudinal Excitations and Spin-Flops in $\text{BaCu}_2\text{Si}_2\text{O}_7$

Andrey Zheludev (Oak Ridge National Laboratory), I. Tsukada (Central Research Institute of Electric Power Industry), E. Ressouche (DRFMC/SPSMS/MDN, CENG), T. Masuda, K. Uchinokura (University of Tokyo), K. Kakurai (Japan Atomic Energy Research Institute)

$\text{BaCu}_2\text{Si}_2\text{O}_7$ is one of the most extensively studied weakly coupled $S = 1/2$ chain quantum antiferromagnets, with a saturation magnetization of only $0.12 \mu_B$ per spin. Neutron diffraction experiments revealed an unusual two-stage spin flop transition in the system. In an external magnetic field $H_c1 = 2$ T, the ordered moment rotates to become perpendicular to the field (conventional spin flop). At $H_c2 = 4$ T, the spin structure undergoes a more unusual second 90° rotation, in the plane perpendicular to the field. The two-stage spin-flop transition allows unique polarization-dependent measurements of quantum spin fluctuations in this quasi-one-dimensional system without using polarized neutrons. It is shown that, unlike in the more three-dimensional KCuF_3 compound, there are no long-lived

longitudinal modes in $\text{BaCu}_2\text{Si}_2\text{O}_7$. The broad inelastic peak seen at the energy where chain-mean-field theories predict the longitudinal mode continuously merges with a diffuse excitation continuum at higher energies.

Tues. 10:30 a.m.–12:00 p.m., Poster, GQ-13

Measuring Lateral Magnetic Structure in Thin Films Using Polarized Neutron Reflectometry

Wai-Tung Lee, S. G. E. te Velthuis, G. P. Felcher (Argonne National Laboratory), F. Klose (Oak Ridge National Laboratory), T. Gredig, D. Dahlberg (University of Minnesota), B. Toperverg (Forschungszentrum Jülich)

Polarized neutron reflectometry (PNR) has long been applied to measure the magnetic depth profile of thin films. In recent years, interest has increased in also observing lateral magnetic structures in a film. While magnetic arrays patterned by lithography and submicron-sized magnetic domains in thin films often give rise to off-specular reflections, micron-sized ferromagnetic domains on a thin film produce few off-specular reflections and the domain distribution information is contained within the specular reflection. In this contribution, we will first show how a long-overlooked characteristic of specular spin-flip reflectivity allows us to measure the distribution of lateral magnetic domains across a thin film. The technique is applied to study the mechanism of magnetization reversal of an exchange-biased Co/CoO bilayer above and below the blocking temperature. In addition, we will present computer simulation studies using the super-matrix formalism to analyze off-specular reflectivity from magnetic arrays.

Tues. 10:30 a.m.–12:00 p.m., Poster, GQ-14

Magnetic Switching of Ferromagnetic Films with Strong Out-of-Plane Anisotropy

Srinath Sanyadanam, G. P. Felcher (Argonne National Laboratory), Paolo Vavassori (University of Ferrara)

The magnetization reversal in CoNiO thin films obliquely deposited and used for magnetic recording has been found to take place by tilting out of the plane until the

external field reverses in magneto-optical studies by P. Vavassori and G. Bottoni [1]. This interpretation is now being tested by polarized neutron reflectivity. Oblique metal evaporation of CoNiO gives rise to columnar structures with columns canted to the tape's normal and along the direction of the tape's length. After inserting the tape in an x-y-z magnet at the POSY I reflectometer of the Intense Pulse Neutron Source at Argonne National Laboratory, the evolution of the magnetic structure is followed as a function of the magnetic field, when applied along the length of the tape and along its width. A coherent rotation of the magnetization takes place without a breakdown of the magnetic film in small domains that would cause broadening of the neutron reflection line. Preliminary measurements indicate that this is the case, when the applied magnetic field is lowered from a saturating value of 3000 Oe. These findings should help explain the behavior of the magnetization and the coercivity, the two main parameters of interest for tapes used in magnetic recording. [1] *J. Appl. Phys.* **90**, 5238 (2001).

Tues. 10:30 a.m.–12:00 p.m., Poster, GQ-15

Epitaxial Nickel films on GaAs(001) by Electroplating

Christian Scheck, Paul Evans, Giovanni Zangari, Rainer Schad (University of Alabama)

Thin ferromagnetic films grown on III/V or II/VI semiconductors using MBE or sputter deposition techniques typically yield unsatisfactory magnetic and electric properties, especially in very thin films, which is due to an interdiffusion at the interface. We deposited nickel films on GaAs(001) substrates using galvanostatic electrodeposition. The thickness range studied is 5 to 100 nm. The film structure is a mixture of two epitaxial orientations, Ni(001) and Ni(011), as verified by out-of-plane and in-plane X-ray diffraction. The saturation moments of these films do not show any reduction towards lower film thickness (down to 5 nm). The thickness dependence of the resistivity does show resistivity values in accordance with Fuchs' Model down to the lowest thicknesses studied. This indicates a strong reduction or absence of interdiffusion problems and better defined interfaces. The magnetic anisotropy is characterized by a superposition of crystalline anisotropy with an uniaxial anisotropy.

Tues. 10:30 a.m.–12:00 p.m., Poster, GQ-16

Spin-Flop Transition in Antiferromagnetic Superlattices

Suzanne G. E. te Velthuis, J. S. Jiang, S. D. Bader, G. P. Felcher (Argonne National Laboratory)

An antiferromagnetically (AF) coupled Fe/Cr(211) superlattice with uniaxial magnetic anisotropy has been used to study the spin-flop transition in an AF with a finite number of layers. It has been predicted that at a field a lower than the bulk spin-flop field, a domain wall is created at the surface and rapidly propagates toward the center of the sublattice[1]. We present extensive polarized neutron reflectivity measurements that give the evolution of the magnetic configuration during the spin-flop transition and prove directly the existence of such a state, in which the superlattice splits in two anti-phase, AF domains. [1] R. W. Wang, D. L. Mills, Eric E. Fullerton, J. E. Mattson, and S. D. Bader, *Phys. Rev. Lett.* **72** (1994) 920.

This work was supported by the U.S. Department of Energy Office of Science under contract W-31-109-ENG-38.

Tues. Morning, GR-Materials

Summit Grand Ballroom II

Tues. 10:30 a.m.–12:00 p.m., Poster, GR-01

Influence of Hydrostatic Pressure on Structural Distortions in La_{1.48}Nd_{0.4}Sr_{0.12}CuO₄

Irina Vasilyevna Pozdnyakova, D. Louca (University of Virginia), T. Egami (University of Pennsylvania), S. Uchida (University of Tokyo)

In La_{1.48}Nd_{0.4}Sr_{0.12}CuO₄, lattice instabilities strongly affect superconducting (SC) properties. In particular, its tetragonal phase stable at low temperatures suppresses SC due to charge stripes pinning. The T_c is pressure dependent in this system. Therefore, a study of the

distortions induced by pressure could reveal possible mechanisms responsible for the onset of SC and the increase in T_c. We have investigated the effects of hydrostatic pressure on the structure of La_{1.48}Nd_{0.4}Sr_{0.12}CuO₄ from 0 to 6 kbars at 4 K, using neutron powder diffraction. The data were collected at the Polaris diffractometer at ISIS. We found that there is a first-order pressure induced phase transformation from the low-temperature tetragonal (LTT) P4₂/ncm to an orthorhombic Pccn phase. The second phase appears at 2 kbars and coexists with the tetragonal phase until at least 6 kbars. Increasing the pressure causes the tilt angle of the CuO₆ octahedra to increase in the Pccn phase. The Cu-O planar bonds have qualitatively different types of distortions in the Pccn phase, while in the LTT the buckling in Cu-O planes remains unchanged. The thermal factors in the second phase are large by comparison with the LTT phase. The influence of structural changes on T_c behavior is discussed. It appears that flat Cu-O bonds favor SC regardless of macroscopic symmetry.

Tues. 10:30 a.m.–12:00 p.m., Poster, GR-02

High-Temperature Structure Refinement of Bi₂O₃-CaO by Neutron Diffraction

Edward Andrew Payzant, Stephen D. Nunn (Oak Ridge National Laboratory), Donald W. Brown, (Los Alamos National Laboratory)

At moderately high temperatures, doped bismuth oxide is a fast oxygen ion conductor with potential application as a membrane for gas separation. The rhombohedral beta-phase of Bi₂O₃ is formed by partial substitution for the bismuth atoms by divalent alkaline earth ions such as calcium, strontium, and barium and is stable at room temperature. The cubic delta-phase of Bi₂O₃ is only stable at high temperatures but can be stabilized by divalent alkaline earth ion dopants to lower temperatures, below which it decomposes into a mixture of monoclinic alpha- Bi₂O₃ and rhombohedral beta- Bi₂O₃-CaO. While conventional X-ray diffraction is useful for structure refinement and determining the cation site distribution, it cannot resolve the oxygen defect distribution on the anion sites in this system. Consequently, an in situ high-temperature neutron diffraction study of the eutectoid composition Bi₂O₃-10.75%CaO was undertaken using the Neutron Powder Diffractometer at the Los Alamos Neutron

Science Center. Diffraction patterns were taken at temperatures above and below the eutectoid temperature, and structure refinements were carried out using GSAS.

Research was sponsored by the Laboratory Directed Research and Development Program of Oak Ridge National Laboratory, managed by UT-Battelle, LLC, for the U.S. Department of Energy under contract DE-AC05-00OR22725. This work has benefited from the use of the Los Alamos Neutron Science Center at Los Alamos National Laboratory. This facility is funded by the U.S. Department of Energy under contract W-7405-ENG-36.

Tues. 10:30 a.m.–12:00 p.m., Poster, GR-03

Phonon Dispersion Measurements of $\text{YBa}_2\text{Cu}_3\text{O}_{6.15}$ and $\text{YBa}_2\text{Cu}_3\text{O}_{6.95}$ by Time-of-Flight Neutron Spectroscopy

Jae-Ho Chung, Takeshi Egami (University of Pennsylvania), Rob McQueeney (Los Alamos National Laboratory), Mohana Yethiraj (Oak Ridge National Laboratory), Masatoshi Arai (KEK)

We report on our recent observations of the strong in-plane anisotropy in the phonon dispersion of $\text{YBa}_2\text{Cu}_3\text{O}_{6.95}$, which changes with the onset of superconductivity. We also report on the high-energy oxygen vibrational modes in the insulating $\text{YBa}_2\text{Cu}_3\text{O}_{6.15}$ with previously unseen details. We used time-of-flight neutron scattering with a large array of position sensitive detectors (MAPS of the ISIS) to observe the wide range of energy-momentum space simultaneously. The in-plane oxygen bond-stretching mode, while nearly dispersionless for the insulating compound, showed strong in-plane anisotropy for the superconducting compound. The dispersion along b-direction showed characteristic softening with continuous dispersion. On the other hand, the dispersion along a-direction showed less softening and split dispersions indicated by the loss of intensity toward the zone boundary, which could be recovered near the b-directional mode. These findings suggest there is a dynamic unit cell doubling primarily along the a-axis. The corresponding TO mode, however, did not show a clear signature of the split dispersion, suggesting that the split dispersion is not the result of simple force constant modification. Below T_c the b-dispersion also showed a

tendency for split dispersion and the anisotropy is reduced in the superconducting phase, showing consistency with the previous triple-axis measurements. This result is consistent with the anisotropy in the underlying electronic structure and the presence of a dynamic stripe structure with 2a periodicity. For the insulating compound, two modes, previously unseen with neutrons, are found to lie above the in-plane bond-stretching mode. These modes are assigned as out-of-phase and in-phase apical oxygen bond-stretching modes, following IR and Raman spectroscopies. In the superconducting phase, they showed even larger zone-center softening than the in-plane modes, indicating that the c-axis Cu-O interaction is renormalized more strongly with charge doping. A few more important comparisons between the two compounds will be discussed as well.

Tues. 10:30 a.m.–12:00 p.m., Poster, GR-04

Synthesis and Characterization of the First 1:2-Ordered Perovskite Ruthenate

Job Thomas Rijssenbeek, Kenneth R. Poeppelmeier (Northwestern University), Sylvie Malo, Vincent Caignaert (Université de Caen)

Perovskite-like mixed metal ruthenates are of interest owing to their varied magnetic properties, which are heavily dependent on the ordering of the transition metals. We report the synthesis and structural characterization, via powder X-ray, electron, and neutron diffraction, of $\text{Sr}_3\text{CaRu}_2\text{O}_9$. The structure is characterized by a 1:2 ordering of Ca^{2+} and Ru^{5+} over the six-coordinate B-sites of the perovskite lattice akin to the well-known dielectric $\text{Ba}_3\text{ZnTa}_2\text{O}_9$ (BZT). The significant bond length mismatch between Ca-O and Ru-O leads to significant tilting, twisting, and deformation of the metal-oxygen octahedra. $\text{Sr}_3\text{CaRu}_2\text{O}_9$ is the first example of this structure-type to include a majority metal with d electrons (Ru(V) , d^3). The relationship of this material to the $n = 1$ Ruddlesden-Popper type $\text{Sr}_{1.5}\text{Ca}_{0.5}\text{RuO}_4$ (i.e., $\text{Sr}_3\text{CaRu}_2\text{O}_8$) highlights the dramatic effects of the ruthenium valence on the resultant structure. Remarkably, each of these structures can be quantitatively converted to the other by the appropriate choice of reaction temperature and atmosphere. X-ray, electron, and neutron diffraction results will be presented along with some preliminary electronic characterization.

Tues. 10:30 a.m.–12:00 p.m., Poster, GR-05

Neutron Powder Diffraction of $\text{Sr}_2\text{MnSbO}_6$, $\text{Sr}_2\text{MnNbO}_6$, $\text{Ca}_2\text{MnSbO}_6$, $\text{Ca}_2\text{MnNbO}_6$, and $\text{Ca}_2\text{MnRuO}_6$: Structure Refinement and Investigation of the Chemistry and Crystallography Using the Software Program SPuDS

Michael Wayne Lufaso, Dr. Patrick Woodward (Ohio State University)

The perovskites $\text{Sr}_2\text{MnSbO}_6$, $\text{Sr}_2\text{MnNbO}_6$, $\text{Ca}_2\text{MnSbO}_6$, $\text{Ca}_2\text{MnNbO}_6$, and $\text{Ca}_2\text{MnRuO}_6$ have been synthesized using conventional solid state techniques. X-ray and neutron powder diffraction (ANSTO) data were collected. The crystal structures were solved by a Rietveld refinement method using the atomic fractional starting positions generated with the software program SPuDS. The refinements indicate long-range disorder on the octahedral site; however, the local coordination environment of the octahedral site suggests the possibility of short-range ordering of the octahedral cations. Octahedral cation ordering in perovskites includes long-range ordering (e.g., Ba_2CuWO_6), short-range ordering (e.g., $\text{Sr}_2\text{MnRuO}_6$), disorder (e.g., $\text{Sr}_2\text{MnNbO}_6$), and charge ordering (e.g., $\text{Nd}_1/2\text{Sr}_1/2\text{MnO}_3$). Structure calculations of SPuDS are utilized in an attempt to extract the effects of octahedral tilting, cation ordering, and Jahn-Teller distortions to enhance the understanding of the crystallography in the synthesized perovskites. The software program SPuDS has been developed to predict the crystal structures of perovskites. SPuDS calculates for ten tilt systems with a single B-site cation, Jahn-Teller distorted B-site cation, or a 1:1 disordered arrangement of B-site cations. SPuDS calculates structures for six tilt systems with two B-site cations in a 1:1 “rock salt” ordered arrangement. A comparison of experimental and SPuDS predicted positions is presented for the synthesized perovskites.

Tues. 10:30 a.m.–12:00 p.m., Poster, GR-06

Structural Tuning in Layered Perovskites

Nattamai S. P. Bhuvanesh, Patrick M. Woodward (Ohio State University)

We have prepared several new layered perovskites belonging to the general formula $\text{Ag}_2[\text{A}_{0.5n}\text{B}_n\text{O}_{3n+1}]$ (A = Ca, Sr; B = Nb, Ta; n = 2, 3, 4) from their lithium analogs by soft topochemical ion exchange. The structure, obtained from the powder X-ray and neutron diffraction data, of the room-temperature phases show significant tilting distortions. We have also characterized, for the first time, interesting phase transitions at higher temperatures, which depend uniquely on the identity of A and B cations. Our structural models for the phase transitions agree very well with the changes in the ionic conductivity in these samples. The details of the structures of these new compounds, various phase transitions, and mechanistic aspects of the transitions based on our structural refinements at various temperatures and impedance measurements will be presented in the poster.

Tues. 10:30 a.m.–12:00 p.m., Poster, GR-07

Inelastic Neutron Scattering Study of the Phonon Density of States of the Vanadium-Based Alloys $\text{V}_{93.75}\text{Ni}_{6.25}$, $\text{V}_{93.75}\text{Pd}_{6.25}$, and $\text{V}_{93.75}\text{Pt}_{6.25}$

Olivier Delaire (California Institute of Technology), Tabitha Swan-Wood, Ryan Monson, Brent Fultz (California Institute of Technology)

Experimental and theoretical investigations have shown the importance of vibrational entropy in the thermodynamics of solid-state phase transitions. In this study we investigated the effect of impurity alloying on the phonon density of states and vibrational entropy of vanadium alloys using inelastic neutron scattering. We examined a series of vanadium-based random substitutional alloys: $\text{V}_{93.75}\text{Ni}_{6.25}$, $\text{V}_{93.75}\text{Pd}_{6.25}$, and $\text{V}_{93.75}\text{Pt}_{6.25}$, on which we measured the phonon density of states (DOS) at room temperature by inelastic neutron scattering. Vanadium is ideal for DOS measurements by neutron scattering because it has a cubic crystal structure (BCC) and because it scatters neutrons incoherently, which allows for reliable extraction of the phonon DOS. All measure-

ments were carried on the LRMECS time-of-flight chopper spectrometer at the IPNS neutron source at Argonne National Laboratory. Previous results have been reported, showing large effects of the dilute alloying on the vanadium phonon density of states and vibrational entropy. These older measurements are somewhat inconsistent however. We compare the data we acquired with these previous measurements carried on the same binary systems at comparable compositions. The elements Ni, Pd, and Pt have the same electronic structure (they are all in the same column of the periodic table), so the differences between the phonon DOS of the three alloys are entirely due to mass and size effects of the impurity atoms. We present preliminary results of Born-von Karman lattice dynamics simulations and interpret the alloying effects of Ni, Pd, and Pt impurity atoms in terms of their difference in atomic mass and metallic radius with the vanadium atoms.

Tues. 10:30 a.m.–12:00 p.m., Poster, GR-08

In Situ Neutron-Scattering Studies of Bragg Glass Melting Transition at the Peak Effect

Sang Ryul Park, X. S. Ling, Ivo Dimitrov, B. A. McClain (Brown University), S. M. Choi (KAIST), J. W. Lynn, D. C. Dender (National Institute of Standards and Technology)

The existence and the nature of the phase transition in the Abrikosov vortex state in weak-pinning type-II superconductors have been a prominent problem in condensed matter physics in recent years. We will present our recent discovery of the hysteresis effect in the structure function of vortex matter using small-angle neutron scattering, providing the first structural evidence for an order-disorder (Bragg glass melting) transition at the peak effect. We will also present our recent rocking curve measurements in which a giant hysteresis effect is observed for the longitudinal correlation length. It is found that the melting of the Bragg glass is a single first-order transition, accompanied by a disentanglement-entanglement transition.

Tues. 10:30 a.m.–12:00 p.m., Poster, GR-09

High Temperature Phases of Barium Indate

Scott Misture, Scott Speakman (Alfred University)

In situ X-ray and neutron diffraction and atomistic computer simulation have been used to study and model brownmillerite-type ceramic oxides such as $\text{Ba}_2\text{In}_2\text{O}_5$. The order-disorder transformations of these materials have been observed and modeled, with particular attention to long-range ordering and its effect on ionic conductivity. In situ high-temperature diffraction using neutrons and X rays provided sufficient data to determine the crystal structures as a function of temperature and to correlate the structures with the ionic conductivity. Thorough structural studies and conductivity measurements demonstrate that the disordering process that leads to fast oxygen ion conduction is a complex three-stage transformation rather than a simple one-step process. The use of chemical substitution to cause a disordered oxygen sublattice that facilitates ionic conduction has been studied using the experimental and computational techniques described above.

Tues. 10:30 a.m.–12:00 p.m., Poster, GR-10

Effects of Lattice Vacancies on the Phonon DOS of FeAl

Tabitha Liana Swan-Wood, Olivier Delaire, Peter Bogdanoff, Brent Fultz (California Institute of Technology)

FeAl alloys are known to have vacancy concentrations as high as 3 to 4%. The equilibrium concentration of thermal vacancies in a material is given by $c(T) = a \exp(-E/kT)$, where E is the energy of formation and $a = \exp[S(\text{vib})/k]$ with $S(\text{vib})$ the vibrational entropy of vacancy formation. From prior experimental work on vacancy concentrations in FeAl, it appears that a is between 200 and 600, giving an $S(\text{vib})$ between 5 and 6 $k_B/\text{vacancy}$. We expected vibrational entropy to be a significant component of the thermodynamics of vacancy formation in FeAl. It is perhaps also significant that the specific volume of a vacancy is 0.5 of that of an atom. A sample with 2% vacancies would have about 16% of its atoms with vacancies as first-nearest neighbors, so we expected

measurable changes in its phonon spectrum. Inelastic spectra were measured on LRMECS at the Intense Pulsed Neutron Source from three Fe-50 at.% Al samples with vacancy concentrations ranging from approximately 0 to 2% (obtained from gravimetric density measurements). Neutron data were also acquired on PHAROS at Los Alamos National Laboratory under similar conditions. Phonon density of states curves were found correcting for multiphonon scattering, Debye-Waller effects, and the thermal factor. The DOS curves showed a low-energy component separated by an energy gap from a high-energy continuum. Lattice dynamics simulations permitted an approximate correction for the neutron-weighting of the measured $S(Q,E)$ and the identification of the low-energy part of the DOS with primarily Fe motions and the high-energy part with Al motions. With increasing vacancy concentration, the Fe modes spread further into the gap. The Al modes also stiffen slightly with vacancy concentration. Nevertheless, the data do not show any significant change in vibrational entropy between the low- and high-vacancy concentrations. If there is an excess entropy of vacancy formation beyond that of configurational entropy, this excess is not accounted for by vibrational degrees of freedom.

Tues. Afternoon, HA-Biological/Biomimetic Systems I

*Chair: Mathias Lösche (Leipzig University)
Tennessee Ballroom A*

Tues. 1:15 p.m., Invited, HA-01

Neutron and X-Ray Scattering Studies of Biomimetic Ultrathin Films

Tonya Lynn Kuhl, Jarek Majewski, Greg Smith (Los Alamos National Laboratory)

In nature, membranes perform several functions of the living cell, from selective transport and recognition to simple sequestration. In general, the membrane consists of a single bilayer or in special cases, such as the lung surfactants, a single monolayer. Using powerful new neutron and X-ray sources, the techniques of reflectivity

and grazing incidence diffraction permit us to obtain structural information on single monolayers and bilayers in an aqueous environment. Recent results on the structure of lipid films including both polymer-grafted bilayers and monolayers, polymer-tethered bilayers, and protein binding and two-dimensional crystallization under lipid layers at the air-water interface will be highlighted, including data on both the in-plane and layer-normal structures.

Tues. 1:30 p.m., Talk, HA-02

Neutron Reflectivity/Interferometry Studies of Vectorially-Oriented Single Monolayers of Membrane Proteins

Larry R. Kneller, Charles F. Majkrzak (National Institute of Standards and Technology), J. Kent Blasie (University of Pennsylvania)

Vectorially-oriented single monolayers of functional membrane proteins tethered to the surface of solid substrates may provide an ultrathin film whose macroscopic response is determined by the protein's molecular function. For example, cytochrome c or Ca^{2+} -ATPase may be utilized to generate energy-dependent electron or ion transport across the film. Cytochrome c and detergent-solubilized Ca^{2+} -ATPase can each be tethered to and thereby vectorially-oriented on soft surfaces of appropriate organic self-assembled monolayers chemisorbed on the surface of silicon substrates. Neutron reflectivity/interferometry data from cytochrome c monolayers and from Ca^{2+} -ATPase monolayers have been collected on the NG-1 reflectometer at the National Institute of Standards and Technology. Results of these experiments will provide the water distribution profiles within both monolayers and the detergent distribution profile within the Ca^{2+} -ATPase monolayers.

Tues. 1:45 p.m., Talk, HA-03

Neutron Reflectometry Characterization of Planar Soft-Supported Membrane-Mimetic Films

Ursula A. Perez-Salas, Susan Krueger, Charles F. Majkrzak, Norman F. Berk (National Institute of Standards and Technology Center for Neutron Research), Elliot Chaikof, Keith M. Faucher (Emory University)

Lipid membranes, the boundaries for cellular and intracellular structures, regulate many crucial biological processes. Planar-supported mimics of cell membranes are of great interest as model systems for the study of membrane structure/function phenomena in fundamental biophysics research. We studied a supported biomedically relevant membrane-mimetic system composed of a polyelectrolyte cushion, a terpolymer, and a self-assembled phospholipid monolayer and obtained a detailed profile characterization of the system by neutron reflectometry. The water-swallowable hydrophilic polyelectrolyte acts as a support for the biomembrane, not unlike the cytoskeletal support found in actual mammalian cell membranes. The “cushion” polymers are fixed to the flat, hard surface by having the polymer interact with it electrostatically. The terpolymer has the following desirable features: it tethers to the polyelectrolyte layer and it creates a hydrophilic and a hydrophobic region. Unilamellar phospholipid vesicle fusion onto the hydrophobic region of the terpolymer creates the hybrid tethered membrane. For added stability to external force fields (such as shear flow), the phospholipid monolayer is then polymerized in situ, effectively anchoring the lipid layer to the hydrophobic region of the terpolymer. Neutron reflectivity measurements were done on the polyelectrolyte layer, the polyelectrolyte layer plus terpolymer, and the polyelectrolyte layer plus terpolymer plus phospholipid. The layers were studied hydrated and under 95% humidity. By using two water conditions (with D₂O and H₂O) on the polyelectrolyte layer plus terpolymer and the polyelectrolyte layer plus terpolymer plus phospholipids, the distribution of water in the layers was obtained. Because this biomimetic membrane has biomedical applications, the work will include a discussion of membrane proteins relevant to clotting.

Tues. 2:00 p.m., Talk, HA-04

Small-Angle Neutron Scattering Characterization as a Tool for Tailoring Micelle Drug Delivery Systems

Rex Paul Hjelm, Beena Ashok, Carol F. Kirchhoff, Hayat Onyuksel, Israel Rubinstein (University of Illinois at Chicago), P. Thiyagarajan, Jaby Jacob (Argonne National Laboratory)

Advanced drug delivery systems based on solubilization by self-assembling amphiphilic systems may provide a means to carry lipophilic drugs safely to target tissues. By tailoring micelle size and shape, the drug can be delivered to the tissue and, because the carrier particles are made of material similar to the target cell membrane, they can serve to enhance the transport of the therapeutic agent into the cell. We describe the morphological characterization of micelles used for advanced drug delivery using small-angle neutron scattering. The micelles are produced by mixing surfactants with different inherent curvature: egg yolk phosphatidylcholine (EYPC) and distearoylphosphatidyl-ethanolamine (DSPE) modified with poly (ethylene glycol) (PEG) with different molecular weight (1, 2, 3 and 5 KDa). The results show how composition controls micelle size and shape. DSPE-PEG 1KDa did not form micelles in either simple or mixed surfactant solutions. DSPE-PEG at 2, 3, and 5 KDa formed monodispersed spherical micelles, with a DSPE core and PEG corona, at sufficiently low concentration. Tube-like micelles formed in mixtures of DSPE-PEG and EYPC, the length and diameter of which was dependent on the composition.

Tues. 2:15 p.m., Invited, HA-05

Diffraction Studies of Peptides in Membranes

Kalina Hristova (Johns Hopkins University), Douglas Tobias, Stephen H. White (University of California, Irvine)

Structural images of peptides in oriented lipid multilayers can reveal the molecular details of peptide-bilayer interactions. Such structural images (profiles) are obtained using lamellar X-ray and neutron diffraction. The usefulness of these images is limited by the very high thermal disorder

that is intrinsic to the natural bilayer state. We have shown, however, that specific labeling of lipid structural groups, combined with neutron and X-ray diffraction difference methods, allows us to determine the transbilayer distributions of the labeled groups with high experimental precision. Furthermore, the methodology allows the bilayer profiles to be decomposed into a collection of transbilayer probability distributions for all lipid groups (phosphates, carbonyls, etc.). Recently, we have developed an X-ray method, referred to as absolute-scale refinement, which permits the determination of the disposition of peptides in fluid bilayers. Now we seek to develop the methodology further by combining the diffraction methods with molecular dynamics simulations. In essence, our goal is to convert one-dimensional experimental data into three-dimensional dynamic images, such that the ensembles of peptide-lipid structures can be explored in detail.

Tues. 2:30 p.m., Keynote, HA-06

Hydrogen and Hydration in Proteins

Nobuo Niimura (Japan Atomic Energy Research Institute)

One of the most important fields today is structural genomics, in which the functions of proteins are analyzed using the results from synchrotron X-ray and nuclear magnetic resonance protein structure analysis. However, it is difficult in an NMR or X-ray crystallographic analysis of a protein to identify all of the hydrogen atoms and the water molecules of hydration, even though they play important roles in innumerable biological processes. In contrast, the neutron diffraction method has the ability to locate hydrogen position absolutely. We have recently developed a neutron imaging plate (NIP) and a neutron monochromator and have successfully used them to construct a neutron diffractometer dedicated to biological macromolecules (BIX-3) in the JRR-3M reactor. The performance of BIX-3 has been certified as one of the best in the world. By using BIX-3, all the hydrogen atoms and most of the solvent molecules of hydration of lysozyme (Hen Egg-white L. at different pH, Human L.), myoglobin, and rubredoxin (wild type and mutant), which are small but fundamentally important proteins, have been unambiguously identified in 1.5-Å resolution. These structural results have provided new and important

discoveries such as the bifurcated hydrogen bonds in α -helices, the fine structure of methyl group, details of hydrogen/deuterium exchange reactions, and the dynamic behavior of hydration in proteins. We have just finished constructing a much higher-performance neutron diffractometer for protein crystallography, and this will be applied for the study of the hydration structure of DNA and the structures of proteins complexed to pharmaceutically active molecules. The start of this new neutron structural biology project, which will use the next-generation neutron source generated by a high-intensity proton accelerator in the United States and Japan, is also coming into view.

Tues. Afternoon, HB—Industrial Applications

*Chair: John Root (National Research Council of Canada)
Tennessee Ballroom B*

Tues. 1:15 p.m., Keynote, HB-01

Putting Polymer Aggregates to Work: An Industrial Perspective on the Use of Neutron Scattering for Probing Polymers in Solution

Hubert E. King (ExxonMobil Research and Engineering Co.), M. Y. Lin (National Institute of Standards and Technology Center for Neutron Research), L. J. Fetters (Cornell University), D. Richter (KFAJ), J. Hutter (University of Western Ontario)

Studies of the structures of individual polymer chains in solution have a long and rich history. However, it sometimes occurs that isolated single-chain structures are superseded by larger, multichain aggregates. In this talk, we will discuss two instances in which small-angle neutron scattering (SANS) studies played a key role in determining the active structures in commercially important, self-aggregating polymer systems. First, we describe our studies of crystalline-amorphous polyethylene-poly(ethylene-propylene) diblock copolymers. Such diblocks exhibit nucleator activity in various diesel fuels, and this nucleating behavior helps solve the problem of low-temperature operation for diesel vehicles. Smaller wax crystals result that do not clog the fuel filter. Through

SANS contrast variation studies, we find that the active structure is a hairy platelet with a crystalline core surrounded by amorphous hairs. Furthermore, when we add wax to this mixture, these molecules go into the hairs, causing them to stretch, and they accumulate on the surface of the plate's core, strongly suggesting that the nucleating effect originates there. In the second example, we describe our studies of poly(N-vinyl-2-pyrrolidone) in aqueous solution. This polymer kinetically suppresses hydrate crystallization. Formation of natural gas hydrate crystals occurs under low T, high P conditions found in gas and oil pipelines, and under such conditions suppression of the crystallization is essential to prevent blockage. We have used contrast variation methods to examine the polymer conformation of the adsorbed layer of this polymer on the crystal surface. Unlike the expected de Gennes self-similar structure, this surface layer exhibits a thickness several times the polymer coil dimension. Nevertheless, the polymer coverage is low. The structural model that results suggests that polymer clumps cover a small (2%) fraction of the available surface. The surface concentration of these self-aggregates is consistent with a growth inhibition mechanism.

Tues. 1:45 p.m., Invited, HB-02

Creep Relaxation of Surface Flaws in Internally Pressurized Tubes

Brian W. Leitch, Nick Christodoulou (Chalk River Laboratories)

The fuel channel in a CANDU™ (CANadian Deuterium Uranium) reactor consists of a Zr_{2.5}Nb pressure tube, which contains the fuel bundles and the pressurized heavy-water coolant, concentric within a Zircaloy-2 calandria tube. Nondestructive techniques have been used for in-service inspections to monitor pressure tubes for the presence of flaws. Depending on the coolant pressure and temperature history, flaws on the inside surface of the pressure tube can be potential sites for crack initiation. However, it is known that the tube material accommodates the presence of such flaws through creep-based relaxation. It is challenging to describe the creep response of the extruded, cold-worked pressure tubes because of the highly anisotropic nature of the Zr_{2.5}Nb material. A theoretical model of the anisotropic creep behavior has been derived using a self-consistent polycrystalline

analysis of the tube material. Integrating this creep model into a finite-element program and analyzing the flaws shows that, for many of the flaws evaluated, cracking would not initiate because the stress relaxes below the initiation threshold. While this theoretical model was developed by using data from creep experiments conducted under simple stress states, an increased level of confidence results if the model predictions are compared with measurements obtained under multiaxial stress states. A blunt-notched compact-toughness specimen (CTS) was machined from a pressure tube and tested at 250°C. In this experiment the CTS was subjected to a constant crack-mouth-opening displacement for approximately 100 hours, while the material in the plane of the notch was being scanned with neutrons. In particular, the stress relaxation was closely monitored near the blunt-notch region. Good agreement was found between experiment and the finite-element model of the CTS, thus validating the constant strain portion of the theoretical model.

Tues. 2:00 p.m., Invited, HB-03

Using Neutron Diffraction as a Complement to other Nondestructive Strain Probes

Lynn Clapham (Queen's University, Canada)

As our modern infrastructure ages, there is a tremendous need to determine its continued fitness for service. Unfortunately, strain in engineering components is notoriously difficult to measure nondestructively. Traditional nondestructive evaluation methods such as eddy current and ultrasonics are stress sensitive, but these stress effects are relatively small and extremely difficult to interpret. Neutron diffraction and magnetic-based techniques represent the best options for nondestructive stress measurement, although magnetic methods are generally only appropriate for ferromagnetic components. The Applied Magnetics Group at Queen's University in Canada has developed Magnetic Barkhausen Noise (MBN) and Magnetic Flux Leakage (MFL) techniques for strain measurement and makes extensive use of neutron diffraction (ND) measurements at Chalk River. Each of the three methods has its own particular advantages and limitations, and together they comprise a suite of complementary techniques that cover a wide range of strain measurement applications. Neutron diffraction is an

excellent tool for measuring stress “at depth” in engineering components. The small beam size enables strain mapping at corners and crack tips, and the penetration enables accurate depth profiles to be obtained. Furthermore, ND produces direct strain measurements. However, although it can handle large components, it is not suitable for “field” strain inspection and is relatively expensive. MBN is very strain-sensitive; furthermore, the technique is relatively portable and inexpensive. However, measurement are limited primarily to the surface layers (<0.2 mm), which necessitates consistent surface preparation. The final technique, MFL, has been applied primarily for the detection of metal loss (e.g., corrosion), and we are now adapting it for stress detection in pipelines. This talk will briefly outline all three of these techniques and their advantages and limitations. Industrial examples will be used to illustrate how they can be used in combination to meet the challenges of strain measurement in engineering components.

Tues. 2:15 p.m., Invited, HB-04

SANS Characterization of Nanoporous Thin Films for the Next Generation of Integrated Circuits

Barry J. Bauer, Hae-Jeong Lee, Ronald C. Hedden, Christopher Soles, Da-Wei Liu, Wen-li Wu (National Institute of Standards and Technology)

The next generation of integrated circuits will be made from dielectric films that have very low dielectric constants (low-k) made possible by forming very small (<50 Å) pores in the matrix material. The nanoporosity not only lowers the average dielectric constant but also changes the strength, permeability, and other crucial properties of the films. Therefore, it is necessary to characterize the nature of the porosity to guide the synthetic efforts and to correlate a variety of electrical and mechanical properties. The small sample volume of 1-mm-thick films and the desire to characterize the film structure on silicon wafers narrows the number of available measurement methods. Small-angle neutron scattering (SANS) has been carried out on samples surrounded by saturated toluene vapor. The SANS signal goes through a minimum at a toluene- h_8 /toluene- d_8 ratio, which is the “match point” at which time the neutron contrast of the wall material is matched by the toluene mixture. The wall density can be calculated from this

composition directly, without assuming any particular morphology type. The match point mixture is then used to fill the pores at various partial pressures of toluene vapor and SANS of these samples provides an independent measure of pore size distribution.

Tues. 2:30 p.m., Talk, HB-05

Characterization of the Controlled Production of the Pore Structure in Catalytic Carbons Prepared from Paper-Mill Sludge Using SANS and BET

Kenneth C. Littrell, Giselle Sandi, P. Thiyagarajan (Argonne National Laboratory), N. Khalili, M. Campbell (Illinois Institute of Technology)

Activated carbons play an important role in many areas of modern science and technology such as purification of liquids and gases, separations of mixtures, and catalysis. Their value for any particular application is determined by the characteristics of their pore structure. In this study we have used small-angle neutron scattering (SANS) and N_2 -BET to characterize the microstructure of a series of activated carbons produced from paper mill sludge using different amounts of $ZnCl_2$ as the chemical activating agent. The size and morphology of the pores and inclusions were determined from the SANS data. The pores in these carbons are roughly rodlike with radii and volumes that increase as the amount of $ZnCl_2$ used for the production of the carbons increase. Contrast-variation SANS studies demonstrate the existence of two different phases, a zinc-rich particle phase and a bulk carbon phase with nanopores. Both phases are accessible to the solvent. Based on these results, we propose a conceptual model describing these carbons as consisting of amorphous carbon containing zinc-rich particles in large voids linked by narrow channels.

Tues. 2:45 p.m., Talk, HB-06

Strain Response to an Applied Compressive Stress Along the Axis of Rod-Textured Zircaloy-2

Thomas M. Holden, D. Brown, S. C. Vogel, C. N. Tome (Los Alamos National Laboratory)

Zircaloy-2 is a hexagonal close-packed material that is plastically anisotropic but elastically nearly isotropic. In the form of extruded rod, it shows marked crystallographic texture: two-thirds of the grains have [-12-10] crystal axes, and one-third of the grains have [10-10] crystal axes aligned along the rod axis. The strain response depends on the modes of slip and twinning in the material. In particular, [1], the residual strains developed under compression were far smaller than those developed under tension because twinning is activated as a mode of deformation under compression. Measurements have been made of the strain response both parallel and perpendicular to the applied stress with the NPD diffractometer at Los Alamos National Laboratory. Twenty-four distinct Bragg reflections were measured, distributed over the complete stereographic triangle. Measurements were made in the elastic regime, in the plastic region below 350 MPa where twinning is not activated, and from 350 to 500 Mpa, where twinning also occurs. The results confirmed and extended previous work [1]. The measurement of initially absent reflections along the direction of the applied stress is of great importance. These give a unique result for the strain in grains that have twinned. The response for [10-10] and [-12-10] grains along the stress direction shows no departure from linear behavior until twinning sets in. The results are compared with earlier work, [1], with previous measurements on the strain response for applied tensile stress, and with an elasto-plastic self-consistent model for zircaloy-2. [1] S. R. MacEwen, N. Christodoulou, and A. Salinas-Rodriguez, *Metall. Trans.*, 21A, (1990) 1083.

Tues. Afternoon, HC—Surfaces and Adsorption

Chair: Dan Neumann (National Institute of Standards and Technology)

Tennessee Ballroom C

Tues. 1:15 p.m., Invited, HC-01

SANS from Aerosols

Barbara E. Wyslouzil (Worcester Polytechnic Institute), Gerald Wilemski (University of Missouri-Rolla), Reinhard Strey (Universität zu Köln)

In the past five years, we have pioneered the use of small-angle neutron scattering (SANS) to study the properties of nanodroplet aerosols. With condensed phase volume fractions on the order of 10^{-6} , aerosol SANS experiments are technically challenging. The results from our experiments to date, however, are already yielding important insight into particle formation processes in nozzles. In multicomponent droplets, there is also strong theoretical evidence for surface enrichment, i.e., that the surface and interior compositions differ significantly. Surface enrichment is important because it affects nucleation, growth, and evaporation kinetics, and the heterogeneous chemistry of aerosol droplets. This talk will focus on our efforts to use SANS to find direct evidence for surface enrichment in nanodroplets.

Tues. 1:30 p.m., Talk, HC-02

Structure and Dynamics of Monolayer P-Phenylene Oligomer Films on GRAFOIL

Edward James Kintzel, S. Rols (Institut Laue-Langevin), K. W. Herwig (Oak Ridge National Laboratory)

The two-dimensional structures and dynamics of monolayer molecular films of p-terphenyl (p-3P), p-quaterphenyl (p-4P), and p-sexiphenyl (p-6P) adsorbed onto the basal plane of graphite have been investigated by neutron scattering. Structural measurements were carried out at sample/substrate temperatures ranging from 22 to 400 K. Analysis of the two-dimensional diffraction peaks for these films, when compared with the bulk structure, indicates that the long molecular axis is oriented parallel to the substrate surface. A change in coherence length at a temperature corresponding to the bulk order-disorder phase transition is seen for p-3P. Initial results from inelastic and quasi-elastic measurements will be presented.

Research supported in part by U.S. Department of Energy grants DE-FG02-97ER45635, DE-AC05-00R22725, and W-31-109-Eng-38.

Tues. 1:45 p.m., Talk, HC-03

Quasielastic Study of H₂ in MCM-48

Yvonne Glanville, Paul Sokol, Bharat Newalker, Sridhar Komarneni (Pennsylvania State University)

The appearance of novel porous materials has allowed us to explore the effect of geometry on many physical properties. MCM-48 is one such material that allows us to explore these effects. MCM-48 is a porous glass with an ordered arrangement of two interwoven but unconnected three-dimensional pores. The pore structures form a simple cubic lattice leading to a well-defined geometry for the system. We have recently performed quasi-elastic neutron-scattering (QENS) studies of H₂ confined to these pores. Preliminary analysis indicates hop diffusion of the H₂ confined in the pores and an enhancement of the freezing temperature of the H₂ due to the confinement.

Tues. 2:00 p.m., Talk, HC-04

Quasi-elastic Neutron Scattering in Nano Science

Yang Ren (Northern Illinois University and Argonne National Laboratory), D. L. Price, S. U. S. Choi (Argonne National Laboratory)

We present quasielastic neutron-scattering (QENS) studies in nano science: H₂ adsorption in carbon nanotubes and dynamical properties of nanofluids. The H₂ storage in carbon nanotubes is of great interest due to its potential application. For single-walled carbon nanotubes (SWNTs), at 80 K, under a H₂ pressure of 110 atm, H₂ molecules gradually condense in the SWNT sample. After pumping out at 25 K and 20 mTorr, the remaining H₂ molecules show a quantum rotational transition at 14.5 meV, with a peak width that increases linearly with increasing temperature from 4.2 to 35 K. The H₂ molecules remain in the sample up to 65 K and then start to desorb with increasing temperature. The time scale of the dynamics is longer than 15 ps even at 200 K. Our results imply that hydrogen molecules are physisorbed in the interstitial tunnels of the SWNT bundles. For multiwalled carbon nanotubes (MWNTs), under an H₂ pressure of 2 atm, with decreasing temperature H₂ are first adsorbed on the internal surface and then below 40 K on the

external surface. It is found that the curved internal surface is more favorite for H₂ adsorption compared to the flat graphite surface. Nanofluids are thermal fluids containing dispersed nanoparticles. It is recently found that the thermal conductivity of carbon nanotube-suspensions is anomalously greater than theoretical predictions and is nonlinear with nanotube concentrations. We have studied the dynamical change of ethylene glycol (EG) mixed with carbon nanotubes. A significant dynamical enhancement of the EG has been found in the mixture. This indicates that the EG on the nanotubes surface has faster movement compared to pure EG, which is expected to play an important role for the large enhancement of the thermal conductivity of the nanofluids.

This work is supported by the state of Illinois under HECA and the U.S. Department of Energy, BES-DMS, under contract W-31-109-ENG-38.

Tues. 2:15 p.m., Invited, HC-05

Quantum Rotations of Confined Methyl Iodide

Robert Michael Dimeo, Dan A. Neumann (National Institute of Standards and Technology Center for Neutron Research)

Rotational tunneling is an extremely sensitive probe of the magnitude and shape of intermolecular potentials. The quantum rotational motion of methyl iodide, a symmetric quantum top, confined to porous glass disks has been measured using high-resolution inelastic neutron scattering. The details of the tunneling line shape in bulk methyl iodide provide direct information on the magnitude and shape of the hindering potential, thus providing a local probe of the molecular environment. When confined to porous glasses of various pore sizes, the motion of the methyl groups is influenced by a distribution of barrier heights due to disorder induced by the confinement, hence altering the tunneling line shape. Line shape analysis and a simple model of the quantum rotations can then be used to extract the distribution of potential barriers. Measurements of the tunneling excitations of methyl iodide confined to porous glass with a nominal pore diameter of 200 Å reveal a substantial deviation from the bulk behavior. Details of the measurement, analysis, and results will be presented.

Tues. 2:30 p.m., Keynote, HC-06

Structure and Rotational Dynamics of Methane films on MgO Surfaces

John Z. Larese (University of Tennessee and Oak Ridge National Laboratory)

Neutrons are not normally viewed as surface-sensitive probes, but elastic and high-resolution inelastic neutron scattering (INS) techniques are surprisingly effective ways to investigate the structural and dynamical properties of films adsorbed on solid surfaces. If adsorption takes place on crystalline powder samples with large surface-to-volume ratios and with highly uniform surfaces, neutron data can yield remarkably detailed pictures of gas-solid interactions. To illustrate the power of this approach, we will describe here what has been learned with neutrons about the structure and rotational dynamics of methane films adsorbed on MgO(100) surfaces. To a large extent the quality of our ability to accurately characterize the gas-solid interaction potential is determined by the quality of the adsorbate used. We will describe how the MgO powders used in these studies were prepared and characterized. Elastic neutron diffraction data show that at low temperatures, solid methane films on MgO form in a layer-by-layer (LBL) pattern, essentially like the growth of the (100) face of the bulk CH₄ solid. Unfortunately, the diffraction data alone cannot be used to uniquely determine the molecular orientation on the surface plane. We will illustrate how high-resolution INS at low temperature can be used to probe the orientational ordering and disordering of the CH₄ molecules in the monolayer solid. Finally, in light of the LBL growth of CH₄ on MgO mentioned above, we have also followed the evolution of the low-temperature rotational properties as the film grows from one to six layers. We will present our most recent findings and discuss those results in terms of how they can be used to follow how INS can be used to track the intermolecular potentials when a system crossovers from two to three dimensions.

Tues. Afternoon, HD—Research Frontiers in Artificially Structured Materials

Chair: Suzanne te Velthuis (Argonne National Laboratory)

Cumberland Room

Tues. 1:15 p.m., Keynote, HD-01

Nanomagnetism and Neutron Scattering

Ivan K. Schuller (University of California, San Diego)

Magnetism at short length scales is one of the interesting and most active areas in solid state physics and materials science. Modern thin-film and lithography techniques allow preparation of artificially structured magnetic materials that have dimensions comparable to interesting magnetic sizes such as dipolar, exchange, spin diffusion, domain wall, etc., length scales. I will describe several examples, from our work, where neutron scattering has been particularly useful in settling key issues in nanostructured magnetism. This includes interfacial magnetic and structural roughness and interdiffusion, coupling in magnetic multilayers, and reversal mechanisms in exchange-biased systems. I will also describe possible new directions in which neutron scattering could provide answers to key issues in the field.

This work is supported by the U.S. Department of Energy and is done in collaboration with J. W. Cable, M. R. Khan, G. P. Felcher, Michael J. Pechan, J. F. Ankner, David M. Kelly, C. F. Majkrzak, M. R. Fitzsimmons, P. Yashar, C. Leighton, J. Nogues, J. A. Dura, A. Hoffmann, H. Fritzsche, and S. G. E. te Velthuis.

Tues. 1:45 p.m., Invited, HD-02

Exchange-Biased Co/CoO Bilayers Studied by Magnetization, Anisotropic Magnetoresistance, and Polarized Neutron Reflectometry

E. Dan Dahlberg, T. Gredig, I. N. Krivorotov, C. Merton, A. M. Goldman, B. K. Hill (University of Minnesota), G. E. Te Velthuis, A. Berger, G. P. Felcher (Argonne National Laboratory)

Magnetic field-induced reversible and irreversible changes of the exchange anisotropy in Co/CoO bilayers were investigated by magnetization measurements, an anisotropic magnetoresistance (AMR) technique, and polarized neutron reflectivity (PNR). The cobalt films were grown by dc magnetron sputtering and then partially oxidized to form the Co/CoO bilayers. After field cooling to temperatures below the Neel temperature, a variable magnitude magnetic field was applied in the film plane at various angles with respect to the exchange bias direction. The magnetization data show strong effects of training with cycling of the magnetic field. Three qualitatively different behaviors of the exchange anisotropy direction were observed by AMR. The particular behavior was determined by the magnitude of the rotation, the magnitude of the applied magnetic field, and the rotation angle. The PNR confirmed the AMR results that in weak fields, perpendicular to the cooling field, the rotation of the magnetization is largely reversible, but, unlike initial AMR results, the rotation is found to be uniform throughout the cobalt layer thickness. The PNR also revealed the onset of spin-dependent diffuse scattering—off the specular reflection—after a training cycle. Such scattering is due to misaligned Co domains.

Tues. 2:00 p.m., Invited, HD-03

Neutron Reflectometry Studies of Interlayer Coupling in All-Semiconductor Ferromagnetic Superlattices

Henryk Kępa (Warsaw University)

Interlayer exchange coupling (IEC) in magnetic/nonmagnetic multilayers has been the subject of intensive studies for more than a decade. It is now firmly established that in metallic systems the transfer of magnetic polarization

from one magnetic layer to another is conveyed by free carriers in the nonmagnetic spacer layer. Recently, similar IEC phenomena have also been observed in multilayers composed exclusively of semiconductor materials where the concentration of free carriers is several orders of magnitude lower than in metals. The results of neutron reflectometry studies of two classes of ferromagnetic semiconductor superlattices (EuS/PbS and GaMnAs/GaAs) that exhibit IEC are reported. In EuS/PbS superlattices, where the spacer PbS is a narrow-gap semiconductor with free electron concentration 10^{17} - 10^{18} cm⁻³, IEC changes its character from antiferromagnetic to ferromagnetic as the thickness of PbS interlayer increases from about 0.5 to 20 nm. The change is gradual and proceeds through a noncollinear phase occurring for PbS thickness about 10 nm. No IEC has been found in EuS/YbSe superlattices, where the YbSe spacer material has the same structure and lattice parameters as PbS but electrically is an insulator. The latter fact suggests a significant role of mobile electrons in transferring the interlayer interactions, as in the case of metallic systems, despite the much lower carrier concentration. In GaMnAs/GaAs superlattices, the very existence in ferromagnetism of GaMnAs as well as the IEC, observed in neutron reflectometry experiments, can be explained in terms of relatively high (10^{20} cm⁻³) free carrier (holes) concentration. Full polarization analysis of the observed reflectivity profiles reveals that the spin order forming in the GaMnAs layers upon cooling in zero external magnetic field consists—in most cases—of a single magnetic domain only.

Tues. 2:15 p.m., Invited, HD-04

Off-Specular Neutron Reflectivity Studies of Magnetic Thin Films

Sunil K. Sinha (University of California, San Diego), M. Fitzsimmons (Los Alamos National Laboratory), D. R. Lee, S. Stepanov (Argonne National Laboratory), R. M. Osgood III (Massachusetts Institute of Technology), V. Metlushko (University of Illinois)

The properties of thin magnetic films have assumed increased importance in recent years owing to their importance for magnetic storage and recording technologies. It is generally accepted that the chemical and magnetic structure at the interfaces plays a central role in

determining their magnetic and transport properties. Neutron scattering via the techniques of specular reflectivity and off-specular diffuse scattering can be an extremely valuable tool in elucidating the nature of the chemical structure and morphology and the magnetic structure of these interfaces and in studying the statistical properties of the domains. The method is complementary to the technique of resonant magnetic X-ray diffuse scattering. We shall illustrate with examples from recent experiments on magnetic thin films. Examples will also be given of studies of so-called patterned magnetic films, involving arrays of magnetic dots or holes, which can also be studied with grazing incidence techniques using polarized neutron beams.

Tues. 2:30 p.m., Talk, HD-05

Magnetic Properties of Ultrathin Iron Oxide Layers in Metal/Native Oxide Multilayers

Geoffrey S. D. Beach, S. K. Sinha, F. T. Parker, A. E. Berkowitz (University of California, San Diego), M. R. Fitzsimmons (Los Alamos National Laboratory), B. Ramadurai, D. J. Smith (Arizona State University)

Recently, magnetically soft, high-resistivity thin films have been fabricated using a metal/native oxide multilayer (MNOM) structure. The structure consists of thin polycrystalline metallic layers of a high-moment $\text{Co}_x\text{Fe}_{100-x}$ alloy that have been exposed, in situ, to oxygen to form oxide surfaces. We present details of a study of the magnetic properties of the native oxide in MNOMs fabricated with pure iron. Polarized neutron reflectivity (PNR) has been used to obtain spatially resolved profiles of the nuclear and magnetic scattering length densities (SLDs). These results are complemented by Mossbauer spectroscopy and bulk magnetization measurements. Under the present oxidation conditions, ~three monolayers of iron oxidizes in each layer. The hyperfine field distribution of the native oxide suggests that a majority is in a well-defined magnetic state, with an average magnetization similar to that of $\gamma\text{-Fe}_{203}$. However, the oxide hyperfine field is significantly different from those of

known bulk iron oxides. As the native oxide is extremely thin and exchange-coupled to the metal, the magnetization of the oxide may be strongly influenced by the metal. PNR can provide important information on the spatial dependence of the magnetization in the oxide layers. The differences between the nuclear and magnetic SLD profiles near the metal/oxide interface will be interpreted as resulting from magnetic influence of the metal on the oxide.

Tues. 2:45 p.m., Talk, HD-06

Tailoring Polarized Neutron Reflectometry for Chiral Magnetic Structures

Kevin V. O'Donovan, Julie A. Borchers, Charles F. Majkrzak (National Institute of Standards and Technology Center for Neutron Research), Olav Hellwig, Eric E. Fullerton (IBM Almaden Research Center)

The twists of Bloch domain walls may be the driving mechanism behind such phenomena as exchange biasing and exchange-spring magnets, and the ability to track their development in magnetic field should help resolve why some of these materials do not behave as expected from current theories. We used spin-polarized neutron reflectometry (PNR) to study the spin structure of an FePt/NiFe exchange-coupled magnetic bilayer in magnetic field and in remanence. We applied our recently developed technique, which improves the sensitivity of PNR to buried magnetic twists. The implementation is straightforward: the neutron reflectivity is measured with neutrons scattering from the back surface as well as the front surface, thus yielding eight spin cross sections instead of the usual four. Our technique quickly identifies the noncollinear magnetism accompanying buried twists, regardless of the presence of chiral domains of clockwise and anticlockwise twists. We have characterized the spin structure of the exchange spring as a function of field, both applied and remanent. We shall discuss the advantages of our PNR technique and the sorts of magnetic structures that benefit most from its use.

Wednesday, June 26, 2002

Wed. Morning, JA—Biological/Biomimetic Systems II

Chair: Kalina Hristova (Johns Hopkins University)
Tennessee Ballroom A

Wed. 8:30 a.m., Keynote, JA-01

Neutrons in the Era of the “New” Biology

Jill Trehwella (Los Alamos National Laboratory)

The sequencing of the human genome, and the accompanying emergence of high-throughput technologies for studying complex biological systems, has led us to contemplate the possibility of having a comprehensive description of the component structures of biological systems from the genetic material to the RNA and protein structures responsible for cellular functions. The next step beyond obtaining the component structures is to understand how they cooperate to form complex molecular machinery, or how they use their exquisitely precise molecular language to communicate messages from the extracellular environment, or perhaps from another part of the cell, and translate them into the desired response. While there are a few examples of large complex structures (such as the ribosome and polymerase), we are more often in the situation of having information on individual components, or even fragments, and limited information on their interactions. Neutrons can play a vital role in unlocking the secrets of how molecular machines are assembled and operate and in decoding the conformational language used to transmit signals in regulatory networks. I will describe examples of how neutrons can provide these critical insights from our work on the structural biology of second messenger mediated signal transduction: calcium-regulated systems (the molecular switch mechanisms in muscle involving troponin and myosin light chain kinase) and the cAMP-dependent protein kinase.

Wed. 9:00 a.m., Talk, JA-02

Microscopic Views on the Structure of Lipid Surface Monolayers: The Quest for Surface-Sensitive Neutron Scattering

Mathias Lösche (Leipzig University)

Nanotechnology and molecular (bio-)engineering are making ever-deepening inroads into everybody’s daily life. Physicochemical and biotechnological achievements in the design of physiologically active supramolecular assemblies have brought about the quest for their submolecular-level characterization. We employ surface-sensitive scattering techniques for the investigation of planar lipid membranes—for the most part, floating monolayers on aqueous surfaces—to correlate structural, functional, and dynamic aspects of biomembrane models. This contribution surveys recent work on the submolecular structure of floating phospholipid surface monolayers—where the advent of third-generation synchrotron X-ray sources has driven the development of realistic, submolecular-scale chemical models [1, 2]—and on the conformational control of water-soluble grafted “polymer brushes” [3, 4]. The very limited availability of neutron beam lines that enable scattering measurements from horizontal fluid surfaces has in the recent past severely impeded further development of this field. Fortunately, as prospects in this area brighten with new sources in various states of planning and commissioning worldwide, this stringent situation is expected to relax considerably. Perspectives for the life sciences and materials engineering of surface-sensitive scattering that are becoming available with state-of-the-art neutron sources will be given.

[1] M. Schälke, P. Krüger, M. Weygand, and M. Lösche, *Biochim. Biophys. Acta* **1464** (2000) 113. [2] M. Weygand et al., *J. Phys. Chem. B* (2002), in press. [3] E. Politsch, G. Cevc, A. Wurlitzer, and M. Lösche, *Macromolecules* **34** (2001), 1328. [4] A. Wurlitzer et al., *Macromolecules* **34** (2001), 1334.

Wed. 9:15 a.m., Invited, JA-03

Slow Relaxation Process: A Key to the Dynamic Transition in DNA and Proteins

Alexei Sokolov (University of Akron)

Hydrated proteins and DNA demonstrate dynamic transition at temperatures $T_d \sim 200$ -230 K. Sharp slowing down of protein functions (rate of biochemical reactions) was observed at the same temperature range. These results suggest a direct relationship between the dynamic transition and biochemical activities of proteins. Thus, understanding of the dynamic transition may be extremely important for understanding how biopolymers function. The dynamic transition shows up as a sharp rise of mean-squared atomic displacement, $\langle x^2 \rangle$, above a particular temperature T_d . Analysis of $\langle x^2 \rangle$, however, does not bring information on microscopic origin of the dynamic transition. One needs time or frequency resolved spectroscopy. We analyzed dynamics of DNA/D₂O at different levels of hydration using neutron-scattering spectroscopy [1, 2]. The results demonstrate that the dynamic transition is related to a slow relaxation process in DNA. Previous neutron-scattering data obtained for various proteins are discussed and compared with the data obtained on DNA. It is shown that in all cases the dynamic transition can be related to a slow relaxation process that activates above T_d . Speculations about the nature of the dynamic transition are presented, and challenges for neutron-scattering spectroscopy of proteins are discussed. [1] A. P. Sokolov, H. Grimm, R. Kahn, *J. Chem. Phys.* 110, 7053 (1999). [2] A. P. Sokolov, H. Grimm, A. Kisliuk, A. J. Dianoux, *J. Biological Physics* 27, 313-327 (2001).

Wed. 9:30 a.m., Invited, JA-04

Dynamics of Cytochrome c by Quasi-Elastic Neutron Scattering

Adam Mathew Pivovar, Dan Neumann (National Institute of Standards and Technology Center for Neutron Research), Mounir Tarek (Universite Henri Poincare)

To deepen our understanding of the molecular motions involved in protein folding, we have employed differential

quasi-elastic neutron scattering (QENS) to measure the dynamics of cytochrome c in the native and several unfolded states at picosecond timescales. In a typical QENS experiment, neutrons exchange both energy and momentum with the sample, allowing one to surmise the characteristic timescale and length scale, respectively, of the molecular motions involved. Another fundamental property of incoherent neutron scattering is the extremely large relative scattering cross section of hydrogen relative to all other atomic species; that is, atoms other than hydrogen remain virtually invisible in the scattering process. Because the hydrogen distribution within a protein is nearly homogeneous, an incoherent QENS experiment reflects the ensemble dynamics of the protein, particularly motions of the nonexchangeable protons of the side chains. Cytochrome c is ideally suited for these preliminary investigations as it has several well characterized and easily accessible nonnative folded states that, in comparison with the native state, permit rationalization of the dynamic behavior. The experimental results are interpreted using a model that allows one to extract an effective diffusion coefficient, determine the timescale of side chain motions, and surmise the apparent geometry of these motions.

Wed. 9:45 a.m., Talk, JA-05

Influence of Hydration and Cation Binding on Protein Dynamics: a Study from Picosecond up to Nanosecond Time Range

Jean-Marc Zanotti (Laboratoire Léon Brillouin and Argonne National Laboratory), J. Parello (Centre National de la Recherche Scientifique), M.-C. Bellissent-Funel (Laboratoire Léon Brillouin)

Hydration, internal dynamics, and function in proteins are intimately associated. Parvalbumins are acidic Ca²⁺ and Mg²⁺ binding proteins of 11.5 kDa with two Ca²⁺/Mg²⁺ binding sites. They belong to the EF-hand superfamily and are ubiquitous in vertebrates. Through its properties of Ca²⁺/Mg²⁺ exchange, parvalbumin is associated with muscle and neuron relaxation after excitation by Ca²⁺. The increase of the quasi-elastic signal observed, upon hydration, by neutron scattering has been interpreted as an increase of the local mobility of side-chains protons, mainly of the hydrogen-rich lysyl residues (17 residues over 109). This result was in agreement with those from a

parallel study of solid-state natural abundance ^{13}C cross-polarization and magic angle spinning NMR. It was shown that the dynamics of surface-charged residues in the picosecond time range, as seen by neutrons, was concomitant with the dynamics of the protein backbone, in the nanosecond time range, as seen by NMR. In the present work, we take advantage of the complementarities in energy resolution of various neutron spectrometers (i.e., time of flight, backscattering, and spin-echo) to extend our previous neutron measurements. We probe the parvalbumin dynamics from a fraction of picosecond to a few nanoseconds. Influence of hydration and of the nature of the cation on parvalbumin dynamics are discussed.

Wed. Morning, JB—Magnetism III

Chair: Jaime Fernandez-Baca (Oak Ridge National Laboratory)

Tennessee Ballroom B

Wed. 8:30 a.m., Keynote, JB-01

Lattice Polarons and Pseudogap in Colossal Magnetoresistance Manganites

Pengcheng Dai, E. W. Plummer (University of Tennessee and Oak Ridge National Laboratory), J. A. Fernandez-Baca (Oak Ridge National Laboratory), C. P. Adams, J. W. Lynn (National Institute of Standards and Technology), Y. Tomioka (Joint Research Center for Atom Technology), Y. Tokura (Joint Research Center for Atom Technology and University of Tokyo)

Since the discovery of the so-called colossal magnetoresistance (CMR) manganites, there has been considerable interest in understanding the mechanism that produce this effect. The basic microscopic mechanism responsible for this behavior is believed to be the double-exchange interaction. It is well known, however, that this mechanism alone cannot account for the magnitude of the observed effect and that other elements have to be introduced, like the intrinsically inhomogeneous electronic ground state and the existence of lattice/magnetic po-

larons. The direct observation of lattice polarons has been reported as diffuse scattering associated with the lattice distortions that accompany the sites containing e_g electrons (Mn^{3+}) and their short-range correlations. Our measurements on $\text{La}_{0.8}\text{Ca}_{0.2}\text{MnO}_3$, $\text{La}_{0.75}\text{Ca}_{0.25}\text{MnO}_3$, $\text{La}_{0.7}\text{Ca}_{0.3}\text{MnO}_3$, $\text{Pr}_{0.7}\text{Ca}_{0.3}\text{MnO}_3$, and $\text{Nd}_{0.7}\text{Sr}_{0.3}\text{MnO}_3$ at the National Institute for Standards and Technology reactor have revealed the presence of short-range polarons and their correlations. We establish the temperature dependence of the coherence lengths associated with these distortions and show that a scale T^* is needed to describe the formation of these short-range charge clusters. Such results are consistent with recent theoretical proposal for the existence of a pseudogap in CMR manganites.

Wed. 9:00 a.m., Invited, JB-02

Competing Charge, Orbital, and Magnetic Order in Layered CMR Manganites

Raymond Osborn, B. Campbell, D. N. Argyriou, S. Rosenkranz, J. F. Mitchell (Argonne National Laboratory), L. Vasiliu-Doloc (Northern Illinois University), J. W. Lynn (National Institute of Standards and Technology), S. K. Sinha (University of California, San Diego)

It is now well established that colossal magnetoresistance (CMR) in manganite compounds is strongly enhanced by the delicate balance of magnetic, charge, and orbital interactions just above the ordering temperature, whether the low-temperature ground state is a ferromagnetic metal or a charge-ordered insulator. Diffuse neutron and X-ray scattering data give detailed insight into the nanoscale phenomena that result from this competition in the paramagnetic phase of optimally doped layered manganites. The ferromagnetic correlations show nearly conventional two-dimensional scaling, but we also observe polaron correlations, in the form of both longitudinal Jahn-Teller stripes and checkerboard charge fluctuations. This short-range order characterizes a dense polaronic fluid, with interactions generated by strongly overlapping strain fields and electronic wave functions. Below the ferromagnetic transition and above a critical field line, the polarons are delocalized by the magnetic order. Comparison with field-dependent magnetization shows that the

bilayer compound with 40% hole doping is on the threshold where the competing order parameters drive the magnetic transition first order.

This work was supported by the U.S. Department of Energy Office of Science under contract W-31-109-ENG-38.

Wed. 9:15 a.m., Invited, JB-03

Dynamics in Single Crystals Measured on the MAPS Spectrometer

Toby George Perring (Rutherford Appleton Laboratory)

The scientific program on the new inelastic scattering spectrometer MAPS has been under way for over a year at the pulsed neutron source ISIS. MAPS is a direct geometry spectrometer that has been optimized to measure collective excitations in single crystals, particularly magnetic excitations. Its principal innovation is the use of position sensitive detectors that provide close to continuous coverage over a large detector area. This allows an unparalleled survey of the excitations throughout the Brillouin zone, with the freedom to take cuts from the data on any plane or direction in reciprocal space, with the resolution tunable in software. The design and technical specification of MAPS will be outlined, and the use of the spectrometer to measure excitations in single crystals will be illustrated by a variety of experimental data taken from the scientific commissioning program. Examples will include data from model magnetic systems in one and two dimensions, transition metal oxides, and transition metal ferromagnets.

Wed. 9:30 a.m., Invited, JB-04

Spin Dynamics of Frustrated Pyrochlore Magnets

Jason Stewart Gardner (National Research Council, Canada)

In the past six years, there has been considerable interest in the physics of geometrically frustrated magnets [1] where the underlying geometry of the spins (the lattice) and the nearest neighbor interaction (bonds) are not

compatible. This results in the system being unable to minimize the total classical ground state energy by minimizing the energy of each spin pair. A subset of these compounds have been given the label “spin ice” because the disorder of the magnetic moments at low temperatures is precisely analogous to the proton disorder in water ice. Neutron-scattering studies on one geometrically frustrated magnet, namely $\text{Tb}_2\text{Ti}_2\text{O}_7$ [3, 4], will be presented. In this compound, the Tb^{3+} ion has a Curie Weiss temperature of -19 K and a paramagnetic moment of 9.7 Bohr magnetons. Spatial correlations between the Tb ions begin to buildup below 100 K. However, unlike the spin ices, this system remains dynamic down to 15 mK. I will present neutron diffraction and high-resolution neutron scattering, including neutron spin echo, data to elucidate the strong, low-temperature dynamics in this spin liquid. [1] A. P. Ramirez, *Annu. Rev. mater. Sci.* 24 (1994) 453. [2] S. T. Bramwell and M. J. P. Gingras, *Science*, 294, 14 (2001). [3] J. S. Gardner et al., *Phys Rev Lett.* 82, 1012 (1999); J. S. Gardner et al., *Phys Rev B.* 64, 224416 (2001). [4] M. Kanada et al., *J Phys Soc. Japan* 68, 3802 (1999).

Wed. 9:45 a.m., Invited, JB-05

Protectorate in a Geometrically Frustrated Magnet

Seung-Hun Lee, Q. Huang (National Institute of Standards and Technology and University of Maryland), C. Broholm, G. Gasparovic (Johns Hopkins University), W. Ratcliff, S.-W. Cheong (Rutgers University), T. H. Kim (Massachusetts Institute of Technology)

Despite progress in both theoretical and experimental physics of geometrical frustration, the nature of the ground state and that of low-energy spin fluctuations are yet to be fully understood. In this talk, I would like to address this issue by discussing our recent inelastic neutron-scattering data obtained from single crystals of ZnCr_2O_4 , where Cr^{3+} ions form a corner-sharing tetrahedra (or pyrochlore) with uniform antiferromagnetic nearest neighbor interactions only. We have discovered that novel composite spin degrees of freedom emerge from the magnetic interactions in the spin liquid phase of ZnCr_2O_4 . Instead of fluctuating individually, groups of six spins self-organize into weakly interacting antiferromagnetic hexagonal loops, whose spin directors govern the

low-temperature dynamics. The hexagon directors are decoupled from each other, and hence their reorientations embody the long-sought local zero energy modes for the pyrochlore lattice.

Wed. Morning, JC–Hydrides and Hydrogen Bonds

Chair: Juergen Eckert (University of California, Santa Barbara, and Los Alamos Neutron Science Center)

Tennessee Ballroom C

Wed. 8:30 a.m., Keynote, JC-01

Single-Crystal Neutron Diffraction and the Study of Metal-Hydrogen Interactions

Thomas F. Koetzle (Argonne National Laboratory and Brookhaven National Laboratory)

Ever since the seminal studies of simple hydrogen-bonded materials that were carried out in the 1950s at the Oak Ridge and Harwell reactor facilities, single-crystal neutron diffraction has been exploited to reveal structural details involving hydrogen atoms in a wide variety of molecular crystals. This lecture will focus on crystallographic studies in the area of organometallic chemistry, at both reactor and spallation sources, which are exploring the bonding of hydrogen ligands to transition-metal centers. In particular, structures of transition-metal hydride and dihydrogen complexes are being investigated because of their central importance in hydrogen activation and chemical catalysis. Recent studies in this area will be discussed, including several where novel binding modes have been uncovered. For example, the structure of a binuclear tantalum hydride complex that possesses a novel bridging imine ligand was studied recently on the Intense Pulsed Neutron Source SCD instrument, in collaboration with Xue and coworkers from the University of Tennessee, Knoxville, and Schultz and Wang from Argonne National Laboratory. This study has provided a direct observation of the formation of an

[eta]-2 imine system through [beta]-hydrogen abstraction between amide ligands, a type of reaction mechanism that may prove to be important during the incorporation of nitrogen impurities into chemical vapor deposition-deposited films. In the future, the advent of the Spallation Neutron Source promises to enhance single-crystal diffraction data acquisition efficiencies by up to two orders of magnitude relative to that at existing sources. This should stimulate the extension of the SCD technique in many areas, such as parametric studies where the effects on structure of thermodynamic variables, including temperature and pressure, will be increasingly explored, and the determination of charge and spin-density distributions in complex systems. This lecture will offer some speculations on the future trends.

Wed. 9:00 a.m., Invited, JC-02

A Chemist's View of Inelastic Neutron Scattering

Bruce Samuel Hudson (Syracuse University)

Inelastic neutron scattering is a unique tool for molecular vibrational spectroscopy. The absence of selection rules, the sensitivity to isotopic substitution, the ability to calculate spectral intensities directly from normal mode calculations, and the application of this technique to bulk samples all contribute to the attractiveness of this technique as a method for obtaining reliable information on the dynamics and potential energy functions of polyatomic molecules. This methodology is greatly enhanced by rapid advances in computational methods in quantum chemistry, including those that treat the solid state. Several examples of comparisons of INS spectra with *ab initio* computations will be presented, beginning with alkanes where intermolecular interactions are minimal. In this case, calculations based on an isolated molecule model appear to be adequate. In the case of hydrogen-bonded solids, inclusion of intermolecular interaction is obviously important. Examples of cluster calculations for several hydrogen-bonded systems will be described. Ionic systems provide additional challenges, as will be discussed.

Wed. 9:15 a.m., Talk, JC-03

Dynamics and Structural Phase Transitions of Solid Mesitylene

*Ireneusz Natkaniec (Frank Laboratory of Neutron Physics and Institute of Nuclear Physics),
K. Holderna-Natkaniec (Institute of Physics)*

Mesitylene, or in other words, 1,3,5-trimethylbenzene, $C_6H_3(CH_3)_3$, seems to be a promising material to make a cold neutron moderator because of its high hydrogen density and anticipated rotational freedom of methyl groups in the solid phase. Inelastic incoherent neutron scattering (IINS) and neutron powder diffraction (NPD) investigations of hydrogenous and deuterated mesitylene were performed simultaneously on the NERA spectrometer at the IBR-2 pulsed reactor of JINR in Dubna. In the solid samples obtained from a liquid state by cooling at a rate of 2 K/min, reversible structural phase transitions were detected between 90 to 100 K for mesitylene- D_0 and between 100 to 110 K for mesitylene- D_{12} . Two more but nonreversible structural phase transitions were observed in the temperature ranges 190 to 200 K and 210 to 220 K at further heating of both samples. These two high-temperature solid phases can be also frozen down to 20 K at a cooling rate of 2 K/min. Thus, three different solid phases of mesitylene can be stable at 20 K. The vibrational spectra of these three solid phases at 20 K and their temperature behaviors are compared. The frequencies of internal modes are interpreted based on DFT calculations of an isolated molecule of mesitylene.

Wed. 9:30 a.m., Talk, JC-04

Ternary Europium Hydrides

Holger Kohlmann (University of Nevada), Klaus Yvon (University of Geneva)

Europium compounds have rarely been investigated by neutron diffraction due to the excessively high neutron absorption of natural europium. It is demonstrated that these difficulties can be circumvented by optimizing experimental parameters (i.e., by taking advantage of the wavelength dependence of the neutron absorption, working on advanced neutron diffractometers at a high flux source, and modifying the sample geometry). This

approach allowed for the first time the full crystal structure determination of europium hydrides by a combination of X-ray (synchrotron) and neutron powder diffraction. Fifteen ternary europium hydrides in the systems Eu-Li-H, Eu-Mg-H, Eu-Pd-H, and Eu-Ir-H have been synthesized and fully structurally characterized. Their crystal chemistry and magnetic properties are discussed in the context of metal hydride chemistry and physics.

Wed. 9:45 a.m., Talk, JC-05

Neutron Scattering Study of the High-Pressure Metal Hydrides

Alexander I. Kolesnikov (Argonne National Laboratory)

Hydrides of the group VI-VIII transition metals were synthesized under high hydrogen pressures and studied by neutron diffraction (ND) and inelastic neutron scattering (INS). The monohydrides of Cr, Mn, Fe, Co, Ni, Mo, Rh, and Pd have close-packed metal sublattices with hcp, fcc, or dhcp structure, in which hydrogen atoms occupy octahedral interstitial positions. The energy of the optical H peak exhibits a monotonous increase as a function of the hydrogen-metal distance, R , in the hydrides of both 3d- and 4d- metals. The increase in R should imply weakening interatomic interactions. The observed opposite effect indicates a significant increase in the hydrogen-metal interaction with decreasing atomic number of the host metal, which outweighs the influence of the accompanying R decrease in the hydrides. The spectra for fcc NiH and PdH appear anisotropic at energy transfers above the fundamental band of optical hydrogen vibrations, while those for fcc PdD do not show a directional dependence at energies of the second optical D band. In dilute hydrogen solutions in hcp Ru and Re with nearly cubic symmetry of the octahedral interstices enclosing hydrogen atoms, the fundamental H band might be expected to be reduced to a narrow line of 3-fold degenerate, non-interacting isotropic local oscillators. Experiments, however, show that the fundamental H band of ϵ -ReH_{0.09} and ϵ -RuH_{0.03} is split into two peaks at about 100 and 130 meV, and 115 and 126 meV, respectively. The results for single crystals demonstrated that these peaks originate from a non-degenerate mode of hydrogen vibrations along the c-axis and a two-fold degenerate mode in the basal plane, respectively. ND study has

shown that H atoms in α -Mn occupy the position in a double-well potential with very short distance between the minima of $2d = 0.68 \text{ \AA}$. INS investigation of α -MnH_{0.07} and α -MnD_{0.05} at $T = 1.7$ -200 K over a wide range of energy and momentum transfers were carried out. Together with the high energy bands of the optical vibrations, pronounced peaks at 6.3 and 1.6 meV were observed in the spectra of samples loaded with H and D, respectively. Temperature, momentum-transfer, and isotope dependence of the spectra demonstrated the tunneling origin of these peaks. The H tunneling peak in the INS spectrum of α -MnH_{0.073} shows an anomalously high energy of 6.3 meV, which is 30 times larger than for H in other metals. Deuterium tunneling in metals has not been detected previously by neutron spectroscopy.

the flat perfect crystal, $I(0)$ cannot be calculated by means of the ordinary Debye-Waller factor, ultrasound leads to the increasing $I(0)$ due to the existence of the standing LAW. $I(0)$ is almost independent from W for the case of Bragg geometry: W is small at the crystal plate surface, and therefore $I(0)$ is almost the same as without ultrasound. (2) PG-graphite—the total intensity of scattering, I_t , is independent vs W ; the elastic scattering is simply transformed to the inelastic. (3) Mosaic KBr—we observed decreasing $I(0)$ and moderate, $\sim 15\%$, increasing of I_t that was explained as the result of the secondary extinction effect at INSU. Recently we observed the similar, $\sim 50\%$, effect for the case of mica s.c. (4) Our AWs are incoherent for the case of strong crystal excitation. NSE allows us to observe INSU in the wide class of samples and to study ultrasonic field parameters.

Wed. Morning, JD—Nuclear/Particle/Astrophysics with Neutrons II

Chair: David Jacobson (National Institute of Standards and Technology)

Cumberland Room

Wed. 8:30 a.m., Talk, JD-01

Inelastic Neutron Scattering by Ultrasound in Solids

Eugene Iolin, Dr. E. Raitman, Dr. L. Rusevich (Institute of Physical Energetic), Dr. Bela Farago (Institut Laue-Langevin), Dr. Ferenc Mezei (Hahn-Meitner Institute)

It was supposed that inelastic neutron scattering (INSU) by the bulk ultrasonic wave could not be studied due to the very small value of energy of the ultrasonic phonon. We observed INSU in single crystals by means of neutron spin echo technique (NSE). Neutron wavelength $\lambda_N = 0.54$ to 1.1 nm, NSE time $t = 6$ to 62 ns, ultrasonic frequency $f = 28$ to 210 MHz. The intensity of the elastic $I(0)$, one $I(1)$, . . . phonon scattering were measured as ultrasound amplitude, W , function. The observed INSU is depended from the s.c. mosaic structure and ultrasonic field parameters. (1) Silicon—small amplitude ultrasound leads to the strong decreasing of $I(0)$ in the deformed silicon in an agreement with theory. Even for the case of

Wed. 8:45 a.m., Talk, JD-02

Reflectivity Measurement for Multiple Bragg Reflections off a Channel-Cut Perfect Silicon Crystal

Helmut Kaiser (University of Missouri), Thomas Dombek (Fermilab), Donald D. Koetke (Valparaiso University), Roy Ringo, Murray Peshkin (Argonne National Laboratory), Keary Schoen, Samuel A. Werner (University of Missouri and National Institute of Standards and Technology), Daniel Dombek (Cornell University)

The reflectivity for multiple Bragg reflections off a channel-cut perfect silicon crystal was measured as a preliminary step for a neutron electric dipole moment (EDM) experiment. Our technique uses successive Bragg reflections for neutrons ($\sim 1.92 \text{ \AA}$ near back scattering) as they travel down channels cut along the (440) planes of a perfect silicon crystal. These measurements are in good agreement with model calculations and indicate that as many as 21,000 multiple Bragg reflections are possible before there is a significant loss of neutron intensity. Before conducting an EDM experiment, a “calibration experiment,” that is, Schwinger scattering experiment, will be carried out. Schwinger scattering occurs when the moving magnetic dipole moment (MDM) interacts with an electric field. In this spin-orbit coupling experiment, we will try to measure the spin rotation induced by the MDM interaction with the atomic electric fields as the neutron

undergoes multiple Bragg reflections along its path down the channel. The reflectivity measurement, as well as the proposed Schwinger scattering experiment, will be discussed.

Wed. 9:00 a.m., Talk, JD-03

A New Technique for Measuring the Electron-Antineutrino Correlation in Neutron Decay

Alexander Karl Komives, F. B. Bateman, M. S. Dewey, A. K. Thompson (National Institute of Standards and Technology), B. Trull, F. E. Wietfeldt (Tulane University), R. Anderman, G. L. Jones (Hamilton College), F. W. Hersman, M. B. Leuschner (University of New Hampshire), L. Goldin, B. G. Yerozolimsky (Harvard University), S. Balashov, Yu. A. Mostovoy (Kurchatov Institute)

Measurements of neutron decay properties can be used to test the Electroweak Standard Model. The parameter λ , the ratio of axial vector-to-vector weak coupling strengths, links this model to neutron decay measurements. Presently, the most precise determinations of λ come from the polarized neutron-electron momentum correlation, “A.” In principle, the electron-antineutrino momenta correlation, “a,” can be used to provide equally precise measurements of λ without the problems associated with measuring neutron polarization precisely. Past measurements of “a” have relied on careful determinations of the proton energy spectrum shape, which are difficult due to the proton’s low energy. A new technique, presented here, sidesteps this problem. The immediate goal is the reduction of the 5% error in λ from “a” to 2%. This experiment will be performed at the National Institute of Standards and Technology Center for Neutron Research.

Wed. 9:15 a.m., Talk, JD-04

About Radiative Corrections in Neutron Beta Decay

Vladimir Gudkov (University of South Carolina)

New experiments on the study of neutron beta decay are about to reach the accuracy level where they become

sensitive to radiative corrections. We discuss the origin of different parts of radiative corrections and how they affect some parameters in neutron beta decay. The main attention is paid to radiative corrections related to the nucleon structure and strong interactions at low energy. The classical methods, using QCD perturbation theory, and alternative methods to calculate these strong interaction dependent parts are discussed.

Wed. 9:30 a.m., Keynote, JD-05

Quasi-Elastic Wall Reflections of Ultracold Neutrons

Albert Steyerl, B. Yerozolimsky (Harvard University), A. Serebrov, M. Lasakov, I. Krasnosheikova, A. Vasilyev (Petersburg Nuclear Physics Institute), N. Achiwa (Kyushu University), P. Geltenbort (Institut Laue-Langevin), Yu. Pokotilovski (Joint Institute for Nuclear Research), O. Kwon (University of Rhode Island)

Ultracold neutrons (UCN) are lost from traps if they are quasi-elastically scattered from the wall with an energy gain sufficient to exceed the Fermi potential for the wall. Possible mechanisms of quasi-elastic energy transfer are, for instance, scattering from hydrogen diffusing in an impurity surface layer or on capillary waves at a liquid wall. Using two different experimental methods at the UCN source of the Institut Laue-Langevin we have investigated both the energy-gain and the energy-loss side of quasi-elastic UCN scattering on walls coated with Fomblin grease. For Fomblin oil and similar new types of oil we report up-scattering data as a function of temperature and energy transfer. These low-temperature oils may be used in an improved measurement of the neutron lifetime, which requires a wall coating with extremely low reflection losses.

Wed. Morning, KP-Instrumentation*Summit Grand Ballroom II***Wed. 10:15 a.m.–12:00 p.m., Poster, KP-01****Single-Crystal Diffractometer for the Spallation Neutron Source***Christina Hoffmann (Oak Ridge National Laboratory)*

A single-crystal diffractometer (SCD) employs area detectors and the time structure of pulsed-neutron sources to measure Laue diffraction patterns. The efficiency of sampling the reciprocal lattice simultaneously in both direction (area detection) and length (time resolution) of the probe wave vector is a powerful advantage of pulsed-source diffractometers [1]. The current generation of instruments in the United States can accumulate sufficient data at 10 to 50 sample orientations over a period of several days to determine structures of moderate complexity. By using the enhanced flux of the SNS, increasing the detector coverage, and employing focusing optics, we can reduce this data collection time to a matter of minutes [2]. More importantly, the vastly increased flux on sample will make possible measurements of smaller samples and more complicated structures. Single-crystal neutron diffraction is a continuously evolving technique that has numerous important applications. With the new, most powerful spallation neutron source coming on-line in 2006, a quantum leap for single-crystal neutron diffraction will be achieved. We can explore scientific problems that are very important for the properties of the material through diffraction patterns of chemically important molecular structures and inorganic atomic arrangements. Single-crystal neutron diffraction can look at subtle features like diffuse scattering next to strong Bragg patterns. Diffuse scattering includes nano-scale information. Important structural features, such as active centers in proteins involving hydrogen bonds, can be characterized. Neutron diffraction is a most sensitive tool to locate hydrogen atoms in crystalline structures. Hydrogen is merely “invisible” for X rays. [1] A. J. Schultz, *Trans. AM. Cryst. Assoc.* 29 (1993). [2] J. F. Ankner and J. K. Zhao, ES-1.1.8.4-6018-RE-A-00 (1999).

Wed. 10:15 a.m.–12:00 p.m., Poster, KP-02**ARCS—A Wide Angular Range Chopper Spectrometer at the Spallation Neutron Source***Douglas L. Abernathy (Oak Ridge National Laboratory)*

The U.S. Department of Energy has funded a wide angular range chopper spectrometer, ARCS, to be constructed on beam line 18 at the Spallation Neutron Source. ARCS will be optimized to provide a high neutron flux at the sample and a large solid angle of detector coverage. The source-sample distance will be 13.6 m, and the secondary flight path will be 3.0 m at all angles, from -30 to 140° horizontally and $\pm 30^\circ$ vertically. The dense array of position-sensitive detectors will detect the direction and velocity of neutrons scattered into almost one quarter of the solid angle around the sample. The spectrometer will be capable of selecting from the full energy spectrum of neutrons provided by an ambient water moderator, making it useful for studies of excitations from a few to several hundred millielectron volts. A supermirror guide in the incident flight path will boost the performance at the lower end of this range. ARCS strives to be the most efficient high-energy chopper spectrometer at any spallation neutron source. In addition to the instrument hardware, the ARCS project includes a significant effort for software development.

Wed. 10:15 a.m.–12:00 p.m., Poster, KP-03**High-Performance Hybrid Spectrometer for Single-Crystal Inelastic Neutron Spectroscopy at the Spallation Neutron Source***Igor Zaliznyak, S. Shapiro, V. Ghosh, L. Passell (Brookhaven National Laboratory)*

We describe a direct-geometry, hybrid inelastic spectrometer with a vertical-focusing crystal monochromator and time-of-flight (TOF) analyzer for investigations of correlated phases and coherent excitations in single crystals at the pulsed Spallation Neutron Source. In contrast with the chopper TOF spectrometers currently under development for the Spallation Neutron Source, which are designed for high-resolution or broad survey studies, our instrument is optimized to use as much as possible of the monochro-

matic neutrons generated by the source, while providing the highest signal-to-background ratio in the detector, at a good-to-moderate energy resolution. We performed an extensive set of Monte-Carlo simulations, which established the remarkable superiority of the hybrid spectrometer over the traditional multi-chopper TOF setup. The instrument will operate in the thermal and subthermal neutron range of 2.5 to 90 meV, have a polarized beam option, and resolution comparable to that of a reactor-based triple-axis spectrometer.

Wed. 10:15 a.m.–12:00 p.m., Poster, KP-04

POWGEN3—A High-Resolution, Third-Generation Powder Diffractometer at the SNS

Jason Paul Hodges (Oak Ridge National Laboratory)

POWGEN3 is a fundamental departure from previous designs for a powder diffractometer at a spallation neutron source. POWGEN3 may be considered the world's first third-generation, time-of-flight powder diffractometer. For the first time, a high-resolution powder diffractometer is able to take advantage of a high source repetition rate. Combined with the use of a straight supermirror neutron guide system, POWGEN3 is a very efficient instrument. The high count rates thus achieved together with high-resolution characteristics present a big leap forward in performance over previous diffractometer designs. POWGEN3 will thus provide unprecedented opportunities for new science in the study of crystalline materials.

Wed. 10:15 a.m.–12:00 p.m., Poster, KP-05

SNS Liquids Reflectometer

John Francis Ankner (Oak Ridge National Laboratory), Roger L. Kellogg (Argonne National Laboratory)

Barring a monumental failure of design execution or of performance estimation, the liquids reflectometer at the Spallation Neutron Source (SNS) will provide unprecedented capabilities for the study of liquid and solid surfaces. Design of the instrument is well under way, and procurement of the guide system and shielding has begun.

Neutrons from a coupled 20-K supercritical hydrogen moderator will be delivered via a multichannel supermirror bender and tapered guide onto either a horizontal or tilted surface. Collimating slits select the beam incident angle from a 0 to 5° vertical intensity distribution provided by the optics. Bandwidth choppers and frame-overlap mirrors define a 3.75-Å-wide wavelength band that can be chosen from $2 \text{ \AA} < \lambda < 14 \text{ \AA}$. The user will be able to collect data using either a $1.5 \times 1.5\text{-mm}^2$ -resolution, two-dimensional position-sensitive detector or a single ^3He tube. With the SNS running at 2 MW, the instrument will be able to accumulate a complete specular reflectivity scan from D_2O ($R < 10^{-7}$, $Q > 0.5 \text{ \AA}^{-1}$) in less than 5 minutes. By tilting a solid surface, a user will be able to measure specular reflectivities $R \sim 2 \times 10^{-10}$ ($Q > 1.5 \text{ \AA}^{-1}$) from large samples in less than 2 hours. The instrument is also designed to facilitate off-specular and grazing-incident small-angle neutron scattering measurements. We will describe the instrument design, discuss time-dependent measurements, report on procurement progress, and present background and performance estimates.

Wed. 10:15 a.m.–12:00 p.m., Poster, KP-06

Design and Performance of the Spallation Neutron Source Backscattering Spectrometer

Kenneth W. Herwig, S. Keener (Oak Ridge National Laboratory)

When the Spallation Neutron Source is operational in 2006 at Oak Ridge National Laboratory, it will provide the most intense pulsed neutron beams in the world for research. This poster describes the expected performance of the near backscattering, crystal-analyzer spectrometer designed to provide extremely high-energy resolution at the elastic peak (2.2 to 2.7 μeV , varying with sample dimension). The design requires a long initial guide section of 84 m from moderator to sample in order to achieve the requisite timing resolution. The design is optimized for quasi-elastic scattering but will provide 0.1% resolution in energy transfer up to energy transfers of 18 meV. This spectrometer will provide an unprecedented dynamic range near the elastic peak of $\pm 258 \mu\text{eV}$. For experiments that require the full dynamic range available at comparable reactor-based instruments (or

greater), this spectrometer is expected to have an effective count rate ~64 times that of the current best spectrometers, although at lower energy resolution.

Wed. 10:15 a.m.–12:00 p.m., Poster, KP-07

VULCAN, Roman God of Fire and Metal Working

Xunli Wang (Oak Ridge National Laboratory)

The VULCAN diffractometer at the Spallation Neutron Source is designed to tackle a broad range of problems in materials science and engineering. The primary use of this instrument is for stress-related studies, including mapping of the residual stress distribution in components and the determination of deformation behaviors under applied load. Other uses include in situ measurements of materials kinetics in chemistry, stress, texture, and microstructure. For mapping experiments, the measurement time with a sampling volume of 1 mm³ will be minutes. This will make possible parametric studies of components subjected to different fabrication or operating conditions. Load-frame and furnaces will be an integrated part of the instrument. With its high flux and a large detector array, VULCAN is also ideally suited for the study of texture and transformation kinetics. Equipped with a two-dimensional area detector, which would enable simultaneous small-angle neutron scattering measurements, VULCAN will become a great tool for understanding the intricate interplay between stress, texture, and microstructure in materials.

Wed. 10:15 a.m.–12:00 p.m., Poster, KP-08

Development of Neutron Beam Facilities for the Australian Replacement Research Reactor

Elliot Paul Gilbert, Shane Kennedy, Robert Robinson (Australian Nuclear Science and Technology Organisation)

Australia is building a research reactor to replace the HIFAR reactor at Lucas Heights by the end of 2005. Like HIFAR, the replacement research reactor will be multipurpose with capabilities for both neutron beam research and radioisotope production. It will be a pool-type reactor with four times the neutron flux of HIFAR, a

cold neutron source, and large neutron guide hall. Cold and thermal neutrons will be transported to the neutron beam instruments with modern supermirror guides. INVAP S.E. has been contracted to build the reactor and associated infrastructure, with the exception of the neutron beam instruments. With the conceptual design complete, detailed engineering is well advanced and site preparation has commenced. The Australian Nuclear Science and Technology Organisation is developing an initial suite of eight neutron beam instruments in close consultation with the Australian user community. Design of six of the neutron beam instruments is progressing well. This presentation will include a review of the planned scientific capabilities, a description of the neutron beam facility, and a status report on progress to date on the instrument development program.

Wed. 10:15 a.m.–12:00 p.m., Poster, KP-09

Neutronic Performance of the Spallation Neutron Source

Erik B. Iverson, Phillip D. Ferguson (Oak Ridge National Laboratory)

We discuss the performance characteristics of the Spallation Neutron Source (SNS). The SNS moderators—one decoupled hydrogen, one decoupled water, and two coupled hydrogen—will provide intense pulsed thermal neutron beams for a variety of neutron-scattering instruments. Optimal design of these instruments requires accurate prediction of the source performance characteristics, and their optimal performance requires careful tuning of various features of the source itself. In addition, we will present the results of various sensitivity studies performed during the course of the SNS design process.

Wed. 10:15 a.m.–12:00 p.m., Poster, KP-10

Neutron Scattering Facilities at Budapest Research Reactor

Mike Makai (KFKI Atomic Energy Research Institute)

The Budapest Neutron Center (BNC) operates a 10-MW research reactor that provides users with a thermal and fast flux $\sim 2 \times 10^{14}$ n/cm²/s, $\sim 1 \times 10^{14}$ n/cm²/s, respec-

tively. The fluxes at beam port exits exceed 10^9 n/cm²/s. The reactor is equipped with a liquid hydrogen type cold neutron source. Five measuring sites are installed on the cold neutron beam: a reflectometer, a triple-axis spectrometer (TAS), a time-of-flight spectrometer (TOF), a small-angle neutron scattering (SANS), and a prompt gamma activation analysis (PGAA) device. Recently, a neutron-induced prompt-gamma ray spectrometer has been implemented at the PGAA site. At present, the TOF is being relocated to the thermal beam; its implementation is due in 2003. On the thermal beam, five measuring sites and a fast rabbit system (RNAA) are implemented in the reactor hall: Powder diffractometer (PDS), static- and dynamic neutron radiography (SNR and DNR), biological irradiation (BIO), and a material testing diffractometer. The European Union (EU) supports visitors from EU and candidate countries to perform measurements on SNR, BIO, PGAA, RNAA, SANS, TAS, and PDS at BRR. Technical specifications of the measuring sites are provided at www.BNC.hu. The full text gives examples of experimental results selected from the last BNC progress report, which is being prepared.

Wed. 10:15 a.m.–12:00 p.m., Poster, KP-11

Novel Investigations and New Neutron Sources

Yuri Andreevich Alexandrov (Joint Institute for Nuclear Research)

This report discusses the direct and indisputable relationship of almost all fundamental and applied researches with the start of operations of powerful sources of high-energy particles (accelerators) and of neutrons with a wide range of energies. This report provides examples of new investigations in neutron physics that appeared due to creation of powerful thermal reactors (expended research in neutron properties and fundamental interactions, ultracold neutron studies, diffractometric investigations in condensed matter physics, biology, materials science, etc.), fast neutron reactors [discovery of Schwinger neutron scattering, search of deformation (polarizability) of the neutron, etc.], and pulsed and spallation neutron sources [investigations in fundamental and applied physics in Los Alamos, Oak Ridge, Dubna, England (ISIS), etc.]. An analysis of the evolution of science and technology, including neutron physics, shows that further advances are almost impossible without new neutron sources.

Wed. 10:15 a.m.–12:00 p.m., Poster, KP-12

Debye-Scherrer Cone Corrections for Linear Position-Sensitive Detector Arrays in Neutron Powder Diffraction

Ronald R. Berliner, Bjorn C. Hauback, Helmer Fjellfaag, O. Steinsvoll (Institute for Energy Technology)

In the classical powder diffractometer, a fine cylindrical beam intersects a point-like polycrystalline specimen, creating cones of diffracted radiation. The diffraction pattern is then sampled by a collimated detector element that rotates about the specimen position to record the intensity as a function of scattering angle. The reactor-based neutron powder diffractometer adopts this basic configuration and employs a cylindrical specimen placed perpendicular to the scattering plane and a slit-collimated detector to sample the diffracted radiation. In comparison to the point specimen, the cylindrical sample leads to an increase in detector count rate, which is proportional to the irradiated sample volume and height of the detector slit. Additional data throughput improvements can be obtained by increasing the size of the detector, either by using a multidetector with numerous Soller-collimated elements or a one-dimensional position-sensitive detector such as a Banana. In both cases, extending the height of the detector (perpendicular to the scattering plane) results in further increases in count rate but at the cost of distortions of the peak shapes and diffraction peak position at small scattering angles. Peak shape and peak position distortions in neutron powder diffraction experiments can be substantially avoided when using a two-dimensional powder diffractometer detector. The detector for our instrument is composed of an array of one-dimensional linear position-sensitive proportional counters that form a plane. In this case the corrections to the raw data at small scattering angle are conceptually simple but mathematically awkward. We will present the form of the peak shape and peak position data corrections and demonstrate their effect on diffraction data at small scattering angles. The importance of this result is that the height of neutron powder diffractometer detector systems can be increased substantially, at little or no cost in resolution, further improving the performance of these instruments.

Wed. 10:15 a.m.–12:00 p.m., Poster, KP-13

A New Thermal Neutron-Scattering Kernel for Liquid Hydrogen

J. Rolando Granada (Argentine Atomic Energy Commission)

We have used recent experimental data on the dynamics of liquid hydrogen to produce a new description of the interaction of slow neutrons with this cryogenic moderator. The molecular translational motion, for both diffusive and collective degrees of freedom, has been reanalyzed and represented by a different spectral frequency distribution compared to existing ones. We also included explicitly the molecular vibrations into the physical model. Recent structural studies on liquid deuterium were considered in the present work to produce by a density-scaling procedure a realistic structure factor for the calculation of the scattering law at different temperatures within the range corresponding to the liquid phase of H₂. This model was employed as input data to generate new scattering cross-section libraries using the NJOY code. The preliminary validation tests performed so far using the new library indicate that they are able to produce results in good agreement with the available experimental information.

Wed. 10:15 a.m.–12:00 p.m., Poster, KP-14

IDEAS, Instrument Design and Experiment Assessment Suite

W.-T. Lee, X.-L. Wang (Oak Ridge National Laboratory)

IDEAS is a general-purpose computer program for simulating neutron-scattering instruments. Instruments with single or multiple beam paths can be flexibly constructed by arranging self-contained subroutine modules (e.g., source and guide) in series. By using appropriate modules, a user can perform absolute flux calculations, simulate time-of-flight instruments, as well as evaluate polarized neutron devices. The precompiled modules are loaded dynamically at run time, allowing rapid prototyping of an instrument. An integrated user interface reduces the work for constructing and changing an instrument set up to virtually the click of a button. IDEAS has adopted

standard specifications for both the neutron parameters and the subroutine interface structure. This not only ensures a smooth passage of data between the modules but also guarantees the reusability of existing modules. In addition, users can readily incorporate their own modules coded in C or Fortran. IDEAS has been used to simulate existing and conceptual instruments at the Spallation Neutron Source, High Flux Isotope Reactor, Intense Pulsed Neutron Source, FRMII, and Hahn-Meitner Institut. Examples of these simulations will be discussed.

Wed. 10:15 a.m.–12:00 p.m., Poster, KP-15

Neutron Imaging by Reflection Superposition

Alexandru D. Stoica, X.-L. Wang (Oak Ridge National Laboratory)

Arrays of reflecting elements can be assembled together to create imaging devices for neutron-scattering instruments. The reflection could be either at grazing angles by total external reflection or at high angles by diffraction. Examples of the first kind include equally spaced silicon wafers coated with supermirrors. Multiwafer crystal assemblies are examples of the second kind. A common optical approach has been found for evaluating the image aberrations. The optimum optical configurations for each kind of devices will be presented. Slop errors of the silicon wafers strongly affect the quality of the image. Aberrations due to slop errors have been estimated and will be discussed.

Wed. 10:15 a.m.–12:00 p.m., Poster, KP-16

Development of an 0.89-nm Monochromator for Use with a Superthermal Helium Ultracold Neutron Source

Paul R. Huffman, C. E. H. Mattoni, K. J. Alvine, S. N. Dzhosyuk, D. N. McKinsey, L. Yang, J. M. Doyle (Harvard University), C. P. Adams, D. L. Jacobson (National Institute of Standards and Technology), R. Golub, K. Habicht (Hahn-Meitner Institut), H. Zabel (Ruhr Universitat Bochum)

Production of ultracold neutrons using the superthermal process in superfluid helium uses input neutrons only in a

small wavelength band centered around 0.89 nm. To select the material for such a monochromator, we measured the mosaicity and 0.89 nm reflectivity of several possible choices: fluorophlogopite (a perfluorinated mica) and stages 1 and 2 potassium-intercalated highly oriented pyrolytic graphite (IHOPG). Based upon these measurements, stage 2 IHOPG has been selected and we have built a tiled monochromator with overall dimensions of 6 by 15 cm. The mosaic angles of the individual pieces range from 1.1 to 2.1 degrees, and the assembled monochromator reflects more than 80% of the 0.88- to 0.90-nm neutrons diverging from a ^{58}Ni -coated guide. Performance of the monochromator coupled with the UCN source will be reported.

Wed. 10:15 a.m.–12:00 p.m., Poster, KP-17

Spallation with High-Energy Protons as a Source of High Spin $^{178\text{m}2}\text{Hf}$ Isomeric Nuclei

Claudiu Rusu (University of Texas, Dallas, and National Institute of Physics and Nuclear Engineering and Induced Gamma Emission Foundation), C. B. Collins (University of Texas, Dallas), S. A. Karamian, J. Adam, D. V. Filossov, V. G. Kalinnikov, N. A. Lebedev, A. F. Novgorodov (Joint Institute for Nuclear Research), D. Hanusova, V. Henzl (Nuclear Physics Institute), I. I. Popescu, C. A. Ur (National Institute of Physics and Nuclear Engineering and Induced Gamma Emission Foundation)

The ^{178}Hf nucleus with its exotic high spin (16^+) long lived ($T_{1/2} = 31$ years) isomer represents an attractive point for both fundamental and applied physics research. One of the main obstacles for using it is its limited availability and difficult production process. Until now, this isomer resulted as a by-product of various types of nuclear reactions but they were never optimized for its production. We have performed a systematic experimental study of the spallation reactions at proton energies ranging from 100 to 660 MeV for the accumulation of ^{178}Hf isomers. Our study aims to identify the best conditions (target and proton beam energy) that lead to the maximum production cross section combined with the highest isomer-to-ground state ratio in the presence of a lowest possible radioactive background of the samples. Targets of natural tantalum and rhenium were irradiated at the JINR, LNP Dubna synchrotron. Many radioactive products of the spallation

and fission reactions were identified, and their yields were compared with the LAHET code simulations. For some high-spin isomers (as ^{178}Hf , ^{179}Hf), we estimated the isomer-to-ground state ration. A qualitative method for optimizing this ratio was developed based on the calculated spin distribution of the spallation residues.

Wed. Morning, KQ-Chemistry

Summit Grand Ballroom II

Wed. 10:15 a.m.–12:00 p.m., Poster, KQ-01

Synthesis and Structure of Subnitrides and Their Intercalates

Amy Bowman, P. V. Mason, D. H. Gregory (University of Nottingham)

Alkaline earth metal subnitrides, A_2N ($\text{A} = \text{Ca}, \text{Sr}$) crystallise in the anti CdCl_2 structure. This consists of layers of NA_6 edge-sharing octahedra with large interlayer gaps containing free electrons (i.e., $\text{A}_2^{2+}\text{N}^{3-} \cdot [\text{e}^-]$). The presence of these “excess electrons” between layers yields two-dimensional metals in which electrons are confined between ionic insulating $[\text{A}_2\text{N}]^+$ layers. Subnitrides (A_2N , $\text{A} = \text{Ca}, \text{Sr}$) can act as hosts for novel anion intercalation. Here we describe how the first nitride mixed halides ($\text{A}_2\text{N}(\text{X}, \text{X}')$, $\text{X}, \text{X}' = \text{Cl}, \text{Br}, \text{I}$) have been synthesized and characterized by powder X-ray (PXD) and neutron diffraction (PND). The halide anions are disordered between the positively charged layers of the hosts $[\text{A}_2\text{N}]^+$ and crystallize in anti-alpha- NaFeO_2 or anti-beta- RbScO_2 structures. The final structures and dimensionality of these and other nitride-mixed anion materials, e.g., with $\text{X} = \text{H}$ or F , as determined by PXD and PND, are sensitive to the relative anion sizes (N^{3-} vs X^- vs X'^+). The structural flexibility of these hosts also allows intercalation of more complex guest anions of varying geometry and charge, e.g., $(\text{CN}_2)^{2-}$ in $\text{Ca}_{11}\text{N}_6(\text{CN}_2)_2$ and $\text{Ca}_4\text{N}_2(\text{CN}_2)$. Neutron diffraction methods have been key in locating anions, resolving ion distributions, and distinguishing between isoelectronic species [e.g., $(\text{CN}_2)^{2-}$ and N_3^-].

Wed. 10:15 a.m.–12:00 p.m., Poster, KQ-02

Comparison of the Crystalline, Glass, and Liquid Structures of a Sodalite-Type Halozeotype

Stephen Joseph Goettler, James D. Martin (North Carolina State University)

Network glasses and liquids such as ZnCl_2 are known to exhibit significant intermediate range order (IRO). Using a zeolite-type synthetic strategy, by which equimolar amounts of an alkylammonium chloride salt and Copper(I) chloride are added to zinc chloride, it is possible to template specific patterns of intermediate range order into the amorphous network. In a glass prepared with the trimethylammonium cation as the network template, the $[\text{CuZn}_3\text{Cl}_{12}]$ amorphous network adopts the sodalite-type geometry with two distinct low Q diffraction peaks that are strongly correlated with its crystalline structure. Further network modification is observed upon melting. The relation between the crystalline, glass, and liquid neutron scattering will be discussed.

Wed. 10:15 a.m.–12:00 p.m., Poster, KQ-03

Investigation of ^3He in Erbium Ditrifide

James F. Browning, Michael A. Mangan, Dale M. Blankenship, Steven D. Balsley (Sandia National Laboratories), Gregory S. Smith, Rex Hjelm, Jr. (Los Alamos National Laboratory), Gillian M. Bond (New Mexico Institute of Technology), Kirk L. Shanahan, David R. Bell (Savannah River Technology Center)

Tritium storage in metal hydride systems generates ^3He via beta decay of the tritium nuclei. It is well known that much of the helium generated does not readily diffuse from the host matrix but becomes trapped in low-energy sites such as interstices, defects, etc. Because of its limited solubility, ^3He tends to cluster at these sites forming high-density, high-pressure bubbles. The resulting accumulation of sufficient quantities of helium will greatly affect the physical, chemical, and mechanical properties of the host material. The energetics and formation kinetics of these clusters are poorly understood phenom-

ena. Migration and coalescence of ^3He bubbles are dependent upon internal gas pressure, which is related to internal atomic density. In this work we present new data in the investigation of the behavior of ^3He in metal hydride systems using neutron-scattering techniques. Neutron reflectometry is used to study helium concentration and depth distribution as a function of time in erbium ditritide. Small-angle neutron scattering is used to investigate bubble formation and kinetics as well as to measure the bubble parameters of size, density, and pressure in erbium ditritide.

Sandia is a multiprogram laboratory operated by Sandia Corporation, a Lockheed Martin Company, for the U.S. Department of Energy under contract DE-AC04-94AL85000.

Wed. 10:15 a.m.–12:00 p.m., Poster, KQ-04

Structure of Liquid Anhydrous Hydrogen Fluoride Using Neutron Diffraction with H/D Substitution

Sylvia E. McLain (University of Tennessee and Argonne National Laboratory), Chris J. Benmore, Joan E. Siewenie, Jacob Urquidi (Argonne National Laboratory), John F. C. Turner (University of Tennessee)

The partial structure factors of liquid hydrogen fluoride have been measured for the first time using neutron diffraction with H/D substitution. The experiments were performed at 295 K and 1.09 bar and are in good agreement with previous neutron diffraction experiments of liquid DF. The neutron data show strong intermolecular hydrogen bonding in the liquid, and the structure has been interpreted using a Reverse Monte Carlo modeling technique. The results presented are compared at the partial structure factor level to existing ab initio calculations and to molecular dynamics simulations using both non-polarizable and polarizable potential models, which all predict linear chains in the liquid. A comparison to electron diffraction data measured on gaseous phase of HF, where cyclic hexamers dominate the structure, is also made. The existence of linear chains and molecular clustering in the measured liquid phase is discussed.

Wed. 10:15 a.m.–12:00 p.m., Poster, KQ-05

Structures of Molecular Deuterium and Oxygen Adsorbed on Carbon Nanotube Bundles

Oscar Edgardo Vilches, Tate Wilson, Matthew DePies (University of Washington), Michel Bienfait, Jean-Pierre Palmari (CRMC2 and Faculte des Sciences de Luminy), Peter Zeppenfeld (J. Kepler Universitat), Nicole DuPont-Pavlovsky (Universite H. Poincare), Mark Johnson (Institut Laue-Langevin)

We have studied the adsorption and structures of molecular deuterium and oxygen on single-wall, closed-end carbon nanotube bundles. We have measured adsorption isotherms to determine the heats of adsorption on the various possible adsorption sites (interstitials, outside channels, outside surface of the bundles) and have performed elastic neutron-scattering (ENS) experiments at selected adsorption coverages to look at both the effect of adsorption on the nanotube bundles lattice and at the structure of the adsorbates. The ENS experiments have been performed using the Institut Laue-Langevin (ILL) D1B and D20 diffractometers. We do not observe any expansion of the nanotube lattice with deuterium adsorption. Both deuterium and oxygen form linear chains of molecules, presumably on internal three or more tubes interstitial sites and outside channels between two tubes, as well as quasi two-dimensional structures on the outside (graphene) surface of the bundles. These two-dimensional structures are somewhat similar to those formed on basal plane graphite. Details of the results will be reported in the poster.

Our research is supported by NSF DMR 0115663 and 0976763, Centre National de la Recherche Scientifique, and the ILL.

Wed. 10:15 a.m.–12:00 p.m., Poster, KQ-06

Nature of the Ag_2S Precipitate in Ag_2S - AgPO_3 Amorphous Electrolytes

M. F. Collins, C. C. Lovekin (McMaster University), E. Kartini, S. Suminta, A. Purwanto (Nuclear Energy Agency), E. C. Svensson (Chalk River Laboratories)

Rapid quenching of $(\text{Ag}_2\text{S} \times (\text{AgPO}_3)_{1-x})$ gives rise to a superionic-conducting glass. For samples with $x > 0.7$, the glass phase is mixed with a polycrystalline precipitate phase. Samples with $x = 0.8$ and 0.9 exhibit high ionic conductivities of about 10^{-3} S/cm at room temperature. Neutron-scattering experiments have been performed to study the structure of the precipitate in these samples as a function of temperature. The results at room temperature show that the Bragg peaks from the precipitate correspond to the monoclinic structure of crystalline Ag_2S (P21/c). For both samples, neutron-scattering and differential thermal analysis data show a phase transition in the precipitate at about 175°C .

Wed. 10:15 a.m.–12:00 p.m., Poster, KQ-07

Optical Implications of Crystallite Symmetry, Structure, and Texture in Potassium Niobate Tellurite Glass Ceramics

Josef W. Zwanziger, Robert T. Hart, Matthew A. Anspach, Brian J. Kraft, Barry Stein (Indiana University), Peter J. DeSanto, W. M. Keck (University of Delaware), Jaby Jacob, Papannan Thiyagarajan (Argonne National Laboratory)

Glass of composition $(\text{K}_2\text{O})_{15}(\text{Nb}_2\text{O}_5)_{15}(\text{TeO}_2)_{70}$ forms a glass ceramic when heated somewhat above T_g . The resulting material shows strong optical second harmonic generation—it can be seen by the naked eye in a dark room. This response was somewhat puzzling because the X-ray diffraction pattern was indexed to a face-centered cubic crystalline phase. Conservation of momentum forbids unpoled glasses and FCC crystals from showing SHG because both contain a center of inversion. In this work, neutron scattering has revealed several additional peaks, resulting in the proposal of an orthorhombic unit cell for the crystallites. These peaks can be assumed to

arise due to disordered planes of predominantly oxygen ions. This poster will show how such a model arises in the absence of a definite unit cell or structural model by combining results of wide-angle neutron and X-ray scattering, SAXS, and TEM. The lower symmetry of the orthorhombic cell allows discussion of the optical response of the material in terms of Lines's theory of d-metal oxide hypolarizability using the results of NMR and Raman spectroscopies. These models allow us to understand the optical response of this material without appealing to exotic mechanisms for SHG.

Wed. 10:15 a.m.–12:00 p.m., Poster, KQ-08

Deep Inelastic Neutron Scattering of H₂ Adsorbed in Britesorb

David George Narehood, Paul Sokol (Penn State University), Rob Dimeo (National Institute of Standards and Technology), Don Brown (Los Alamos National Laboratory), Nathan Grube

Deep inelastic neutron scattering (DINS) provides a unique microscopic perspective of the state of adsorbed molecules in Britesorb. We report DINS studies of H₂ in bundles Britesorb. DINS studies yielded spectra consisting of multiple peaks due to rotational transitions with widths determined by the translational momentum distribution $n(p)$. These measurements help characterize the interaction of the H₂ with the Britesorb. The mean kinetic energy provides information on the extent of the localization of the H₂, while the extracted rotational transitions give insight into the local environment of the adsorbed molecules. In these measurements, the H₂ used was converted from n- H₂ (75% J = 1 to 25% J = 0) to entirely p- H₂ (J = 0). This simplifies the analysis greatly with only rotational transitions to odd J state being observable.

This research was supported by the U.S. Department of Energy through its support of the Intense Pulsed Neutron Source and by the National Science Foundation under grant 9970126.

Wed. Morning, KR—Soft Condensed Matter

Summit Grand Ballroom II

Wed. 10:15 a.m.–12:00 p.m., Poster, KR-01

“Slow” Diffusive Motions in Tetracosane Monolayers Adsorbed on Graphite

Leah Criswell, A. Diama, H. Mo, H. Taub (University of Missouri-Columbia), K. W. Herwig (Oak Ridge National Laboratory), F. Y. Hansen (Technical University of Denmark), U. G. Volkmann (Catholic University of Chile), R. Dimeo, D. Neumann (National Institute of Standards and Technology)

Tetracosane ($n\text{-C}_{24}\text{H}_{50}$ or C_{24}) monolayers serve as prototypes for studying the interfacial dynamics of more complex polymers. Using the High-Flux Backscattering Spectrometer (HFBS) at the National Institute of Standards and Technology, we have investigated the relatively slow diffusive motion in these monolayers adsorbed on exfoliated graphite substrates on an energy/timescale of ~ 1 to $35 \mu\text{eV}$ (~ 0.1 to 4 ns). Upon heating, we first observe quasi-elastic scattering (QNS) in the crystalline monolayer phase at ~ 160 K. From the crystalline-to-smectic phase transition at ~ 215 to ~ 230 K, we observe the QNS energy width to be dispersionless, consistent with molecular dynamics simulations showing rotational motion of the molecules about their long axis. At ~ 260 K, the QNS energy width begins to increase with wave vector transfer, suggesting onset of bounded translational diffusion. We continue to observe QNS up to the monolayer melting temperature at ~ 340 K, where our simulations indicate that translational diffusion has become too rapid to be observed within the dynamical range of the HFBS. According to our simulations, the only motion slow enough to be observable within our energy window results from intramolecular and rotational diffusion of the more globularly shaped C_{24} molecules, which contain many gauche defects.

Wed. 10:15 a.m.–12:00 p.m., Poster, KR-02

“Fast” Diffusive Motion in Tetracosane Monolayers Adsorbed on Graphite

Armand Diama, L. Criswell, H. Mo, H. Taub (University of Missouri-Columbia), K. W. Herwig (Oak Ridge National Laboratory), F. Y. Hansen (Technical University of Denmark), U. G. Volkmann (Catholic University of Chile)

We are using quasi-elastic neutron scattering (QNS) to study molecular diffusion in tetracosane ($n\text{-C}_{24}\text{H}_{50}$) monolayers over a range of energy/time scales. With the upgraded QENS spectrometer at Argonne's Intense Pulsed Neutron Source, we are investigating the relatively fast diffusive motion in these monolayers on an energy/time scale of ~ 0.1 to 5 meV (~ 1 - 40 ps). Our most interesting result is that, unlike our molecular dynamics simulations, we observe a decrease in the energy width of the QNS as the temperature increases from 215 to 285 K in the “smectic” monolayer phase. However, at ~ 300 K and above, the QNS energy width increases with the temperature as predicted by the simulations. Throughout both temperature ranges, the QNS intensity increases monotonically with heating. The discrepancy between the experiment and the MD simulations is not understood at present. We speculate that the molecular diffusion may involve torsional motion of the end methyl groups, which are not included in the simulation.

Wed. 10:15 a.m.–12:00 p.m., Poster, KR-03

Neutron Investigations of Liquid Dynamics in the Polymer Gels

Valeri V. Klepko (National Academy of Sciences of Ukraine), L. A. Bulavin, V. I. Slisenko (Institute of Macromolecular Chemistry), Taras Shevchenko (Kyiv State University)

Investigations of molecules' mobility in porous media represent a very interesting problem that is connected to the description of dynamics of different size particles in the field of randomly distributed obstacles. Besides the obvious fundamental interest, such investigations are highly important for a variety of technologies, such as biomedical membranes, gel permeation chromatography,

membrane separation and filtration, proton conducting gel electrolytes, etc. In this report we present the results of the experimental investigation of the diffusion processes in the polymer gels of different chemical natures. Using quasi-elastic neutron scattering (QENS) and neutron transmission techniques, the self-diffusion and mass transfer of liquid molecules in aqueous [gelatin, poly(acrylamide)] and nonaqueous [silica, poly(vinyl chloride)] polymer gels have been studied. Using these techniques, we have covered a wide timescale ranging from microscopic (10-12-10-10 s, QENS) to macroscopic (101 to 104 s, neutron transmission) times. QENS data were interpreted according to the conception of the hierarchy of molecular motions timescale: slow collective motions of the molecules in the content of Lagrange's clusters and rapid single-particle motions (jump-diffusion mechanism). Using this approach, the collective and single-particle diffusion coefficients of liquids in the gels of different concentrations were determined. Theoretical analysis of the neutron transmission data shows that in the macroscopic range, the diffusion of the liquid molecules in hydrogels have the effective medium concept behavior for semidilute polymer gel matrixes. The influence of the obstacles concentration, thermodynamic state, and ion complexes on the liquids mobility in the polymer gels have been also studied and interpreted on the basis of modern theoretical predictions.

Wed. 10:15 a.m.–12:00 p.m., Poster, KR-04

Structure of PEO-PPO-PEO Gels in Mammalian Cell Medium for Tissue Engineering Applications

Surita Rani Bhatia, Julie Matthew (University of Massachusetts)

We investigate gels of a poly(ethylene oxide)-poly(propylene oxide)-poly(ethylene oxide) copolymer, Pluronic F127, in mammalian cell culture medium for applications in tissue engineering and cell encapsulation. It is well known that aqueous solutions of F127 will gel at physiological temperatures and that this transition corresponds to formation of a close-packed cubic assembly of spherical micelles. Previous work in our groups has shown that in both mammalian cell minimum essential medium (MEM) and MEM with added fetal bovine serum (MEM-FBS), the gel phase boundary shifts to lower temperatures and concentrations as compared to pure

water. Our small-angle neutron scattering (SANS) studies indicate that F127 in cell medium also forms a close-packed cubic micellar gel, suggesting that the mechanism of gelation is the same in both pure water and MEM. Fits to the neutron spectra show no appreciable difference in the micelle size or aggregation number between MEM and water. However, the gels in MEM exhibit stronger ordering and sharper peaks, perhaps indicating stronger intermicellar interactions in the presence of MEM. Finally, our SANS spectra on dilute solutions (2 to 5 wt % polymer) of F127 in MEM indicate strong correlations between micelles, whereas no correlation peak is observed for these concentrations of F127 in water. This stronger repulsive interaction may be the cause of the shift in the liquid-gel phase boundary that is observed.

Wed. 10:15 a.m.–12:00 p.m., Poster, KR-05

SANS Study of Structure and Interaction of Triblock Copolymer Micelles: Effects of Molecular Weight and Temperature and Sodium Carbonate Salt

Lixin Fan, P. Thiyagarajan (Argonne National Laboratory)

We have investigated the micellization and interaction in aqueous solutions of triblock copolymers of 5 wt % F38, F68, F88, F98, and F108 using small-angle neutron scattering (SANS) as a function of temperature and concentration of sodium carbonate. The critical micellization temperatures and concentrations and the thermodynamic parameters of micellization were obtained for F108 in presence of salt. SANS data were fitted by using appropriate form factor and structure factors to extract the information on the size of the core, corona, interparticle distance, aggregation number, and the volume fraction of the micelles. These studies show that the temperature, molecular weight of the triblock copolymers, and sodium carbonate have a strong effect on the micellization. As the molecular weight increases, the micelle aggregation number and the radii of the core, corona, and hard sphere increase. However, the temperature, at which the saturation of the volume fraction of the micelles (completion of the micellization) occurs, decreases with increasing molecular weight. The presence of sodium carbonate decreases both critical micellization temperature and micellization completion temperature, as well as the temperature of transition from spherical to

cylindrical micelles. Furthermore, the micellization and transition temperatures decrease with increasing molecular weight of the copolymer as well as the salt concentration. The mechanism of the micellar structure and the phase separation is through gradual dehydration of the copolymer chains with an increase in either the temperature and/or the salt concentration. Progressive dehydration occurs in the core at lower temperature, whereas progressive insertion of PEO units into the core occurs at higher temperature ($T > 50^\circ\text{C}$).

Wed. 10:15 a.m.–12:00 p.m., Poster, KR-06

Using Internal/External Contrast Variation To Study the Role of Counterion Binding in Micellar Structure

Zhibin Li, Lee Magid (University of Tennessee), Paul D. Butler (Oak Ridge National Laboratory)

Unlike the nonpenetrating counterions—such as chloride and bromide—2,6-dichlorobenzoate can penetrate into the cetyltrimethylammonium (CTAX) micelles to change the micellar structure in order from globular micelles, to short rod, to elongated wormlike micelles, and back to globular micelles as the concentration increases. Small-angle neutron scattering has been used to determine the rodlike and spherical micellar internal structure by the methods of external and internal contrast variation. By using deuterated sodium 2,6-dichlorobenzoate, deuterated surfactant, and changing the $\text{D}_2\text{O}/\text{H}_2\text{O}$ content in the solution, we can get detailed information on counterion binding.

Wed. 10:15 a.m.–12:00 p.m., Poster, KR-07

SANS Study of the Micellization of PEO-PPO-PEO Triblock Copolymers in Aqueous Electrolyte Solutions

Sathish K. Sukumaran, G. Beaucauge (University of Cincinnati), P. Thiyagarajan (Argonne National Laboratory)

Small-angle neutron scattering was used to study the effects of several potassium salts (K_3PO_4 , $\text{K}_2\text{P}_4\text{O}_{13}$, KNO_3 , KF , and KCl) on the structural evolution and inter-aggregate interactions of the Pluronic F88 ($\text{P}(\text{EO})_{103}$ -

P(PO)₃₉-P(EO)₁₀₃ in aqueous (D₂O) solution. Addition of the salts lowered the micellization temperature. The progression of the micellar structures (from spherical to cylindrical) with a variation in the salt concentration is similar in nature to that observed with a change in temperature in the F88/pure D₂O system with the differences found only in the temperature(s) at which the structural transformation(s) takes place. Dimensions of the micelles were obtained by modeling the scattering data using analytical expressions for the scattered intensity. The calculated dimensions of the micelles, coupled with certain assumptions, were used to obtain several quantities of interest, like the amount of water in the core. The quantities thus obtained were then used to interpret the mechanism of the structural behavior in terms of the effects of the different salts studied. It appears that the process of progressive dehydration of the copolymer is the cause of all the structural transformations observed. The obtained values for the characteristic sizes of the micelles indicated that the salts were effective in the order K₂CO₃ ~ K₃PO₄ ~ K₂P₄O₇ > KF ~ KNO₃ > KCl in promoting micellization.

monolayers provide well-defined surfaces for studying protein adsorption behavior and also a potential means of creating monomolecular coatings for surface modification. The hydrophobicity of SAMs has been of great interest in studying surface interactions with proteins. An important property that can be varied to control adsorption is the packing density of the SAM alkyl chains. The adsorption behaviors of delipidized HSA and lipidized HSA (fatty acid bound) to SAMs were compared using ex situ X-ray reflectivity measurements that are extremely sensitive to adsorbed layer thickness. The adsorption tenacity was seen to vary strongly with the alkyl chain packing in the SAM for delipidized HSA for which the binding sites are free to interact with the surface. The tenacity of adsorption of lipidized HSA was insensitive to SAM packing. In situ neutron reflectivity measurements were used to complement the X-ray reflectivity measurements. A larger contrast among different components of the system can be obtained when using neutron reflectometry by exploiting deuterium labeling of the SAM and the use of D₂O.

Research support from The Whitaker Foundation and the Army Research Office (MURI contract DAAH4-96-1-0018) is gratefully acknowledged.

Wed. Morning, KS-Biology

Summit Grand Ballroom II

Wed. 10:15 a.m.–12:00 p.m., Poster, KS-01

Role of Binding Sites in Human Serum Albumin Adsorption to Self-Assembled Monolayers

Eugene J. Choi, Mark D. Foster (University of Akron), Charles Majkrzak (National Institute of Standards and Technology), Peter Witte, Henning Menzel (Technical University of Brunswick)

A comparison of the adsorption behaviors of Human Serum Albumin (HSA) with and without its fatty acid binding pockets filled suggests that these specific binding sites play an important role in determining the tenacity with which HSA binds to hydrophobic self-assembled monolayers (SAMs). Since the interactions between proteins and surfaces are key in dictating biocompatibility, an ability to control adsorption tenacity by engineering monomolecular coatings is attractive. Self-assembled

Wed. 10:15 a.m.–12:00 p.m., Poster, KS-02

Neutron Diffraction of Alpha, Beta, and Gamma Cyclodextrins: Hydrogen Bonding Patterns

Brian E. Hingerty (Oak Ridge National Laboratory), V. Zabel, C. Betzel, W. Saenger (Frie Universität Berlin)

Cyclodextrins (CDs) have proved useful as model systems for the study of hydrogen bonding. They are torus-shaped molecules composed of six(α), seven(β), or eight(γ) linked glucoses. Because of their particular geometry, they are able to act as “hosts” to form inclusion complexes with “guest” molecules very much like enzymes. CDs have been shown to exert catalytic activity on suitable included-substrate molecules; they catalyze the hydrolysis of phenylacetates, of organic pyrophosphates, and of penicillin derivatives. They also accelerate aromatic chlorinations and diazo coupling by means of their primary and/or secondary hydroxyl groups so that the rates of hydrolysis are enhanced by up to a factor of 400. In order to understand the hydrogen bonding in these

enzyme models, neutron diffraction data were collected to unambiguously determine the hydrogen atom positions, which could not be done from the x-ray diffraction alone. The two different structures for α -CD correspond to an "induced-fit" like mechanism. Both β -CD and γ -CD possess an unusual "flip-flop hydrogen bond" with the disordered water and hydroxyl structure of the type O-H...H-O representing an equilibrium between two states: O-H...O and O...H-O. This study demonstrates that hydrogen bonds are operative in disordered systems and display dynamics even in the solid state.

This work was supported by Oak Ridge National Laboratory, which is managed by UT-Battelle, LLC, for the U.S. Department of Energy under contract DE-AC05-00OR22725; the National Institutes of Health Grant GM 34687-05 (B. H. and V. Z.); the Bundesministerium für Forschung and Technologie (Grant FKZ 03 B72 A079); and the Fonds der Chemischen Industrie (V. Z. and W. S.).

Wed. 10:15 a.m.–12:00 p.m., Poster, KS-03

Effect of Zinc (Zn^{2+}) Ions on Self-Assembly of β -amyloid(10-21) Studied by Small-Angle Neutron Scattering

Jaby Jacob (University of Chicago and Argonne National Laboratory), Jijun Dong, D. G. Lynn, D. M. Morgan (Emory University), P. Thiyagarajan (Argonne National Laboratory)

The primary component of the amyloid plaques of Alzheimer's disease is the 39 to 43 amino acid peptide, β -amyloid. Recently, a combination of small-angle neutron scattering (SANS) and solid-state nuclear magnetic resonance experiments on the aggregated state of $A\beta(10-35)$ allowed us to propose an experimentally justified model of the $A\beta(10-35)$ fibril. This model predicts the spatial clustering of like amino acids throughout the fiber, including His 13 and His 14, and therefore suggests an explanation for another observation from the Alzheimer's disease literature, that Zn^{2+} and other multivalent cations increase the rate at which $A\beta$ peptides self-associate. Our current efforts are directed at clarifying the relationship between Zn^{2+} and the structure and kinetics of fiber formation. We have carried out SANS measurements on $A\beta(10-21)$, a short amyloid fragment whose sequence

emphasizes the putative metal binding site. Our experiments indicate that $A\beta(10-21)$ in the absence of Zn^{2+} aggregates to form a long cylindrical species that has a cross-sectional radius of ~ 29 Å at pH 5.4. We do not observe a dependence of either the size or the concentration of the cylinders with time over a period of ~ 15 hours. However, in the presence of Zn^{2+} , the cylindrical fibrils formed have a smaller cross-sectional radius of ~ 23 Å (at pH 5.4). We also note that the fibrils are formed within a few minutes of dissolving the peptide in the buffer in contrast to the case where fibrils were observed only 4 to 5 hours after dissolving the peptide in the absence of Zn^{2+} .

This work benefited from the use of the Intense Pulsed Neutron Source at Argonne National Laboratory, which is funded by the U.S. Department of Energy (DOE) Office of Basic Energy Sciences, and was carried out under the auspices of the Nuclear Energy Research Initiative of the U.S. DOE under contract W-31-109-ENG-38.

Wed. 10:15 a.m.–12:00 p.m., Poster, KS-04

Electron-Phonon Coupling in the Light-Harvesting Complex II of Green Plants

Joerg Pieper, R. E. Lechner (Hahn-Meitner Institut Berlin), K.-D. Irrgang, G. Renger (Technische Universität Berlin)

The primary steps of photosynthesis comprise the generation of electronically excited states by light absorption in antenna pigment-protein complexes and rapid excitation energy transfer (EET) to reaction center complexes. The major constituent of the antenna of green plants is the light-harvesting complex II (LHC II). The LHC II protein is embedded into the thylakoid membrane of green plants and forms a trimer of subunits, each of which consists of 12 to 13 chlorophyll molecules, at least two carotenoids, one amphipathic, and three membrane-spanning α -helices. In antenna complexes, the coupling of the electronic transitions to low-frequency vibrations of the protein matrix (phonons) plays an essential role in light harvesting as well as in ultrafast EET. Thus, a detailed understanding of ultrafast EET requires thorough analyses of electron-phonon coupling. In the present study, inelastic neutron-scattering experiments are combined with high-resolution optical spectroscopy in order to quantitatively characterize the phonon density of states of LHC II.

Wed. 10:15 a.m.–12:00 p.m., Poster, KS-05

Chlorophyll-b and the Regulation of Light-Harvesting Processes in Plants

David Worcester, J. J. Katz (Argonne National Laboratory), Nancy Vosnidou (University of Missouri)

This work explores functions of chlorophyll-b (Chl-b) in light-harvesting processes of plants. Chl-b is present only in light-harvesting (antenna) complexes (LHC) but amounts to 1/4 to 1/3 of the total chlorophyll in plants and many algae. LHC size is tightly coupled to Chl-b synthesis, but the mechanisms of this coupling are unknown. Details of Chl-b biosynthesis remained an enigma until the last few years. Although textbooks present Chl-b as serving to absorb light near 500 and 650 nm where Chl-a absorbs poorly, this role is probably minor. Studies of chlorophyll aggregates by neutron scattering and absorption spectroscopy show that Chl-b can inhibit the red-shift in the visible absorption that occurs in Chl-a aggregates. This may serve in vivo to ensure fast energy transfer without the “uphill” steps that have been recently demonstrated for the long wavelength chlorophyll-a of Photosystem I. Without such fast energy transfer, there is increased formation of triplet states in chlorophyll-a, which can react with molecular oxygen to form highly reactive singlet oxygen. We conclude therefore, that chlorophyll-b, like carotenoids, serves the important function of reducing oxidative stress during the primary processes of photosynthesis.

Wed. 10:15 a.m.–12:00 p.m., Poster, KS-06

Small-Angle Scattering Study of Sml1 Protein and its Complex with RNR1 Protein

Peng Yuan, Jinkui Zhao (Oak Ridge National Laboratory), Chris Dealwis (University of Tennessee)

Ribonucleotide reductase (RNR) catalyzes the reduction of ribonucleotides to deoxyribonucleotides. A novel protein called Sml1 was shown to bind to the RNR1 protein. It inhibits the RNR activity. We are interested in the structure of the Sml1 protein, especially its interaction with RNR1. From our neutron and X-ray scattering data, the Sml1 protein appears to form a polymeric aggregate at various buffer conditions and protein concentrations.

However, synchrotron radiation seems to break the aggregate up without noticeably damaging the Sml1 protein. This observation is contrary with many cases where radiation typically induces protein aggregation. Further studies are under way to characterize the Sml1 protein and its complex with RNR1.

Wed. Afternoon, LA–Polymer Structure and Thermodynamics II

*Chair: Robert Briber (University of Maryland)
Tennessee Ballroom A*

Wed. 1:15 p.m., Keynote, LA-01

PNIPAM Grafted Chains at the Silicon/Water Interface: Temperature-Dependent Conformational Changes and Protein Adsorption

Michael S. Kent, H. Yim, Dale Huber (Sandia National Laboratories), K. Shin, S. Satija (National Institute of Standards and Technology), J. Majewski, G. S. Smith (Los Alamos National Laboratory)

Poly(N-isopropyl acrylamide) (PNIPAM) is perhaps the most well known member of the class of responsive polymers. It has a lower critical solution temperature at about 31°C. This very sharp transition (~5°C) is attributed to the disruption of the hydrogen bonding of water molecules around the amide group of the side chain. Proteins adsorb strongly onto PNIPAM layers above 31°C but adsorb only weakly below 31°C. For this reason, PNIPAM layers are being investigated for use in protein preconcentrators for microchemlab applications. In this work, we investigate the conformation of grafted PNIPAM chains at the silicon/water interface using neutron reflection (NR). Grafted PNIPAM layers were prepared both by reacting COOH-terminated PNIPAM to OH-terminated self-assembled monolayers on silicon (“grafting to” method) and by polymerizing NIPAM monomers from silicon (“grafting from” method). Detailed concentration profiles of PNIPAM layers in D₂O and d-acetone were determined by NR. A range of PNIPAM molecular weights from 33 to 220 K have been examined. Surprisingly, whereas the samples all have a

cloud point at about 31°C in aqueous solution, we find little change in the conformation of the grafted PNIPAM chains with temperature. A bilayer profile is required to fit the data for all PNIPAM samples in D₂O, but a smoothly decaying, one layer profile is adequate for the PNIPAM samples in d-acetone. The PNIPAM chains are more collapsed in d-acetone than in D₂O. The adsorption of myoglobin to the grafted PNIPAM layers as a function of temperature will also be discussed.

Wed. 1:45 p.m., Invited, LA-02

Microstructure of High-Pressure Polyolefin/n-Alkane Solutions

John Hollis van Zanten (North Carolina State University), Mark A. McHugh (Virginia Commonwealth University), Todd P. DiNoia (Johns Hopkins University)

A series of dilute and semi-dilute poly(ethylene-co-1-butene)/ simple n-alkane solutions has been investigated with high-pressure small-angle neutron scattering (SANS) and dynamic light scattering. The simple n-alkane solvents considered in these investigations were ethane, propane, butane, and pentane. The solutions have been examined at 130°C and at pressures up to ~2000 bar. In the semi-dilute concentration range, the classic high concentration isotopic labeling technique is used in conjunction with SANS to determine both the solution correlation length and coil dimensions for poly(ethylene-co-1-butene) dissolved in either ethane or pentane. Chain collapse is observed upon approach to the phase boundary in both solvents. For the dilute solution regime, solutions of varying concentration are considered in order to isolate both the polymer diffusion coefficient at infinite dilution as well as the dynamic second virial coefficient, which is primarily dominated by the second osmotic virial coefficient. Interestingly, the supercritical solvents (ethane, propane, and butane) are found to swell the chains to a greater degree than the simple liquid solvent pentane, wherein it is observed that the polymer coil hydrodynamic radius is essentially unchanged throughout the pressure range considered. Coil behavior in the dilute and semi-dilute concentration regimes is compared and contrasted.

Wed. 2:00 p.m., Talk, LA-03

Polymer Thin Films in Supercritical CO₂

Miriam Rafailovich (State University of New York, Stony Brook)

We report an anomalous swelling of polymer thin films in carbon dioxide (CO₂), which is associated (in both locus and form) to the density fluctuation ridge that forms along the extension of the coexistence curve of gas and liquid in the P-T phase diagram. In situ neutron reflectivity showed that CO₂ could be sorbed to a large extent (~60%) in thin polymer films even when the bulk miscibility of the polymer with CO₂ is very poor. The anomalous swelling is found to scale with the polymer radius of gyration (R_g) and extends to a distance approximately 10 R_g. Neutron reflectivity in combination with dynamic secondary ion mass spectrometry measurements showed that this is associated with a decrease in glass transition temperature that occurs only within the narrow region of the phase diagram associated with the density fluctuation ridge. Within the ridge the diffusion coefficients scale as M⁻² and can be approximated by an effective William-Landel-Ferry (WLF) equation.

Wed. 2:15 p.m., Talk, LA-04

Dynamics of Copolymeric Surface Segregation Using Neutron Reflectivity

Mark D. Dadmun, Michael Arlen (University of Tennessee), William A. Hamilton (Oak Ridge National Laboratory)

Surface segregation of a functional additive in a polymer matrix can provide a mechanism by which the surface-sensitive properties (biocompatibility, flammability, etc.) of the polymer may be selectively modified. Moreover, if the additive is polymeric (i.e., a copolymer), its entanglement with the polymer matrix will limit erosion of the surface-active component at the face of the sample. However, there is very little understanding of how the copolymer structure (graft vs comb. vs random) impacts the rate of segregation of the additive to the surface, information that will be important in designing new and useful additives. Moreover, there exist few techniques that can accurately provide this information (i.e., characteristics of the

diffusive behavior of copolymers in a homopolymer matrix). In this talk, we will present neutron reflectivity results that reliably determine the diffusion coefficients of copolymers in a homopolymer matrix and thus provide a mechanism by which the importance of copolymer architecture on its utility as a surface-active additive can be efficiently examined. Furthermore, results will also be presented that will shed light on the importance of copolymer structure and composition on its dynamics.

Wed. 2:30 p.m., Talk, LA-05

Polymer Blends as Theta Systems: New SANS Data and Interpretation

Yuri B. Melnichenko, G. D. Wignall (Oak Ridge National Laboratory), D. Schwahn (Forschungszentrum Jülich)

For two decades, the miscibility of various polymers was studied by small-angle neutron scattering (SANS), based on the de Gennes Random Phase Approximation (RPA). The RPA is essentially equivalent to the assumption that the radius of gyration (R_g) of the polymer blend components remains unchanged on mixing, and thus exhibits the unperturbed dimensions, as in a melt or in a polymer solution at the theta temperature. However, several theoretical, computer simulation, and experimental results have suggested that this assumption may not hold universally and that R_g may shrink or expand with temperature or concentration. Considering a polymer blend as a special case of a polymer solution, one might expect that the RPA should be strictly valid only for “ideal” or theta blends of noninteracting polymers, whereas finite interactions between polymer segments may lead to the variation of R_g , as is observed in dilute solutions of polymers in small molecule solvents. In this talk we discuss recent SANS data on the R_g and the correlation length as a function of temperature and concentration in weakly and strongly interacting polymer blends. We show that macromolecules in miscible polymer blends may behave as good, theta, and poor polymeric solvents for each other and construct a conceptual phase diagram, delineating the range of validity of the RPA, outside of which polymers contract or expand beyond their unperturbed dimensions.

The revealed occurrence of the upper and lower theta points may provide new insight and interpretation of some of the yet unexplained phenomena, such as variation of the interaction parameter with the molecular weight (M_w) and concentration, the M_w -dependence of the Ginzburg number, as well as the crossover between mean field and fluctuation regimes in polymer blends.

Wed. Afternoon, LB–Sample Environment and Neutron Detection

Chair: Jack Carpenter (Argonne National Laboratory)

Tennessee Ballroom B

Wed. 1:15 p.m., Keynote, LB-01

High-Pressure Techniques and Neutron Scattering

Chris A. Tulk (Oak Ridge National Laboratory), J. Parise (State University of New York, Stony Brook), N. Y. R. Hemley (Carnegie Institution of Washington)

The study of materials under conditions of extremely high pressure over a wide range of temperature using neutron-scattering techniques is likely to be a significant growth area for the foreseeable future. With novel large-volume, ultrahigh-pressure devices, either those recently demonstrated or those currently under development, it is reasonable to expect that neutron-scattering studies of samples under pressures ranging from 2-60 Gpa, and even perhaps upwards of 100 Gpa, will be a reality over the next decade. This talk will briefly review the current state-of-the-art, high-pressure neutron instrumentation available at several laboratories within the United States and around the world. Further emphasis will be placed on recent initiatives to produce ultrahigh-pressure/high-temperature devices specifically designed to take advantage of the enhanced flux available at next-generation neutron sources. Finally, several recent scientific examples of neutron scattering from samples held in situ under ultrahigh pressure conditions will be highlighted.

Wed. 1:45 p.m., Invited, LB-02

X-Ray and Neutron Scattering from Levitated Liquids

David L. Price (Centre de Recherches sur les Matériaux à Haute Température—Centre National de la Recherche Scientifique and Argonne National Laboratory), M.-L. Saboungi (Centre de Recherche sur la Matière Divisée), S. Krishnan (Containerless Research Inc.), L. Hennet, C. Landron, D. Thiaudières (Centre de Recherches sur les Matériaux à Haute Température), E. E. Alp, H. Sinn (Argonne National Laboratory)

Measurements of liquid structure, dynamics, and transport are important in advancing condensed matter theory, in developing predictive models, and in establishing structure-property-process relationships in high-temperature materials science. The major experimental difficulties encountered in obtaining structural data on liquids at temperatures above about 1000 K are (1) reactions of the samples with container walls and (2) influence of the containers on the structural measurements. Recently, a number of research groups around the world have attempted to overcome these problems by employing levitation techniques in conjunction with x-ray and neutron scattering to study the properties of high-melting, corrosive liquids. Several key advantages of these methods include (a) the elimination of container interactions and container-derived impurities, (b) rapid access to high temperatures, (c) localized heating conditions, and (d) access to the supercooled liquid and other metastable states. This talk will present recent results on levitated liquids obtained with X-ray and neutron diffraction and inelastic X-ray scattering.

This work was supported in part by the French CNRS and by the U.S. Department of Energy Office of Science under contract W-31-109-ENG-38.

Wed. 2:00 p.m., Talk, LB-03

Polarized ^3He -Based Neutron Spin Filters

Thomas Richard Gentile (National Institute of Standards and Technology)

Several methods exist for polarizing neutrons, such as supermirrors for cold neutron energies, Heusler alloy for thermal neutron beams, and polarized proton filters for epithermal energies. However, certain applications require a new approach. This talk will review the progress by the National Institute of Standards and Technology (NIST) and Indiana University in the development and application of neutron spin filters based on the large spin dependence of the cross section for neutron absorption by ^3He . For cold neutron scattering, ^3He -based spin filters have much greater angular acceptance than supermirrors, which is desirable for diffuse reflectometry and other applications that involve large solid-angle polarization analysis. ^3He -based devices are well matched to time-of-flight analysis at spallation sources because they filter all neutron energies. We are developing two optical pumping methods, spin-exchange (SEOP) and metastability-exchange (MEOP), to produce highly polarized ^3He gas. For SEOP, we have recently developed spin filters with long polarization relaxation times, which is relevant to obtaining high polarization in large diameter cells and also for applications in which the gas is polarized remotely. The SEOP method is relatively simple and compact and is best suited for spin filters that will be continuously optically pumped on a beam line. The MEOP method requires compression of the polarized gas but has the capability of rapid polarized gas production. We will report results of a piston compression system at Indiana University and a compact compressor at NIST. We will also discuss experiments to test the application of ^3He spin filters, which we have carried out at the NG3 Small Angle Scattering Spectrometer at the NIST Center for Neutron Research and the POSY-I reflectometer at the Intense Pulsed Neutron Sources at Argonne National Laboratory and which are also planned for the NG1 reflectometer. Applications to experiments in weak interaction physics will also be presented.

Wed. 2:15 p.m., Invited, LB-04

Lithium Gadolinium Borate Scintillators

J. Bart Czirr (MSI/Photogenics) and Thomas K. McKnight (MSI/Photogenics)

What role will detectors built with fast scintillators play in spallation neutron source instrumentation? To answer this question, an overview of three categories of contemporary detector materials will be presented: gaseous detectors, slow scintillators, and fast scintillators. The various classes of neutron-scattering instruments will be described, and the detector types that could be employed in each will be proposed. A new, fast scintillator, lithium gadolinium borate (LGB), has been incorporated into a 1200-cm² detector module at the ISIS neutron-scattering facility, United Kingdom. This type of detector module is used at ISIS for powder diffractometers such as the General Materials Diffractometer (GEM) and the High Resolution Powder Diffractometer (HRPD). A series of experiments was conducted to make a direct comparison of the performance of LGB to ZnS/LiF scintillator in these types of detectors. An overview of experimental results obtained at the HRPD instrument station will be presented to illustrate the performance characteristics of LGB in powder diffractometers. The physical characteristics of LGB, an inorganic, crystalline scintillator, will be discussed. Future applications will be proposed.

Wed. 2:30 p.m., Talk, LB-05

Exotic Concepts of Neutron Detectors for Spallation Neutron Sources

Jim Schelten (Forschungszentrum Jülich GmbH)

Traditional neutron detection is based on ³He proportional counters and wire chambers and on ⁶Li scintillation detectors. Some attempts were made to detect neutrons with semiconductor pin diodes and ⁶LiF or ¹⁰B¹¹C converters. The latter suffers from low detection efficiency, in particular for thermal neutrons. The discovery in early 2001 that Mg₂B is superconducting at T_c = 39 K allows an efficient detection of thermal neutrons with superconducting tunnel junctions. At an operation temperature of 4.2 K, excellent detection properties are predictable. For scattering experiments at pulsed spallation sources, advanced

beam monitors are needed that provide simultaneously temporal and spatial information without attenuating the primary beam by scattering or absorption. A solution with a dual-ionization chamber in which the middle electrode consists of a thin aluminum foil covered by ⁶LiF converter layer and the two counter electrodes consist of strips in x and y direction is described. The detection efficiency is adjustable within the range 10⁻³ to 10⁻⁶. The strip width at the two counter electrodes determines the spatial resolution. At present, the major problems of neutron detectors are (1) the required large detection areas of up to 10 m², (2) a high instantaneous count rate of 10⁶ events per second, and (3) the demanded low cost limited by \$10 per cm². In the frame of these needs, all detector concepts and experiments should be discussed. The detection of neutrons over areas of 1 to 10 m² is still a serious technical and economical problem, even if one is satisfied with moderate spatial resolution for the large area detectors. Experimental attempts to detect neutrons with ¹⁰B- or ⁶Li-containing insulators are presented. The insulators like Duran glass and sintered Boronitride are available in large quantities and are extremely cheap compared to ⁶Li scintillators, ³He fill gases, and silicon wafers.

Wed. Afternoon, LC-Materials III

Chair: Rob McQueeney (Los Alamos Neutron Science Center)

Tennessee Ballroom C

Wed. 1:15 p.m., Keynote, LC-01

First Principles Calculations to Guide and Interpret Neutron Spectroscopy of Materials

Taner Yildirim (National Institute of Standards and Technology Center for Neutron Research)

We will present several projects at the National Institute of Standards and Technology Center for Neutron Research that exemplify the power of neutron scattering when combined with first-principles calculations. Systems that we will discuss include new 40-K superconductor MgB₂, molecular solid cubane, protonic-conducting oxides, hydrogen-bonded systems, and the cubic negative thermal expansion material ZrW₂O₈. The measured

structural and dynamical properties and their temperature dependencies are compared with those obtained from first-principles calculations. In most cases, impressive agreement was obtained, even for systems as diverse as van der Waals molecular solids and ionic oxides. Therefore, the first-principles computational method with its predictive power should be considered as an indispensable tool for the analysis of neutron-scattering data.

Wed. 1:45 p.m., Invited, LC-02

Phonon Anomalies in Relaxor $\text{Pb}(\text{Mg}_{1/3}\text{Nb}_{2/3})\text{O}_3$

Shuichi Wakimoto, C. Stock, R. J. Birgeneau (University of Toronto), P. M. Gehring (National Institute of Standards and Technology), G. Shirane (Brookhaven National Laboratory), Z.-G. Ye, W. Chen (Simon Fraser University), W. J. L. Buyers (Chalk River Laboratories)

A detailed investigation of soft phonons was carried out for the prototypical relaxor ferroelectric $\text{Pb}(\text{Mg}_{1/3}\text{Nb}_{2/3})\text{O}_3$ (PMN). Relaxors show a broad maximum in the temperature dependence of the dielectric constant at T_{max} , which is significantly frequency dependent. An important clue for such a relaxor behavior is the formation of “polar nanoregions” (PNR) below T_{d} suggested by Burns and Dacol [1]. From a recent series of inelastic neutron-scattering experiments on PMN, Gehring et al. [2] observed a dramatic change of the transverse optic (TO) phonon dispersion from normal one to a “waterfall”-type one across T_{d} . Also, Hirota et al. [3] proposed a simple model to resolve the puzzling problem of diffuse scattering for PMN by introducing the “condensed soft mode with phase shift.” We have extensively investigated the TO and the transverse acoustic (TA) modes down to 11 K. The soft mode, overdamped by polar nanoregions below T_{d} , recovers dramatically below 220 K. The square of the soft phonon energy increases linearly with decreasing temperature. The TA phonon line broadening starts at T_{d} and disappears at 220 K, coincident with the recovery of the TO mode. These results imply that well-developed ferroelectric state is established at low- T instead of a randomly oriented PNR (relaxor) state. [1] G. Burns et al., *Solid State Commun.* 48, 853 (1983). [2] P. M. Gehring et al., *Phys. Rev. Lett.* 87, 277601 (2001). [3] K. Hirota et al., *Phys. Rev B* 65, 104105 (2002).

Wed. 2:00 p.m., Invited, LC-03

Phonon Densities of States and the Electronic Nature of the Volume Collapse Transition in fcc $\text{Ce}_{0.9}\text{Th}_{0.1}$

Michael Edward Manley (Los Alamos National Laboratory)

Phonon density-of-states (DOS) curves were obtained from inelastic neutron-scattering spectra from $\text{Ce}_{0.9}\text{Th}_{0.1}$ at several temperatures from 10 to 300 K. The low-temperature alpha-phase (collapsed fcc) showed an 80% decrease in its highest energy phonon modes when heated from 10 to 140 K. The size of the effect was too large to be explained with anharmonicity, suggesting that electronic excitations are altering the interatomic potential. Despite the 17% volume collapse, the phonon DOS showed little change between the gamma-phase at 150 K and the alpha-phase at 140 K. This is supported by analysis of the magnetic spectra showing that most of the transition entropy can be accounted for with the crystal field and Kondo spin fluctuations. We argue that the anomalous behavior of the phonon DOS originates with the volume dependence of the Kondo spin fluctuations.

Wed. 2:15 p.m., Invited, LC-04

Dynamic Local Jahn-Teller Fluctuations in Cobaltates

Despina Louca (University of Virginia)

The cobalt perovskite, $\text{La}_{1-x}\text{Sr}_x\text{CoO}_3$, is fundamentally distinct from other perovskites because of its unique spin transitions, subjecting the system to variable spin-lattice coupling depending on the configuration. In pure LaCoO_3 spin, transitions occur with increasing temperature from the ground state low spin configuration (LS) to either a high-spin (HS) or an intermediate-spin (IS) configuration. The IS state is distinct because it is an eg Jahn-Teller (JT) active state. With doping, similar excitations are expected and when x exceeds 18%, ferromagnetism is established concomitant with the onset of metallic conductivity. Such spin fluctuations would be accompanied by distortions in the local atomic structure corresponding to and reflecting the type of transition in the presence of strong eg-lattice coupling. With the combination of time-averaged and

time-resolved neutron-scattering techniques, it has been possible to obtain information on the type of atomic distortions and how they fluctuate in time. The local atomic structure determined as a function of temperature and composition using the pair density function analysis showed that the octahedral environment changes in a way that corresponds to activation from the LS to the IS-JT state at low temperatures. Measurements of the dynamic structure function, $S(Q, \omega)$, provided additional evidence that lattice dynamics (strong momentum transfer dependence) indeed change with temperature and composition as seen by the change in the intensity of several phonon peaks. These modes become active with temperature in a way that is consistent with the local lattice becoming “glassy,” while no crystallographic structural phase transition is observed. The magnitude of their intensity is indicative of a collective excitation consistent with a phase transition that is not otherwise observed with macroscopic measurements.

Wed. 2:30 p.m., Invited, LC-05

Neutron-Scattering Studies of Vortex Matter in Type-II Superconductors: Peak Effect and Bragg-Glass Melting

Sean Ling, S. R. Park, I. Dimitrov (Brown University), J. W. Lynn, D. Dender (National Institute of Standards and Technology), S. M. Choi (National Institute of Standards and Technology and KAIST)

I'll discuss the recent breakthroughs in the field of vortex matter physics using neutron-scattering techniques. A well-known Imry-Ma theorem in statistical physics says that systems such as the Abrikosov vortex lattice in type-II superconductors cannot have positional long-range order due to the quenched random defects in the atomic lattice. For many years, a genuine symmetry-breaking phase transition of the solid-liquid type was considered unlikely for vortex matter systems. However, it has been proposed recently that a Bragg glass phase with topological order may exist in weak-pinning type-II superconductors. I'll discuss the results of a Brown-National Institute of Standards and Technology experiment [1], which demonstrated a first-order Bragg glass melting transition at the peak effect, a well-known flux-pinning anomaly ubiquitous in weak-pinning type-II superconductors. [1] X. S. Ling et al., *Phys. Rev. Lett.* 86, 712 (2001).

Author Index

A

Abernathy, Doug 70
 Abernathy, Doug L. 34
 Abernathy, Douglas L. 101
 Adam, J. 106
 Adams, C. P. 95, 105
 Adams, Mark 60
 Aeppli, G. 21
 Agamalian, Michael 59, 65
 Aldona, Rajewska 48, 49
 Alexandrov, Yuri Andreevich 104
 Allgaier, Jürgen 57
 Allis, Damian 40
 Allis, Damian G. 41
 Alp, E. E. 117
 Alvine, K. J. 105
 Anand, Dave K. 33
 Anderman, R. 100
 Anghel, V. N. P. 58
 Ankner, John F. 31
 Ankner, John Francis 102
 Anspach, Matthew A. 24, 108
 Arai, Masatoshi 77
 Argyriou, D. N. 73, 95
 Arlen, Michael 115
 Aronson, M. C. 73
 Aronson, Meigan C. 28
 Aso, N. 64
 Aswal, Vinod Kumar 48
 Azuah, Richard 60

B

Bader, S. D. 76
 Badica, E. 71
 Badyal, Yaspal Singh 23
 Baglioni, Piero 23
 Balashov, S. 100
 Balsley, Steven D. 107
 Barker, J. G. 32
 Barker, John 30
 Barkhouser, R. 34
 Barnes, A. C. 23
 Barry, Dwight D. 33
 Bateman, F. B. 100
 Bauer, Barry J. 84
 Baxter, David V. 57
 Beach, Geoffrey S. D. 89
 Beaucage, G. 111
 Beaucage, Gregory 26

Behr, G. 73
 Beitz, James V. 60
 Belch, H. 69
 Bell, David R. 107
 Bellissent-Funel, M.-C. 94
 Benmore, C. J. 42
 Benmore, Chris J. 107
 Benmore, Christopher 44, 68
 Berger, A. 88
 Berk, Norman F. 81
 Berkowitz, A. E. 89
 Berliner, Ronald R. 67, 104
 Betzel, C. 112
 Bewley, R. I. 73
 Bhatia, Surita Rani 20, 110
 Bhuvanesh, Nattamai S. P. 78
 Biancaniello, Frank S. 30
 Bienfait, Michel 108
 Birgeneau, R. J. 21, 119
 Blankenship, Dale M. 107
 Blasie, J. Kent 80
 Bogdanoff, Peter 79
 Bond, Gillian M. 107
 Bonn, D. 21
 Borchers, Julie A. 89
 Bourke, M. A. M. 45
 Bourke, Mark A. M. 29, 30, 45
 Bowman, Amy 106
 Boyce, Donald 29
 Braden, Dale 40
 Brand, P. C. 34
 Brand, Paul C. 33
 Briber, Robert M. 25, 51
 Broholm, C. 28, 34, 96
 Broholm, Collin Leslie 33
 Brown, Craig 23
 Brown, D. 84
 Brown, D. E. 71
 Brown, Don 109
 Brown, Donald W. 76
 Browning, James F. 107
 Buchannan, Michelle 34
 Bulavin, L. A. 110
 Bunz, Uwe H. F. 26
 Butler, J. 46
 Butler, P. D. 19, 49
 Butler, Paul 34
 Butler, Paul D. 50, 111
 Butler, W. 74
 Buttrey, D. 74
 Buyers, W. J. L. 21, 119

C

Caignaert, Vincent 77
Cameron, J. M. 57
Campbell, B. 95
Campbell, Branton J. 71
Carpenter, J. M. 59
Carpenter, John Marland 58
Cava, Robert 19
Chaikof, Elliot 81
Chakoumakos, B. C. 67
Chakoumakos, Bryan 46
Chakoumakos, Bryan C. 44, 61
Chatterjee, A. 36, 38
Chatterjee, Alok 37
Chen, W. 119
Cheong, S.-W. 96
Chinta, Sivadinarayana 39
Chmaissem, Omar 71
Cho, J. R. 30
Choi, Eugene J. 112
Choi, S. M. 79, 120
Choi, S. U. S. 86
Choi, S.-M. 32
Choi, Sung-Min 56
Chojnowski, David B. 70
Choo, Hahn 45
Choudhar, T. V. 39
Christensen, N. B. 21
Christodoulou, Nick 83
Chung, Jae-Ho 77
Ciezak, Jenn 40, 41
Ciezak, Jennifer A. 40
Circone, Susan 44
Clapham, Lynann 83
Clausen, Bjørn 29
Clausen, K. N. 21
Coakley, K. J. 63
Collins, C. B. 106
Collins, M. F. 108
Colmenero, J. 55
Colmenero, Juan 55
Conlon, Kelly Timothy 30
Connatser, Robert W., Jr. 66
Coulter, Kevin Patrick 64
Crichton, Mark 20
Criswell, L. 110
Criswell, Leah 109
Crow, J. E. 27
Czirr, J. Bart 118

D

Dabrowski, B. 71
Dadmun, Mark D. 115
Daemen, L. L. 39
Dahlberg, E. Dan 88
Dai, Pengcheng 71, 95
Darling, T. 61
Dawson, Paul Richard 29
Daymond, Mark 30
De Lurgio, Patrick 37
De, Udayan 46
Dealwis, Chris 114
Delaire, Olivier 78, 79
Deming, Tim 25
Demler, Eugene 20
Dender, D. 120
Dender, D. C. 79
DePies, Matthew 108
DeSanto, Peter J. 24, 108
Dewey, M. S. 64, 100
Diama, A. 109
Diama, Armand 110
Dimeo, R. 109
Dimeo, Rob 109
Dimeo, Robert Michael 86
Dimitrov, I. 120
Dimitrov, Ivo 79
DiNoia, Todd P. 115
Doerr, M. 73
Dombeck, Daniel 99
Dombeck, Thomas 99
Dong, Jijun 113
Doyle, J. M. 63, 105
Dunand, David C. 30
DuPont-Pavlovsky, Nicole 108
Dye, David 30
Dzhosyuk, S. N. 63, 105

E

Eccleston, R. S. 73
Ecker, J. 39
Egami, T. 76
Egami, Takeshi 77
Egelstaff, P. A. 42
Ely, T. M. 47
Enderle, M. 28
Engels, Ralf 38
Epstein, A. J. 27
Erwin, R. W. 27
Espada, Loren I. 66
Evans, Paul 75

F

Fan, Lixin 111
 Farago, Dr. Bela 99
 Faraone, Antonio 23
 Faucher, Keith M. 81
 Felcher, G. P. 75, 76, 88
 Felcher, Gian P. 69
 Ferguson, Phillip D. 103
 Fernandez-Baca, J. A. 26, 95
 Fernandez-Baca, Jaime A. 71
 Fetters, L. J. 82
 Fieramosca, Joseph S. 70
 Filossov, D. V. 106
 Fishman, Randy Scott 72
 Fitzsimmons, M. 88
 Fitzsimmons, M. R. 89
 Fjellfaag, Helmer 104
 Foster, Mark D. 49, 112
 Fratini, Emiliano 23
 Frielinghaus, Henrich 57
 Frost, C. 27
 Fujita, M. 74
 Fullerton, Eric E. 89
 Fulton, J. L. 23
 Fultz, Brent 78, 79

G

Gardner, Jason Stewart 96
 Gasparovic, G. 96
 Gast, Alice P. 25
 Gehring, P. M. 28, 119
 Geltenbort, P. 100
 Gentile, Thomas Richard 117
 Ghosh, V. 101
 Gilbert, Elliot Paul 65, 103
 Gilliam, D. M. 64
 Glanville, Yvonne 86
 Glinka, Charles Joseph 32
 Gnäupel-Herold, Thomas H. 30
 Goettler, Stephen Joseph 107
 Goldin, L. 100
 Goldman, A. M. 88
 Golub, R. 63
 Gonzalez, Juan 50
 Goodman, D. W. 39
 Gottlieb, Moshe 50
 Goyal, P. S. 48
 Goyette, R. J. 69
 Graf, M. J. 61
 Granada, J. Rolando 105
 Granroth, Garrett Earl 34
 Gredig, T. 88

Greene, G. L. 64
 Gregory, D. H. 106
 Greven, M. 28
 Grube, Nathan 109
 Gudkov, Vladimir 100

H

Habicht, K. 105
 Haen, P. 73
 Haen, Pierre 28
 Hamilton, W. A. 19
 Hamilton, William A. 115
 Hamilton, William Anthony 49
 Hammond, R. L. 58
 Hammonds, J. 36
 Hammonds, John P. 37
 Hammouda, B. 32
 Hansen, F. Y. 109, 110
 Hanusova, D. 106
 Hardy, W. N. 21
 Hart, Robert T. 24, 108
 Hartman, M. 67
 Hauback, Bjorn C. 104
 Haynes, T. E. 46
 Heath, Christopher H. 43
 Hedden, Ronald C. 84
 Hedrick, James L. 25
 Heffner, R. H. 61
 Hellwig, Olav 89
 Hemley, N. Y. R. 116
 Hennet, L. 117
 Hersman, F. W. 100
 Herwig, K. W. 85, 109, 110
 Herwig, Kenneth W. 102
 Hill, B. K. 88
 Hill, Teresa Anne 49
 Hingerty, Brian E. 112
 Hinks, David G. 62
 Hjelm, Rex, Jr. 107
 Hjelm, Rex Paul 66, 81
 Hodges, Jason Paul 102
 Hoffmann, Christina 101
 Holden, T. M. 45, 47
 Holden, Thomas M. 84
 Holderna-Natkaniec, K. 41
 Hoteling, Nathan 40
 Hristova, Kalina 81
 Hu, Hegui 40, 41
 Huang, Q. 27, 96
 Hubbard, C. R. 47
 Huber, Dale 114
 Hudson, Bruce 40, 41
 Hudson, Bruce Samuel 97

Huffman, Paul R. 63, 105
Hussey, N. E. 21
Hwang, Jonghwi 49

I

Iland, Kristina 43
Indrakanti, Ananth 51
Iolin, Eugene 99
Iolin, Eugene M. 39
Irrgang, K.-D. 113
Ishii, Yoshinobu 44, 61
Islamov, A. H. 48
Iverson, Erik B. 103

J

Jacob, Jaby 24, 108, 113
Jacobson, D. L. 105
Jakobs, ritta 57
Jenkins, Tim 41
Jenkins, Timothy 40
Jenkins, Timothy A. 40
Jeong, Il-Kyoung 61
Jiang, J. S. 76
Jiao, X. 43
Jiao, Xuesong 50
Jirmanus, M. N. 69
Johnson, Jacqueline Anne 45
Johnson, Mark 108
Jones, C. Y. 61, 67
Jones, Camille Y. 44
Jones, G. L. 100
Jones, Gavin 40
Jones, Ronald L. 51
Jordan, Aszetta 46
Jorgensen, James D. 62
Jorgesnen, J. D. 71

K

Kaiser, Helmut 99
Kakurai, K. 74
Kalinnikov, V. G. 106
Karamian, S. A. 106
Kartini, E. 108
Katano, S. 26
Katsaras, J. 58
Katsumata, K. 28
Katz, J. J. 114
Kawano-Furukawa, H. 71
Keck, W. M. 24, 108
Keener, S. 102
Kemmerling, Guenter 36
Kennedy, Shane 103
Kent, Michael S. 114

Kepa, Henryk 88
Khalili, N. 84
Khan, Amjad 43
Khaykovich, Boris 72
Kim, T. H. 96
King, Hubert E. 82
Kintzel, Edward James 85
Kirby, S. H. 61
Kirby, Stephen H. 44
Klepko, Valeri V. 110
Kline, S. R. 32
Kline, Steven R. 56
Klose, Frank 65, 68, 69
Klug, D. D. 42
Kmety, Carmen R. 27
Kneller, Larry R. 80
Kockelmann, W. 73
Koetke, Donald D. 99
Koetzle, Thomas F. 97
Kohlmann, Holger 98
Kolesnik, S. 71
Kolesnikov, Alexander I. 98
Komarneni, Sridhar 86
Komives, Alexander Karl 100
Kopp, Daniel M. 37
Kopp, Manfred K. 37
Korobkina, E. I. 63
Kraft, Brian J. 108
Krasnoshekova, I. 100
Krishnan, S. 117
Krist, Thomas 32
Krivorotov, I. N. 88
Krueger, Susan 81
Kuhl, Tonya Lynn 80
Kuklin, A. I. 48
Kumar, Sanat K. 51
Kupcho, Kevin 66
Kwon, O. 100

L

Lake, B. 27
Lake, Bella 21
Lake, Bella A. 72
Lal, Jyotsana 56, 57
Lamoreaux, S. K. 63
Lan, Yanmei 40, 41
Lance, M. J. 46
Landron, C. 117
Lara, P. D. 38
Lara, Patrick D. 70
Larese, John Z. 87
Larsson, Cecilia 45
Lasakov, M. 100
Lawson, A. C. 61

Leao, Juscelino Batista 73
 Lebedev, N. A. 106
 Lechner, R. E. 113
 Lee, D. R. 88
 Lee, Hae-Jeong 84
 Lee, S.-H. 74
 Lee, Seung-Hun 96
 Lee, Seung-Yub 29
 Lee, Wai Tung 68
 Lee, Wai-Tung 69
 Lee, Young S. 21
 Lefmann, K. 21
 Leitch, Brian W. 83
 Leuschner, M. B. 100
 Leuschner, Mark 63
 Li, Zhibin 111
 Liang, R. 21
 Lieutenant, Klaus 35
 Lin, M. Y. 82
 Ling, C. D. 73
 Ling, Sean 120
 Ling, X. S. 79
 Littrell, K. C. 59
 Littrell, Kenneth C. 84
 Liu, Da-Wei 84
 Liu, Li 23
 Liu, Sam 72
 Liu, Zhentong 46
 Lodge, Timothy P. 24
 Loewenhaupt, Michael B. 73
 Loong, C.-K. 36, 38
 Lösche, Mathias 93
 Louca, D. 76
 Louca, Despina 119
 Lovekin, C. C. 108
 Lufaso, Michael Wayne 78
 Lumsden, Mark D. 22
 Lynn, D. G. 113
 Lynn, Gary W. 34
 Lynn, J. W. 27, 28, 34, 71, 79, 95, 120

M

MacEwen, Stuart 29
 Magid, Lee 50, 111
 Mais, J. 71
 Majerz, I. 41
 Majewski, J. 114
 Majewski, Jarek 80
 Majkrzak, Charles 112
 Majkrzak, Charles F. 80, 81, 89
 Makai, Mike 103
 Malo, Sylvie 77
 Mandrus, D. 22
 Mang, P. K. 28

Mangan, Michael A. 107
 Mangkorntong, N. 21
 Manson, L. J. 27
 Manley, Michael Edward 119
 Maple, Brian 28
 Marshall, S. L. 67
 Martin, James D. 22, 107
 Martter, Teresa D. 49
 Mason, P. V. 106
 Mason, T. E. 21
 Masuda, T. 74
 Matejicek, Jiri 30
 Matsuda, M. 26
 Matthew, Julie 110
 Mattoni, C. E. H. 63, 105
 Maxwell, S. 63
 Mayers, J. 58
 Mayes, Anne M. 50
 Maziasz, Philip 46
 McCall, S. 27
 McClain, B. A. 79
 McHugh, Mark A. 115
 McKinsey, D. N. 63, 105
 McKnight, Thomas K. 118
 McLain, Sylvia E. 107
 McMorrow, D. F. 21, 22
 McQueeney, Rob 77
 Meissner, M. 28
 Melnichenko, Yuri B. 116
 Mendelsohn, Jonas 50
 Menzel, Henning 112
 Merl, Robert B. 39
 Merton, C. 88
 Mezei, Dr. Ferenc 99
 Mezei, F. 32
 Mezei, Ferenc 33, 35, 58
 Middleton, Chris 40, 41
 Mihailescu, Mihaela 57
 Mikkelson, D. 38
 Mikkelson, Dennis 36, 37
 Mikkelson, R. 36, 38
 Mikkelson, Ruth 37
 Miller, Joel S. 27
 Mixture, Scott 79
 Mitchell, J. F. 71, 95
 Mo, H. 109, 110
 Molitsky, Michael 70
 Monkenbusch, M. 55
 Monkenbusch, Michael 35, 57
 Monson, Ryan 78
 Montfrooij, Wouter 28, 73
 Morgan, D. M. 113
 Morton, Maurice 49
 Mostovoy, Yu. A. 100

Murani, Amir 28
Mydosh, J. 73

N

Naday, Istvan 37
Nagler, S. 64
Nagler, S. E. 72
Nagler, S.E. 22
Nagler, Stephen E. 27, 34
Nann, H. 57
Narehood, David George 109
Natkaniec, I. 41
Natkaniec, Ireneusz 41
Nelson, Ronald O. 39
Neuefeind, J. 42
Neuman, Dan 94
Neumann, D. 109
Neumann, Dan A. 86
Neumeier, J. J. 73
Newalker, Bharat 86
Nico, Jeffrey S. 64
Niemann, Ralph 70
Niimura, Nobuo 82
Novgorodov, A. F. 106
Nowak, Andy 25
Nunn, Stephen D. 76

O

O'Donovan, Kevin V. 89
O'Hare, Dermot 22
Ohl, Michael 35
Orndorff, J. D. 34
Orndorff, Joseph D. 33
Osborn, R. 71
Osborn, Ray 28
Osborn, Raymond 95
Osgood III, R. M. 88

P

Padmini, P. 74
Pakstis, Lisa 25
Palmari, Jean-Pierre 108
Pandey, R. K. 74
Pappas, Catherine 35
Parello, J. 94
Parizzi, Andre 68
Parizzi, Andre de Azevedo 69
Park, S. R. 120
Park, Sang Ryul 79
Park, Stella Yoon-Sun 50
Parker, F. T. 89
Passell, L. 101
Payzant, Edward Andrew 47, 76

Pearce, Jonathan Vaughan 60
Peets, D. 21
Perahia, D. 43
Perahia, Dvora 26, 49, 50
Perez-Salas, Ursula A. 81
Perring, Toby George 96
Peshkin, Murray 99
Peterson, P. F. 36, 38
Peterson, Peter 37
Pieper, Joerg 113
Pike, T. D. 34
Pivovar, Adam Mathew 94
Platzman, Phil 58
Plummer, E. W. 95
Pochan, Darrin J 25
Poepfelmeier, Kenneth R. 77
Pokotilovski, Yu. 100
Popescu, I. I. 106
Pople, John A. 25
Popovici, M. 67
Popovici, Mihai P. 32
Porcar, L. 49
Porcar, Lionel 19
Porter, Rodney 37
Pozdnyakova, Irina Vasilyevna 76
Price, D. L. 86
Price, David L. 117
Proffen, Thomas E. 35
Prud'homme, Robert K. 57
Purwanto, A. 108
Pynn, Roger 59

Q

Qiu, Y. 34
Qiu, Yiming 33
Quirk, Roderic P. 49

R

Rafailovich, Miriam 115
Rainford, B. D. 73
Rainford, Brian 28
Raitman, Dr. E. 99
Ramadurai, B. 89
Rangaswamy, Partha 45
Ratcliff, W. 96
Rawn, C. J. 61, 67
Rawn, Claudia J. 44
Reed, Roger 30
Reeves, T. 34
Regnault, L. P. 74
Regnault, L.-P. 28
Rehm, Christine 65
Reich, D. 28

Reiter, George F. 58
 Ren, Yang 86
 Renger, G. 113
 Ressouche, E. 74
 Richardson, J. W. 31, 47
 Richter, D. 82
 Richter, Dieter 35, 57
 Richter, Dieter Oswald 55
 Rijssenbeek, Job Thomas 77
 Ringo, Roy 99
 Robinson, Robert 103
 Rogge, R. B. 58
 Rogge, Ronald 29
 Rols, S. 85
 Rondinone, A. J. 61
 Rondinone, Adam J. 44
 Rondinone, Adam Justin 67
 Rønno, H. M. 21
 Rose, Chris R. 38, 70
 Rosenkranz, S. 71
 Rosov, Nicholas 56
 Rotter, M. 73
 Rubner, Michael F. 50
 Rusevich, Dr. L. 99
 Russina, Margarita 56
 Rusu, Claudiu 106

S

Saboungi, M.-L. 117
 Sachdev, Subir 20
 Saenger, W. 112
 Sales, B. C. 22
 Sandí, Giselle 84
 Santodonato, Louis Joseph 68
 Sanyadanam, Srinath 75
 Sasagawa, T. 21
 Satija, S. 114
 Schad, Rainer 74, 75
 Scharfstein, G. 34
 Scharfstein, Gregory 33
 Scheck, Christian 75
 Schelten, Jim 118
 Schneibel, J. H. 47
 Schneider, Joel 25
 Schoen, Keary 99
 Schuller, Ivan K. 87
 Schultz, Arthur J. 42
 Schwahn, D. 116
 Serebrov, A. 100
 Shanahan, Kirk L. 107
 Shapiro, S. 64, 101
 Shen, Yue 50
 Shevchenko, Taras 110

Shin, K. 114
 Shirane, G. 119
 Shmueli, Liora 50
 Short, S. 71
 Sieling, M. 28
 Siewenie, Joan 44, 68
 Siewenie, Joan E. 107
 Simonson, J. M. 23
 Sinha, S. K. 89, 95
 Sinha, Sunil K. 88
 Sinn, H. 117
 Skanthakuma, S. 60
 Slisenko, V. I. 110
 Smee, S. A. 34
 Smee, Stephen A. 33
 Smeibidl, P. 21
 Smirnov, A. 46
 Smith, D. J. 89
 Smith, D. W. 43
 Smith, G. S. 114
 Smith, Greg 80
 Smith, Gregory S. 107
 Snow, W. M. 57, 64
 Sokol, Paul 60, 86, 109
 Sokolov, Alexei 94
 Soles, Christopher 84
 Sottmann, Thomas 57
 Sow-Hsin Chen 23
 Speakman, Scott 79
 Spoone, S. 47
 Spooner, Steve 46
 Spraul, Bryan 43
 Stancik, Cheryl Marie 25
 Stein, Barry 24, 108
 Steinsvoll, O. 104
 Stepanov, S. 88
 Stern, L. A. 61
 Stern, Laura A. 44
 Stettler, M. 38
 Stevenson, K. L. 27
 Steyerl, Albert 100
 Stirling, William 60
 Stock, C. 21, 119
 Stoica, A. D. 31
 Stoica, Alexandru 32
 Stoica, Alexandru D. 105
 Stout, M. 45
 Streletzky, Kiral A. 43
 Strey, Reinhard 43, 85
 Sukumaran, Sathish 26
 Sukumaran, Sathish K. 111
 Suminta, S. 108
 Sur, B. 58

Svensson, E. C. 108
Swan-Wood, Tabitha 78
Swan-Wood, Tabitha Liana 79

T

Taillefer, L. 21
Takagi, H. 21
Tangeman, Jean 44, 68
Tarek, Mounir 94
Taub, H. 109, 110
te Velthuis, G. E. 88
te Velthuis, S. G. E. 69
te Velthuis, Suzanne G. E. 76
Tennant, D. A. 22, 27, 72
Terech, Pierre 20
Thiaudières, D. 117
Thiyagaraja, P. 111
Thiyagarajan, P. 60
Thiyagarajan, P. 84, 111, 113
Thiyagarajan, Papannan 24, 108
Thompson, A. K. 63, 100
Thompson, J.R. 22
Tobias, Douglas 81
Toby, B. H. 61
Toby, Brian H. 44
Tokura, Y. 71, 95
Tomberli, B. 42
Tome, C. N. 84
Tomioka, Y. 71, 95
Traiphol, R. 43
Traiphol, Rakchart 26
Tranquada, John M. 74
Trehella, Jill 93
Trull, B. 100
Tsukada, Andrey Zheludev I. 74
Tselik, Alexei 28
Tulk, C. A. 42
Tulk, Chris A. 34, 64, 116
Tun, Z. 21
Turner, John F. C. 107

U

Uchinokura, K. 74
Ur, C. A. 106
Urquidi, Jacob 42, 107
Üstündag, Ersan 29
Uwakweh, Oswald N. C. 46

V

Vaidyanathan, Raj 30
Vajk, Owen Peter 28
van Zanten, John Hollis 115

Vasiliu-Doloc, L. 95
Vavassori, Paolo 75
Verghese, Jag Kasichainula K. 46
Vilches, Oscar Edgardo 108
Vogel, S. C. 47, 84
Volin, K. 69
Volin, Kenneth James 68
Volkman, U. G. 109, 110
Vorderwisch, P. 28
Vorderwisch, Peter W. 43

W

Wagner, Norman J. 19
Wakimoto, Shuichi 119
Wang, Howard 20
Wang, X.-L. 31, 105
Wang, Xiaoping 42
Wang, Xun-Li 47
Wang, Xunli 103
Wang, Y. D. 47
Wang, Yandong 31
Warr, G. G. 19, 49
Weber, Richard 44, 68
Weizeoric, John 37
Werner, Samuel A. 39, 99
White, Stephen H. 81
Wietfeldt, F. E. 64, 100
Wietfeldt, Fred E. 62
Wignall, G. D. 116
Wignall, George 34
Wilemski, Gerald 85
Wilk, K. A. 48
Willner, L. 55
Wilson, Tate 108
Winn, Barry L. 64
Wischnewski, A. 55
Witte, Peter 112
Wölk, Judith 43
Won, You-Yeon 50
Woodford, John 45
Woodward, Dr. Patrick 78
Woodward, Patrick M. 78
Worcester, David 114
Worlton, T. 36
Worlton, Thomas 37
Worlton, Thomas G. 38
Wu, Wen-li 84
Wyslouzil, Barbara E. 43, 85

Y

Yamada, K. 74
Yang, Bing-Shiou 57
Yang, G. L. 63

Yang, L. 63, 105
Ye, Feng 26
Ye, Z.-G. 119
Yelon, W. B. 67
Yerzolimsky, B. 100
Yerzolimsky, B. G. 100
Yethiraj, Mohana 77
Yildirim, Taner 41, 118
Yim, H. 114
Yoshizawa, H. 26, 64, 71
Young, Albert R. 63
Yuan, Peng 114
Yun, S. I. 25

Z

Zabel, V. 112
Zaliznyak, Igor 101
Zaliznyak, Igor A. 28
Zangari, Giovanni 75
Zanotti, Jean-Marc 94
Zeppenfeld, Peter 108
Zhang, Ying 20
Zhao, Jinkui 35, 114
Zsigmond, Géza 58, 60
Zvinevich, Yury 43
Zwanziger, J. W. 57
Zwanziger, Josef W. 24, 108



Revolve's magnetic bearings enhance your chopper performance!



Revolve can supply 60Hz - 300Hz bandwidth limiting disk type choppers and 600Hz Fermi type neutron choppers complete with control system and disk or slit package.

Revolve's magnetic bearings and control system enable neutron choppers to operate with:

- High reliability
- Accurate phase control with VETO signal for out-of-phase alert
- High efficiency
- No hydrocarbons to breakdown or contaminate
- Minimal particle contamination
- Minimal outgassing
- Built-in diagnostics - no need to add accelerometers or other monitoring equipment
- Safety interlocks
- RS485 communication

Our High Speed Fermi type (E0) Neutron Chopper uses a magnetic bearing control system to smartly control the motor phasing. It operates up to 36,000 RPM in a vacuum and is compatible with up to 2×10^6 rads of gamma radiation.

Revolve sets the standards for:

Phase Control - 100% repeatability of ± 0.25 ms at 600 Hz (i.e. within 0.054 degrees of alignment with its windows on each revolution), providing the best performance and operation in neutron scattering spectrography!

Design - Overhung design allows for easy accessibility to the top payload for quick interchangeability of slit packages.

Motors - Our integrated DC Brushless motors provide a very efficient solution. They allow speeds between 3600RPM and +36,000RPM to be achieved with phase control ability as described above.

Flexibility - Our solutions are adaptable to your application and are extremely easy to use!

Revolve has turnkey and global support solutions for rotating equipment operating in high vacuum environments.

Call us at +403.232.9292 to develop the best solution for you!

or visit our website at

WWW.REVOLVE.COM



VANADIUM SAMPLE CANS

**No more
fabricating
your own
containers!**

Metal Technology, Inc. understands the challenges of neutron-powder diffraction and neutron-scattering experiments. To assist you in meeting those challenges, we've developed Vanadium Sample Cans (in coordination with NIST).

These cans are:

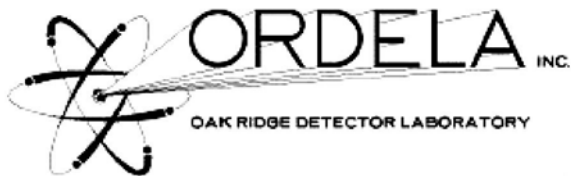
- Seamless
- Virtually indestructible and resistant to holes
- Available with and without flanges or caps
- Vanadium cans, with titanium flanges and aluminum caps
- Also in custom materials, diameters, & sizes
- Allow both low and high temperature work
- Manufactured with a groove in the flange for O-rings or indium seals

Visit our URL, www.mtialbany.com ...

Chances are we have just what you need!

METAL TECHNOLOGY, INC.

173 Queen Ave. SE Albany, OR 97321 U.S.A.
Tel: 800:394:9979 Fax 541:928:0596
E-mail: sales@mtialbany.com



Neutron, X-Ray and Alpha Radiation Detection and Measurement

Neutron

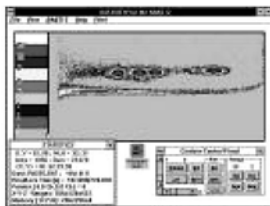


ORDELA, Inc. designs and manufactures radiation detection and measurement instruments for neutrons, x-rays, beam monitors and alphas used at nuclear research facilities worldwide.

Our **Neutron** Instruments are used in such applications as neutron scattering and diffraction research. Our line includes:

- Preamplifier-per-cathode counter design for maximum resolution (*to 1 mm*) and count rate capability (*to 10⁷*).
- Two Dimensional Neutron Counters
- Curvi-Linear Detector Systems
- Linear Detector Systems

Software



- Dual Parameter display for PSPC or PERALS®
- Remote Control to configure, control and process all essential counter operations from computer console.
- One- and Two-Dimensional Position Sensitive Proportional Counters (PSPC)

X-Rays



Beam Monitors



Instrumentation



- Customer-specified sensitive area and efficiency

- High Speed Data Acquisition Systems
- Convenient NIM module format
- Wide variety of multi-function instrumentation available



For further information, contact us!

ORDELA, Inc., 1009 Alvin Weinberg Dr, Oak Ridge, TN 37830, USA

Call 865-483-8675 or FAX 865-483-8404

E-mail: info@ordela.com

Visit our web site: www.ordela.com

ACNS Comment Form

We'd like to have your feedback on this conference. Please fill out this form (name is optional) and return it to the NSSA booth, fax it to James Rhyne at (573) 882-4195, or mail it to the address on the back of the form.

What is your overall opinion of this conference? Has it been informative?

Would you come to another ACNS?

How would you rate the facilities?

Suggestions for future conferences?

Name and address (optional)

We appreciate your input!

James J. Rhyne
Dept. of Physics, Univ. of Missouri
Columbia, MO 65211